# SHEAR STRENGTH OF A COHESIONLESS SOIL UNDER PLANE STRAIN AND TRIAXIAL CONDITIONS

# SHEAR STRENGTH OF A COHESIONLESS SOIL UNDER PLANE STRAIN AND TRIAXIAL CONDITIONS

by

NABIL SALIM EL-NASRALLAH, B.Sc. (Civil Eng.)

A Thesis

Submitted to the School of Graduate Studies

in Partial Fulfillment of the Requirements

for the Degree

Master of Engineering

McMaster University

April, 1976

MASTER OF ENGINEERING (1976) McMASTER UNIVERSITY
(CIVIL ENGINEERING) HAMILTON, ONTARIO.

TITLE: SHEAR STRENGTH OF A COHESIONLESS SOIL UNDER PLANE STRAIN AND TRIAXIAL CONDITIONS

AUTHOR: Nabil Salim El-Nasrallah, B.Sc. (Damascus, Syria)

SUPERVISOR: Professor Nyal E. Wilson

NUMBER OF PAGES: vi, 104

SCOPE AND CONTENTS:

An experimental programme was carried out involving both plane strain and triaxial compression tests on a dry sand. A comparison between both methods is presented to show the influence of the intermediate principal stress on the angle of shearing resistance at failure, the shear characteristics and the failure criterion. The Mohr-Coulomb theory was used as a failure criterion. The angle of shearing resistance at failure in plane strain tests was higher than in triaxial tests. Shear strength values at failure were higher in plane strain tests than in triaxial tests. All stress-strain curves in both plane strain and triaxial tests have a similar shape.

## ACKNOWLEDGMENTS

The author wishes to express his appreciation to Professor Nyal E. Wilson for his assistance and encouragement throughout the research program.

The financial support by the Civil Engineering Department, McMaster University, the extension of the financial support by Dr. B. Allen and Dr. A. Smith and the Defence Committee, are gratefully acknowledged.

The author wishes to thank Dr. J.J. Emery for his support, constructive discussion and comments.

The assistance of Mr. W. Sherriff with the construction of the experimental apparatus is very much appreciated.

The author wishes to thank his fiance, Camille T. Majchrzyk for her continuous moral support, understanding and encouragement throughout the research program.

## CONTENTS

## LIST OF FIGURES

# CHAPTER 1

# INTRODUCTION

In soil mechanics, there is a great dependence on shear testing. Such tests enable geotechnical engineers to measure the shear strength parameters of soils under various controlled conditions of drainage and loading. The results of these tests may be usefully employed in projects such as foundations and embankments.

In this study, triaxial and plane strain conditions are considered from the point of view of comparing soil behavior and failure criteria.

In the triaxial (cylindrical) compression test, three external stresses are involved. The axial stress is the major principal stress ($\sigma_1$), and the other two external stresses surrounding the soil sample represent the intermediate principal stress ($\sigma_2$) and the minor principal stress ($\sigma_3$). In this test, the intermediate principal stress and the minor principal stress are both equal to the confining pressure ($\sigma_2 = \sigma_3 = \sigma_c$). The results of the triaxial test are strictly applicable to axially symmetric problems, for instance, it is particularly applicable to problems dealing with piles, circular footings, square foundations and oil

tanks, etc., if and where the loading is symmetric.

In this respect, many engineers and investigators in the field of soil mechanics are aware of some of the limitations of the conventional triaxial test, because of the fact that the conventional shear strength analysis (Mohr-Coulomb theory) assumes that $\sigma_2$ has no effect on the shear strength of soils. This assumption is conservative and approximate in many practical soil problems approximating to plane strain conditions (long foundations, earth dams, retaining walls, culverts, embankments and pipe lines), where the value of $\sigma_2$ is higher than $\sigma_3$. Plane strain conditions exist when the loading and the geometry of a structure do not vary in the longitudinal direction, and also when the displacements in this direction are equal to zero.

An apparatus has been constructed at McMaster University to measure the shear characteristics of cohesionless materials under plane strain conditions. This apparatus measures the intermediate principal stress ($\sigma_2$) in addition to measuring the major principal stress ($\sigma_1$), the minor principal stress ($\sigma_3$), and the vertical displacement. The technique of preparing and testing dry cohesionless soils, as well as full details of the apparatus and the loading and measuring systems, will be given in the following chapters.

A series of plane strain tests and triaxial compression tests have been carried out on a dense to very dense dry sand, since limited time did not allow for tests over a wide range of densities.

The shear strengths of dry sands in plane strain com-

pression tests are compared with shear strengths in triaxial compression tests. For instance, revealing the results of subsequent chapters, it was shown that the angle of shearing resistance $\phi_f$ at failure in plane strain tests, was about eight degrees higher than the angle of shearing resistance at failure in the triaxial compression test for the densest state.

All stress-strain curves in both triaxial compression and plane strain compression tests have a similar shape, where principal stress ratios rise to a peak value at failure and then continue to decrease with increasing axial strains. Principal stress ($\sigma_1$) values in plane strain tests are greater than principal stress ($\sigma_1$) values in triaxial tests, and occur at smaller strains.

The values of the intermediate principal stress ratio $\sigma_2/(\sigma_1 + \sigma_3)$ are found to be in the range of 0.19 to 0.23 for the very dense samples. Other intermediate principal stress ratios (i.e., $\sigma_2/\sigma_3$, $\sigma_2/\sigma_1$) are plotted versus initial porosity, and compared with results obtained by other researchers.

An analysis of octahedral stresses (normal and shear stresses) was carried out for both test methods. Results showed that octahedral stresses versus axial strain curves had similar shapes to the major principal stress curves.

# CHAPTER 2

# PLANE STRAIN CONCEPT

## 2.1 Plane Strain Concept in Geomechanics

Plane strain conditions occur when the geometry and the loads of a structure do not vary significantly in the longitudinal direction, or conversely, when the dimension of the structure in the z-direction is very large, and the displacements in this direction are prevented (i.e., $\varepsilon_z = 0$).

There are many important engineering applications and problems which fall into this category, as shown in Figure (2.1). In each case, the loads must not vary significantly along the length.

## 2.2 Orientation of Plane Strain Conditions

In plane strain analysis, it is sufficient to consider a slice between two sections each a unit length apart in a coordinate system. Figure (2:2) shows the orientation of the plane strain conditions in relation to the fixed coordinate directions x, y and z. The strain component $\varepsilon_z$ in the longitudinal section z, is equal to zero. According to the theory of elasticity two strain components $\varepsilon_y$ and $\varepsilon_x$ and three stress components $\sigma_x$, $\sigma_y$ and $\sigma_z$, can be calculated in

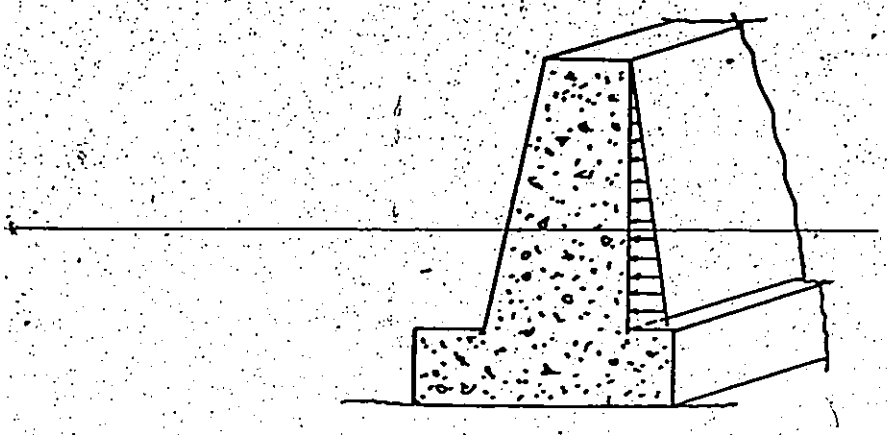

A) Retaining Wall With Lateral Pressure.

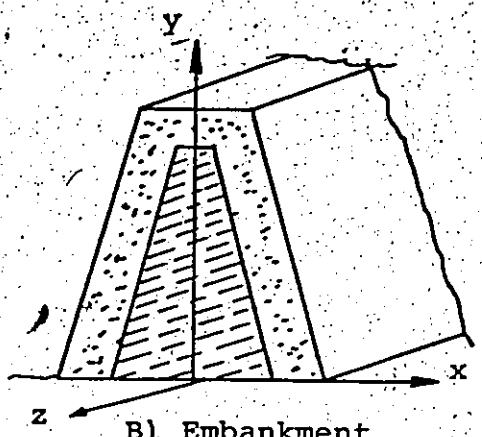


B) Embankment.

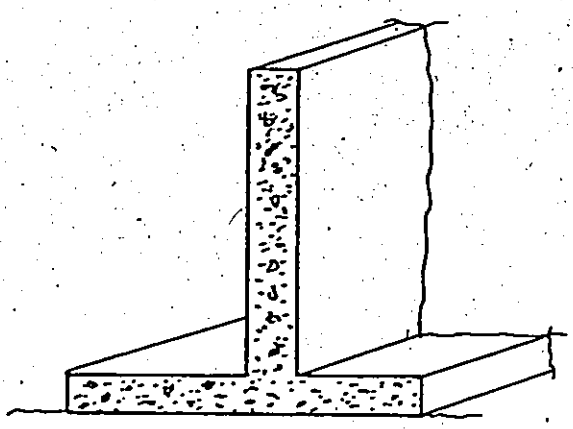

C) Retaining Wall.

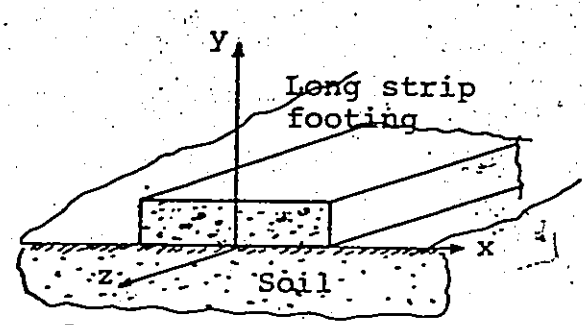


D) Loaded Semi Infinite Half Space.

Figure (2.1) Examples of Plane Strain Conditions.

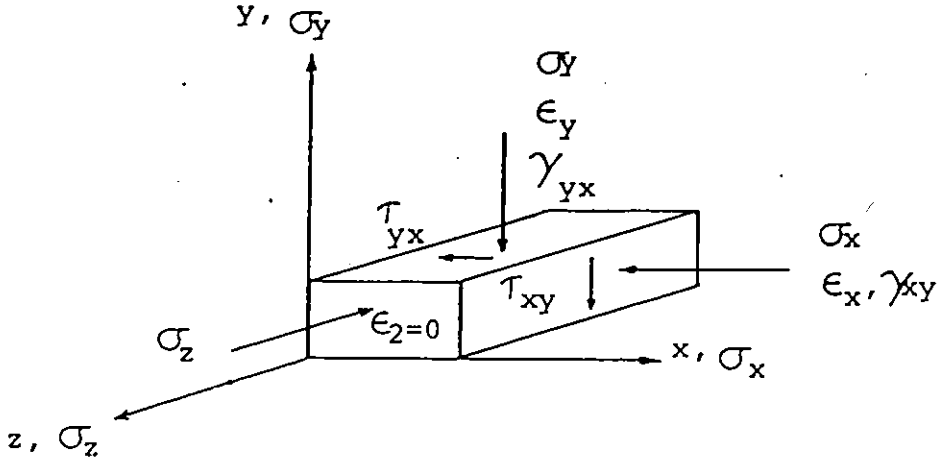


Figure (2.2) Orientation of Plane Strain Conditions.

any plane strain problem, in addition to shear stresses $\tau_{xy}$, $\tau_{yx}$ and shear strains $\gamma_{xy}$, $\gamma_{yx}$.

In plane strain and triaxial compression tests the stresses $\sigma_x$, $\sigma_y$ and $\sigma_z$ in the directions x, y and z will be defined as: the minor principal stress ($\sigma_3$), the major principal stress ($\sigma_1$) and the intermediate principal stress ($\sigma_2$). In triaxial tests $\sigma_2 = \sigma_3$. In addition, the mathematical derivations of principal stresses and planes, the relation between the intermediate principal stress and the other principal stresses, the concept of octahedral stresses, and all stress-strain relationships can be found in any of the textbooks dealing with the theory of elasticity and plasticity (Scott, 1963). These relations will be used in the analysis of the experimental data derived from both triaxial compression and plane strain tests.

# CHAPTER 3

## LITERATURE REVIEW

Kjellman (1936), described an apparatus as shown in Figure (3.1), to test cubical samples and to measure principal stresses: $\sigma_1$, $\sigma_2$, $\sigma_3$. Samples were compressed between frictionless steel pistons and steel reaction plates. Pressure was transferred to the sample on each side by rods with plane end bearings on the sample and spherical ends in contact with the ends of the pistons or the reaction plates. These rods reduce friction on the sides of the sample during shear by being free to move laterally as the sample deforms. The apparatus was supported by a cast-iron frame. Each piston was loaded by a lever system, and a suspended water tank was used in preference to weights.

The applied pressures were read from water levels in the tank, which could provide pressures up to 13 kg/sq. cm. No rubber membranes were used for coarse sand samples; however, thin stretched rubber membranes were used over dry samples to prevent the soil from being squeezed out between the rods.

Tests on dry German standard sand with grain size equal to 1 mm and void ratio equal to 0.67, showed that the strengths

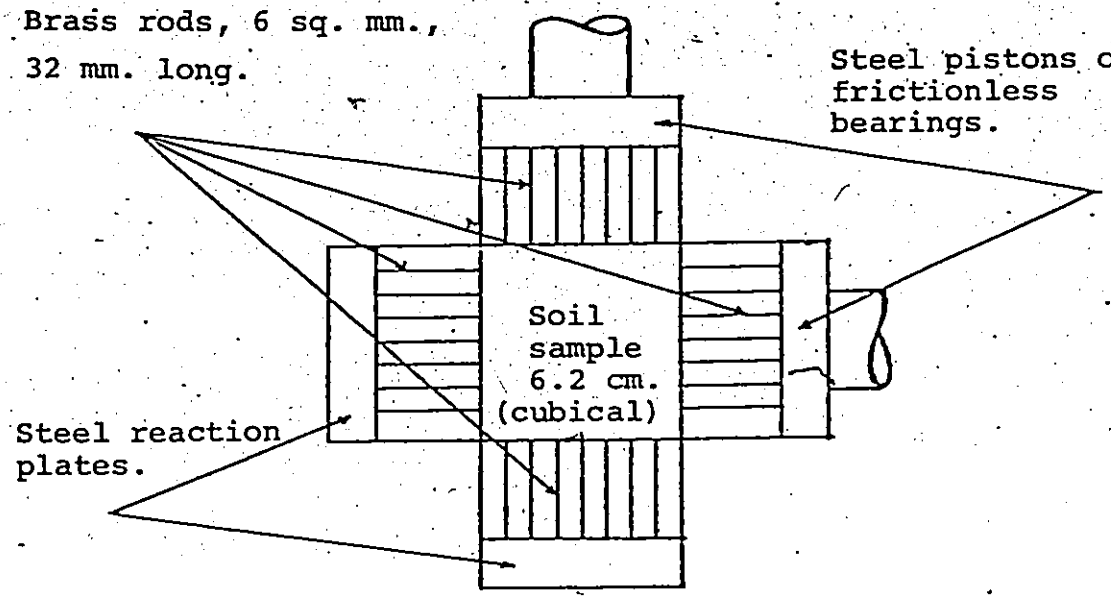


Figure (3.1) Kjellman Apparatus.

Kjellman (1936).

of the sand in tests having the intermediate principal stress greater than the minor principal stress, were higher than the strengths in tests which had the same stress system as the triaxial compression test. The angle of shearing resistance at failure was equal to 35° in triaxial tests, and equal to 43° in tests where $\sigma_2$ was measured. The difference in strength was believed to be due to the influence of the intermediate principal stress.

The Norwegian Geotechnical Institute (Cornforth, 1961), constructed an apparatus which tested a specimen 4 cm. wide, 12 cm. high and 30 or 60 cm. long as shown in (simplified) Figure (3.2). In this type of apparatus there was no form of restraint to prevent deformation in the longitudinal section of the sample during the shear test, but the friction between the specimen and the loading plates was sufficient to induce a plane strain failure. The test specimen was not enclosed in a cell and the effective lateral pressure was obtained by applying a vacuum to the sample. This pressure was negative and held constant during the test and measured by mercury manometers. Vertical loads and displacements were measured in the conventional way. Volume changes, however, were measured by a water-filled burette which was not reliable because it was difficult to hold the negative internal pressure at a constant level. Tests on dry Valgrinda sand were carried out by Kummenje (given by Cornforth, 1961) in this apparatus and the standard triaxial apparatus. Results showed that the plane strain type of tests gave higher strength than standard triaxial compression tests at all

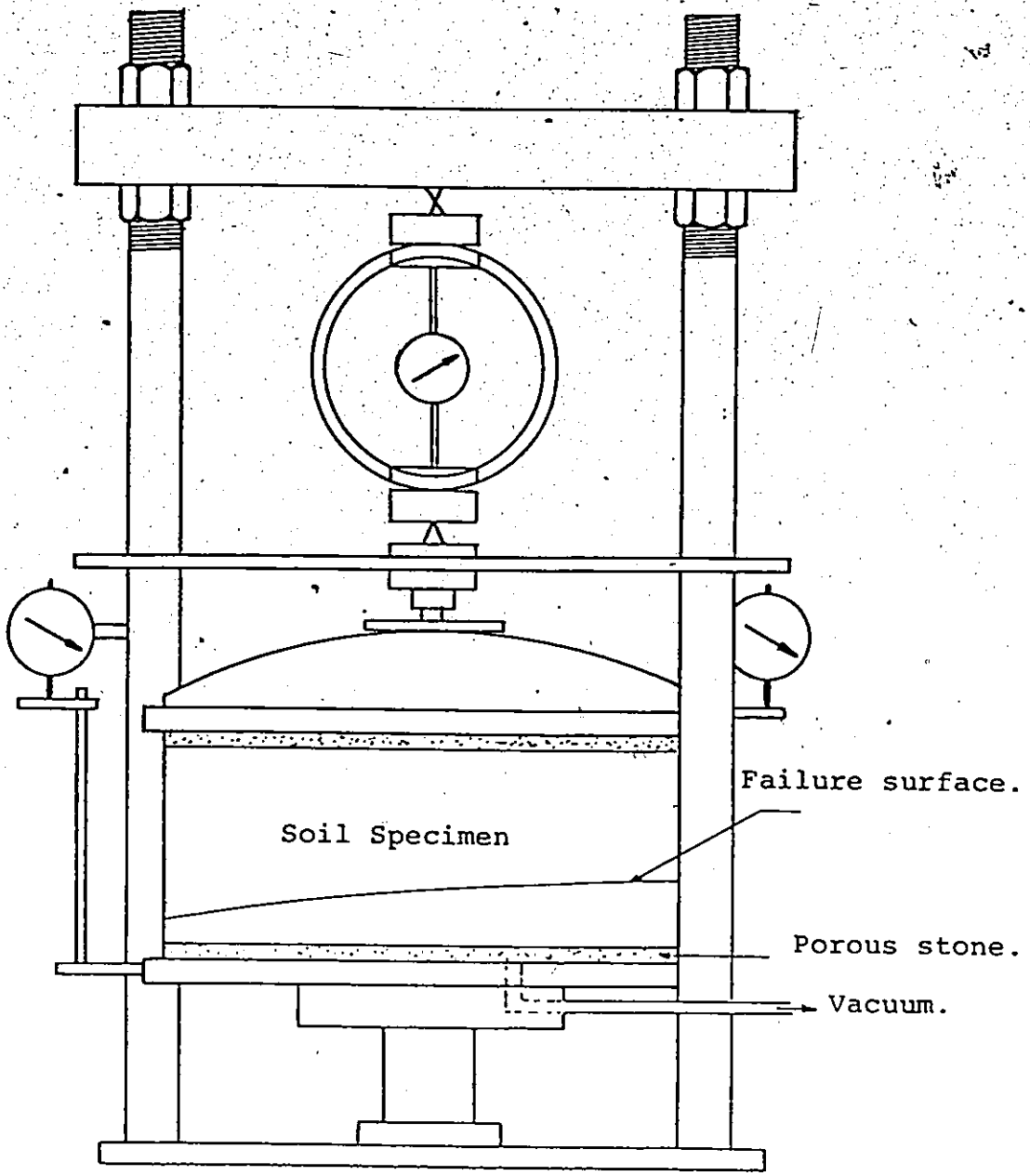


Figure (3.2) The Norwegian Geotechnical Institute Apparatus.
(From Cornforth, 1961).

porosities. The greatest difference in the angle of shearing resistance $\phi_d$ ranged from 2 to 4 degrees.

Wood (1958) constructed an apparatus to measure shear strength characteristics of soils under plane strain conditions. Figure (3.3) shows a simplified diagram of the plane strain apparatus which tested a specimen 16 in. long, 4 in. high and 2 in. wide. The height:width ratio is equal to two. This ratio is the same as in the usual triaxial test. A strain device (end clamp) was used to prevent strain in the longitudinal direction of the sample and to maintain plane strain conditions. The plane strain sample was enclosed by a rectangular rubber membrane. The vertical load was transferred to the sample via two pistons passing through the top of the cell at the quarter-length points. The deviator stresses and the vertical displacements were measured in the conventional way. The intermediate principal stress was measured by a pressure measuring device attached to one of the end clamps which contained a stiff rubber diaphragm.

This apparatus made possible the measurement of $\sigma_1$, $\sigma_2$, and $\sigma_3$ independently, in addition to the pore water pressure and the vertical displacements. Alternatively, Cornforth (1964) carried out an extensive testing program by using the Wood apparatus on Brasted sand in plane strain conditions, triaxial compression, triaxial extension and the shear box. Results showed that the strength of the cohesionless materials was slightly higher in plane strain tests than in triaxial tests. This demonstrates that the intermediate principal stress ($\sigma_2$) has an effect on shear strength character-

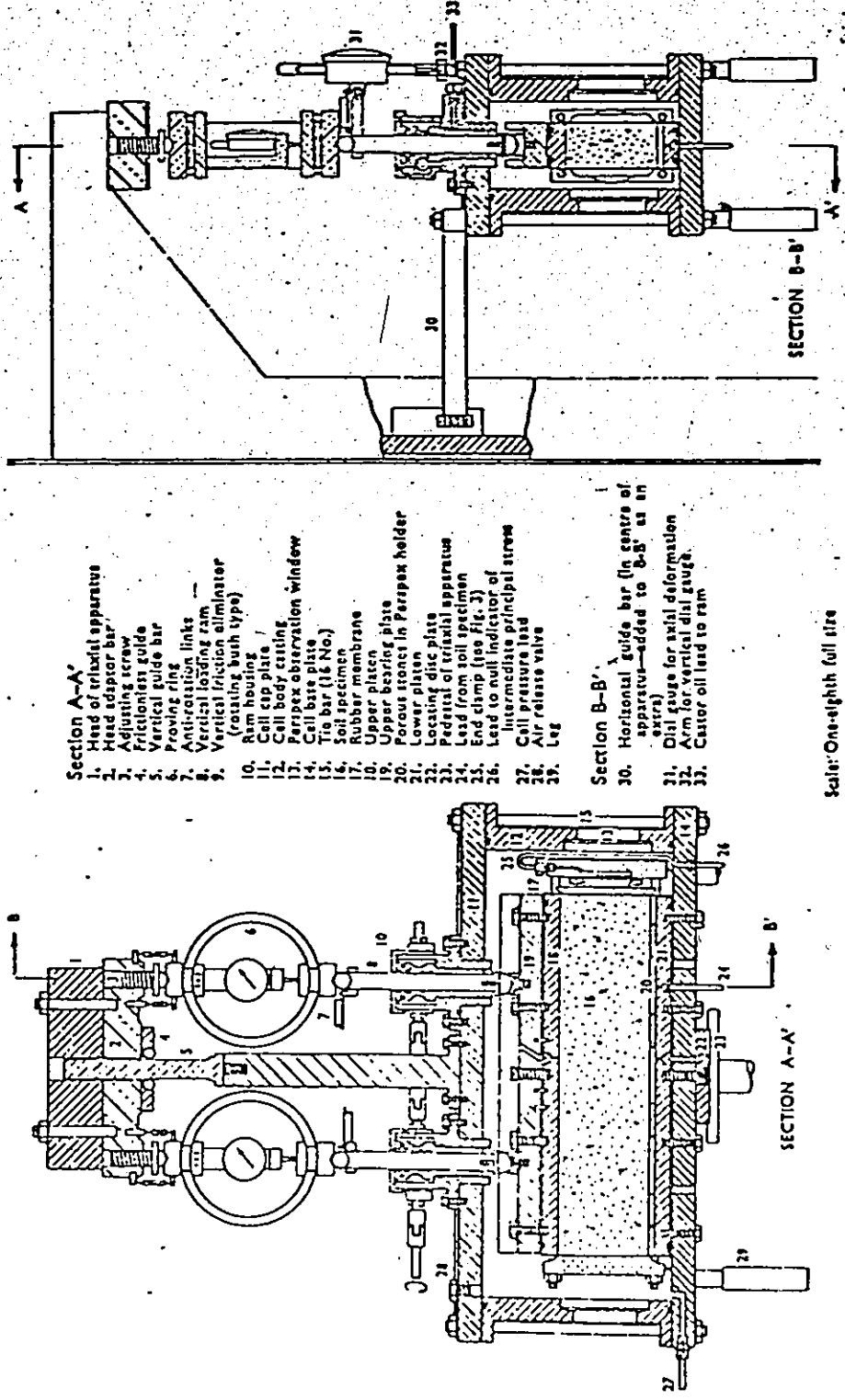


Figure (3.3) Wood Apparatus.
Wood (1958).

istics and on the failure criterion. The angle of shearing resistance in the plane strain test was higher by about 1/2° than the triaxial test on loose sand. This difference was more than 4° for the densest specimens. The ratio of the intermediate principal stress ($\sigma_2$) to the sum of the other two stresses (i.e., $\sigma_1$ and $\sigma_3$) versus the axial strain was almost constant. However, this ratio versus the initial porosity varied from 0.27 for denser specimens to 0.36 for the looser specimens.

Barden, Ismail and Tong (1969) tested cubical samples of sand in plane strain conditions with high confining pressures in the range of 5-1000 lb./sq. in. The 6 in. long, 4 in. wide and 4 in. high sample was formed in a standard 6 in. diameter triaxial membrane which had been drawn into a rectangular section by means of a vacuum connected to a perspex former in order to seal the membrane by O-rings. Discs were attached to the 6 in. by 4 in. rectangular top and bottom platens. The transition from the rectangular to the circular section was smoothed out by a plastic filler. Two side plates with load cells were used to maintain the plane strain conditions and to measure the intermediate principal stress ($\sigma_2$) as shown in Figure (3.4). The test specimens were deformed vertically. The applications and the measurements of the displacements and the principal stresses were performed in the conventional way. High cell pressure tests in the range of 100-1000 psi were carried out by using high pressure nitrogen cylinders controlled by sensitive valves. Drained plane strain tests which were conducted on cohesionless

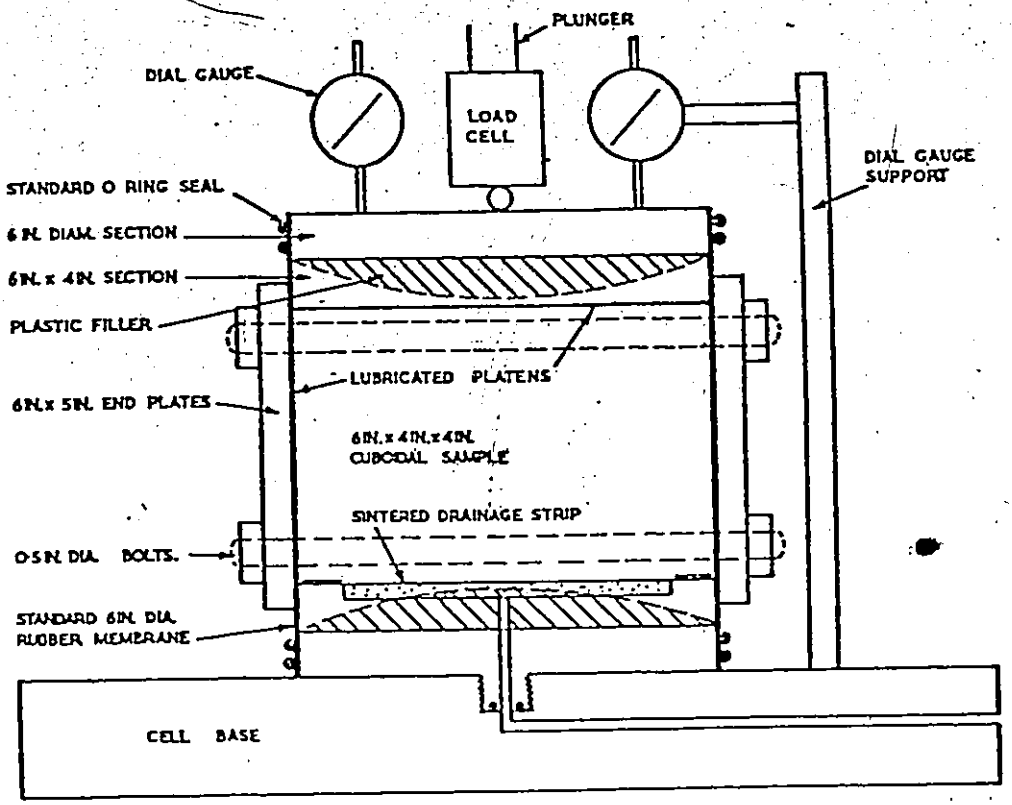


Figure (3.4) Barden, Ismail and Tong Apparatus.
Barden, Ismail and Tong (1969).

materials (River Welland sand, crushed feldspar and bronze ballotini) at low and high confining pressures indicated that the stress dilatancy behaviour provides a simple flow rule and a family of plastic potentials which are independent of the density of the material and the confining pressure. These results were not found to be particularly relevant to this research.

Campanella and Vaid (1973) constructed a plane strain apparatus at the University of British Columbia to test a sample 10 cm. long, 2.5 cm. wide and 5.75 cm. high. The sample was constrained in the direction of its length between two rigid fixed exterior side plates to maintain the plane strain conditions. The sample was enclosed by a rectangular rubber membrane. The intermediate principal stress ($\sigma_2$) was measured by load cells inserted into the end plates. Other principal stresses and displacements were applied and measured in the conventional way. Figure (3.5) shows exploded cross sections of the plane strain apparatus. Undisturbed, saturated marine sensitive clay specimens were used in the testing program to study the influence of stress path on the plane strain conditions. These results dealt with drained and undrained conditions of clay. The angle of shear resistance $\phi'$ was equal to 31.6 degrees in plane strain compression and 34.3 degrees in plane strain extension. The ratio of the principal effective stress $\sigma_y'$ in the direction of zero strain (i.e., intermediate principal stress $\sigma_2'$) to the sum of the other two principal stresses stayed at a value between 0.36 and 0.39 during the shear test.

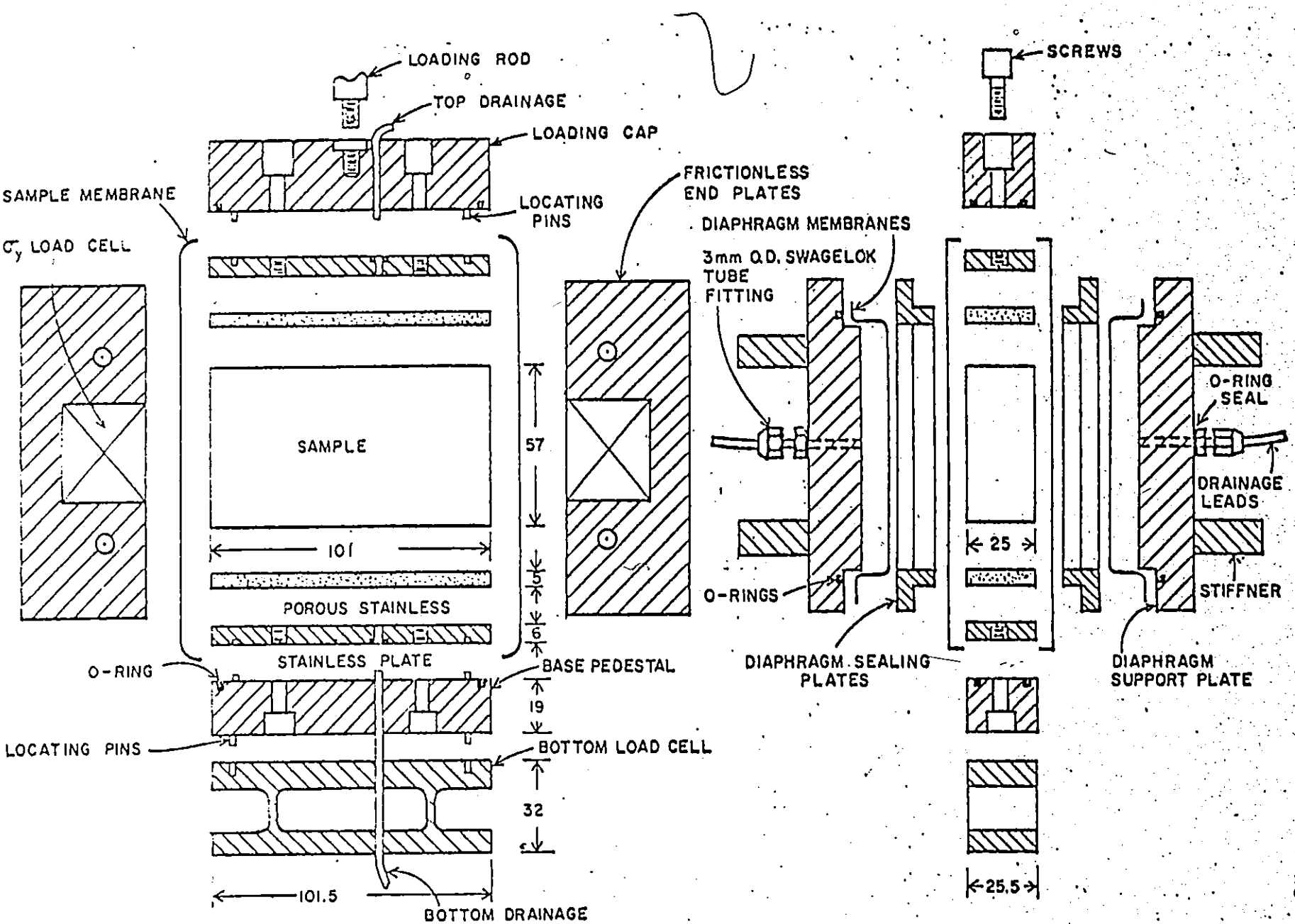


Figure (3.5) Campanella and Vaid Apparatus. (1973)

Mitchell (1973) also constructed an apparatus at Queen's University which measures the soil properties in plane strain conditions. This apparatus was designed to avoid some of the disadvantages of many plane strain apparatuses. In particular, this type proved useful in eliminating the excess friction, the limited deformation range, the side clearance between the sample and the side plates and other difficulties. Figure (3.6) shows the difference between the exterior side plates (used by others) and the interior side plates which were used in the Mitchell plane strain apparatus. This concept provided continuity at all corners of the sample and reduced the boundary friction. A rubber membrane was used by covering the interior plates (slide mechanism), and it was held in tension by springs, so that the membrane would not buckle as deformation progressed. The compressible side plates allow a 20% axial strain. The design of the apparatus was based on independent pressure cells which were placed adjacent to the tested specimen and the compressible side plates (this mechanism provides rigid boundaries in $\sigma_2$ directions). Air pressure was used to provide $\sigma_2$ and $\sigma_3$, the pressure in the independent cells was monitored by tranducers. The vertical load was applied by conventional methods. The volume change of each cell was measured by an air silicone fluid meniscus in a pressurized burette. The specimen was allowed to strain toward the cell and any rupture planes could be observed through the perspex plate. This apparatus has been developed for plane strain conditions and true triaxial by stress strain control and also to test drained and undrained

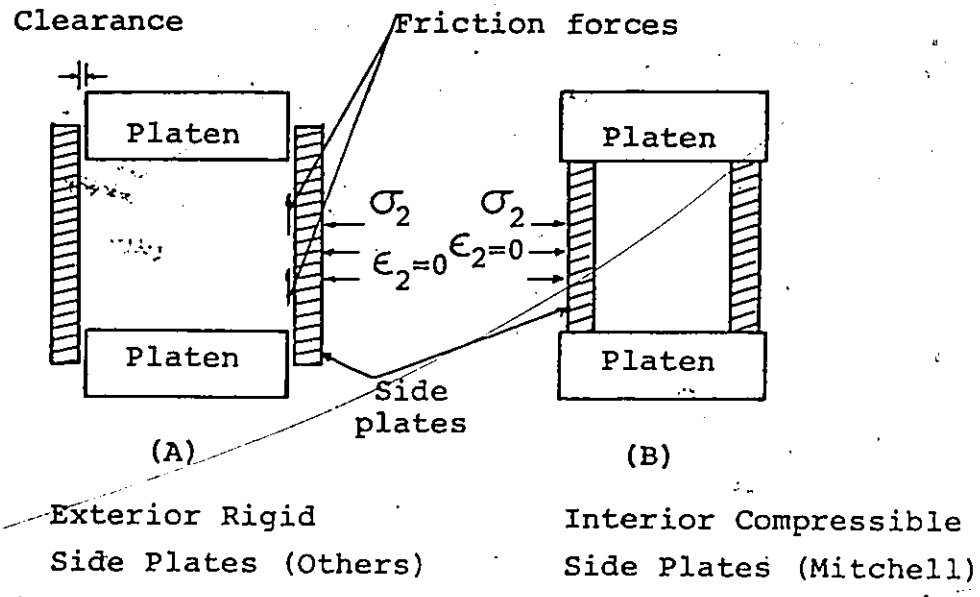


Figure (3.6)
Mitchell (1973)

samples. A series of fully drained plane strain tests have been carried out on Champlain Sea deposits (clays) in this apparatus in conjunction with triaxial compression and extension tests. However, the results of these tests were not published.

The following chapter will describe the main features and details of the plane strain apparatus which was built at McMaster University, in a very simple and inexpensive way. The plane strain apparatus is a modification of the triaxial cell for 4 in. diameter samples. The main aim of this apparatus is to measure the shear strength parameters of dry sand in plane strain conditions and to compare these parameters with those obtained by the standard triaxial compression tests.

# CHAPTER 4

# DETAILS OF PLANE STRAIN APPARATUS

The plane strain apparatus was designed and built in a similar way to the other plane strain apparatuses; it measures the intermediate principal stress ($\sigma_2$) while maintaining $\varepsilon_2 = 0$. The vertical displacements, the deviator stresses ($\sigma_1 - \sigma_3$), and the minor principal stress ($\sigma_3$) were measured in the usual way common in triaxial testing.

The following sections describe the stages of developing this apparatus, and the difficulties faced during the design process.

## 4.1. Sample Description

The plane strain apparatus measures the shear strength of specimens with rectangular cross sections. The specimen dimensions are 1.5 in. wide, 3.5 in. long and 3 in. high, thus retaining the same height to width ratio (i.e., equal to two) as the triaxial test specimen.

Figure (4.1) shows the specimen dimensions in a coordinate system, keeping in mind that the strain in the z-direction is prevented by two rigid plates to maintain the plane strain conditions.

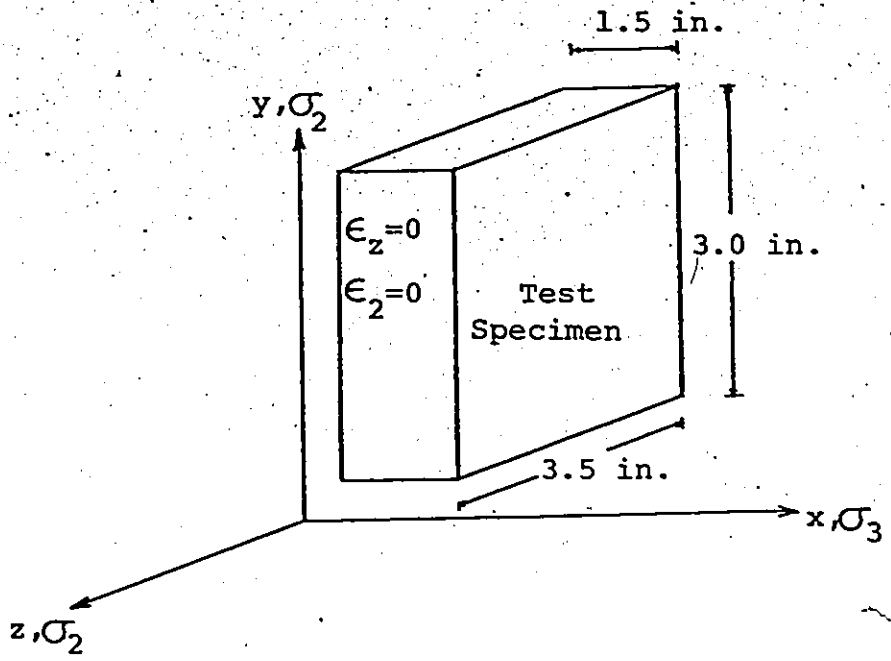


Figure (4.1) Test Specimen in a Coordinate System.

## 4.2 The Main Features of the Plane Strain Apparatus

The plane strain apparatus replaces the cylindrical triaxial specimen (i.e., pedestal, cap, stones, membrane) so that the strain in the z-direction $\varepsilon_2$ is equal to zero. A triaxial cell for 4 in. diameter samples was used to provide the minor principal stress ($\sigma_3$), the deviator stress ($\sigma_1 - \sigma_3$) and the vertical displacement. Figure (4.2) shows a simple sketch of the triaxial cell, with a plane strain sample in place.

The loading and the measuring system which enable the shear test to be performed under the plane strain conditions are described in the schematic layout of Figure (4.3).

The vertical load was applied in a similar manner as in the triaxial test. The deviator stress was measured by means of a proving ring, whereas, the vertical displacement was obtained by using a dial gauge.

The minor principal stress ($\sigma_3$) was applied by an air supply with a maximum capacity of 30 psi. Figure (4.3) shows the connections between the air supply and the cell. The air pressure was controlled by a pressure relief type valve in order to maintain a steady predetermined pressure throughout the shear test.

The intermediate principal stress ($\sigma_2$) was measured by intrumenting the rigid plates with thin diaphragms. These diaphragms transfer the pressure in the z-direction and their deflection is monitored through the attached strain gauges. The strains are monitored by individual strain indicators and a digital recorder as shown in Figure (4.3). These readings are then converted to pressure (i.e., $\sigma_2$) by

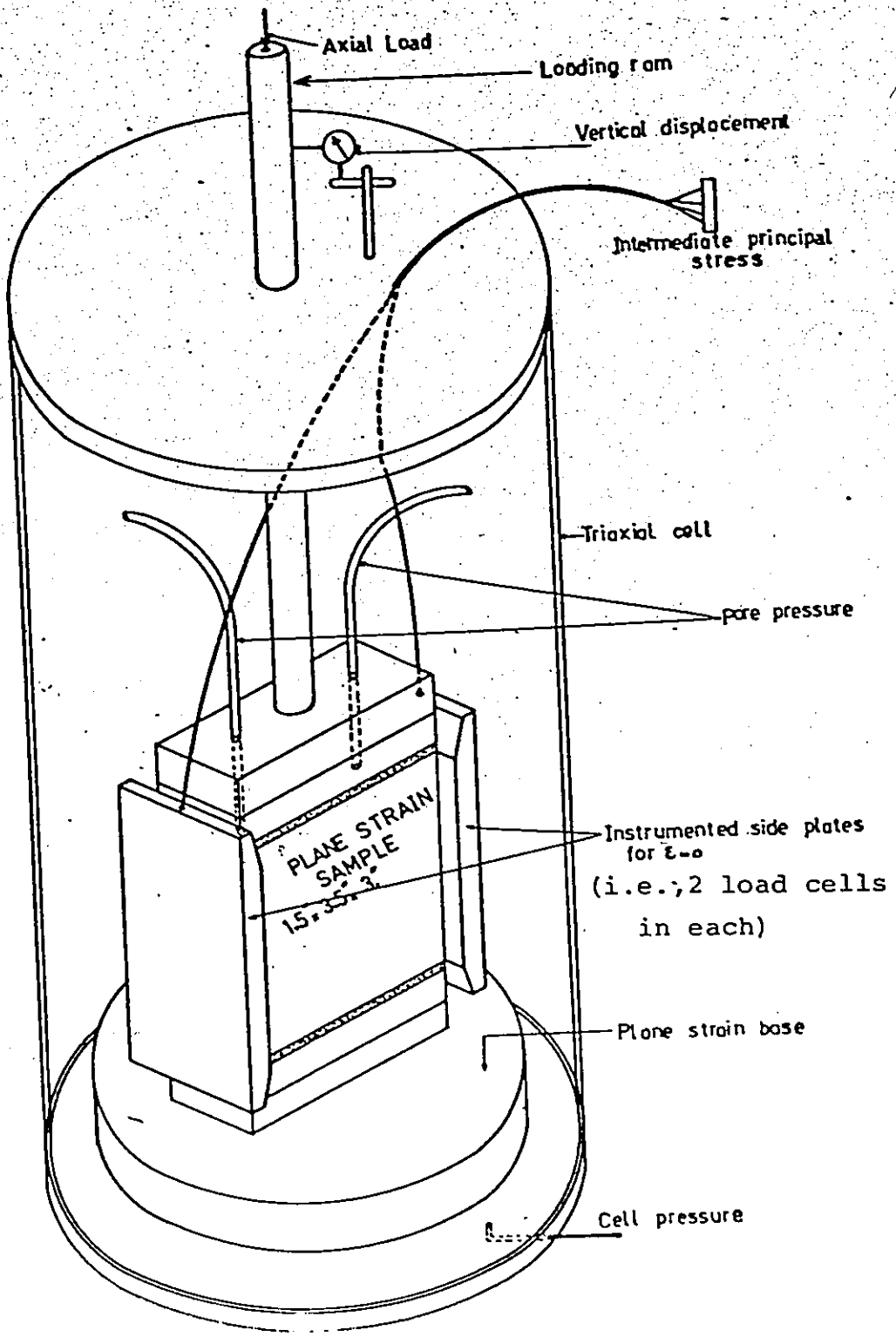


Figure (4.2) Sketch of the Triaxial Cell with Plane Strain Sample in Place.

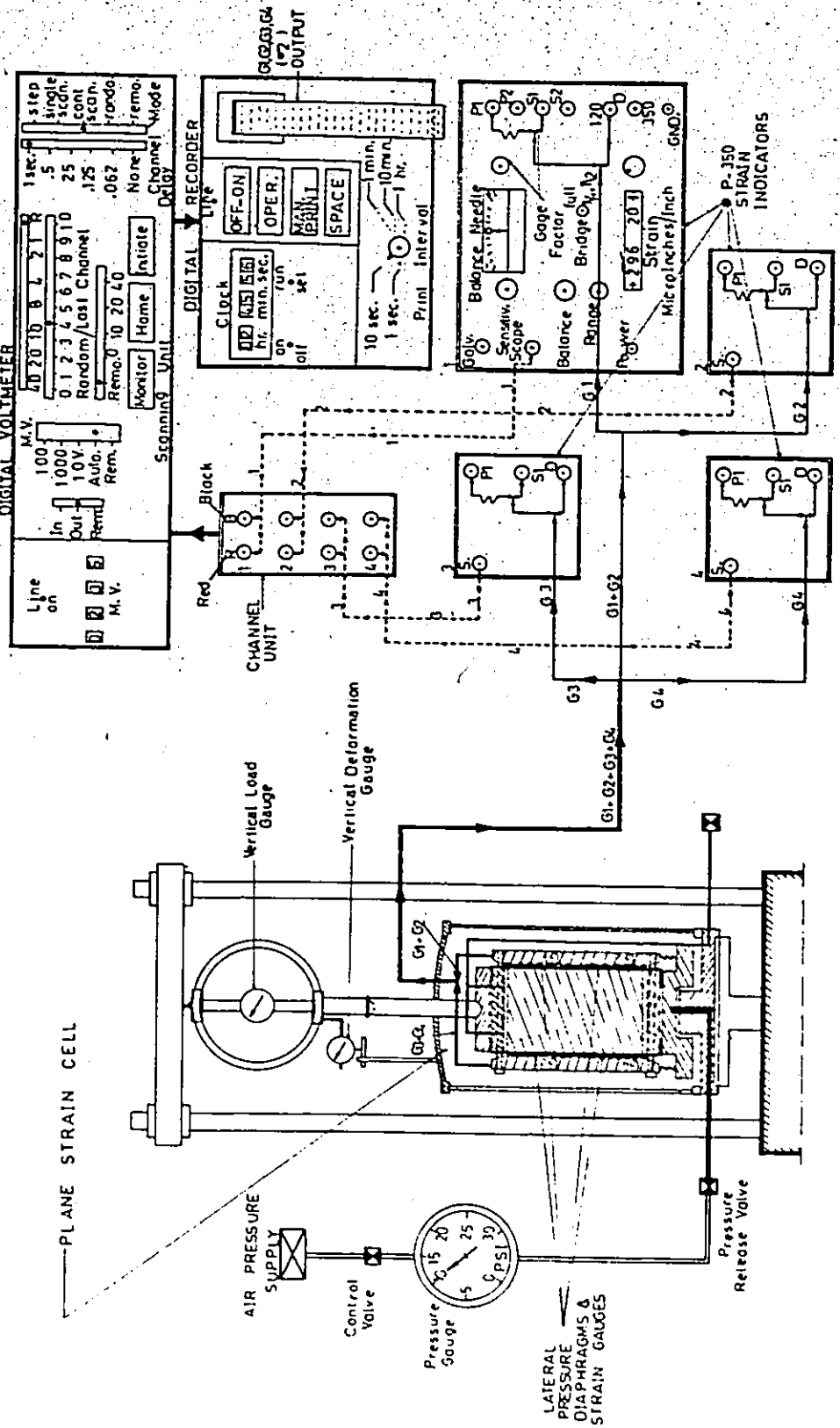


FIG(4_3) SCHEMATIC LAYOUT OF LOADING AND PRESSURE MEASURING SYSTEM.

using the calibration curves of the strain gauges as indicated in Figure (4.6).

The $\sigma_2$ values are used in the analysis of the plane strain condition of cohesionless materials.

## 4.3 Instrumented Side Plates

Two stainless steel side plates were made to prevent the strain in the z-direction (i.e., the longitudinal section of the plane strain sample), and to incorporate circular diaphragms for measuring the intermediate principal stress ($\sigma_2$) by means of four strain gauges.

The instrumented side plates are shown in Figure (4.4). Incorporated in the side plates are circular diaphragms with strain gauges attached. These thin film strain gauges were waterproofed.

### 4.3.1 Diaphragm Design

The stainless steel diaphragms were made first in the Geotechnical machine shop without a design process to determine the desired thickness. The thickness of the diaphragms was confined to .05 in., in view of the fact that machinery limitations precluded production of thinner diaphragms.

The following design process was used to determine the calculated thickness of the diaphragms under the application of the proposed maximum pressure. The thickness of the elastic diaphragm was calculated from the following equation (Bares, 1969), which considers the diaphragm as a circular fixed plate.

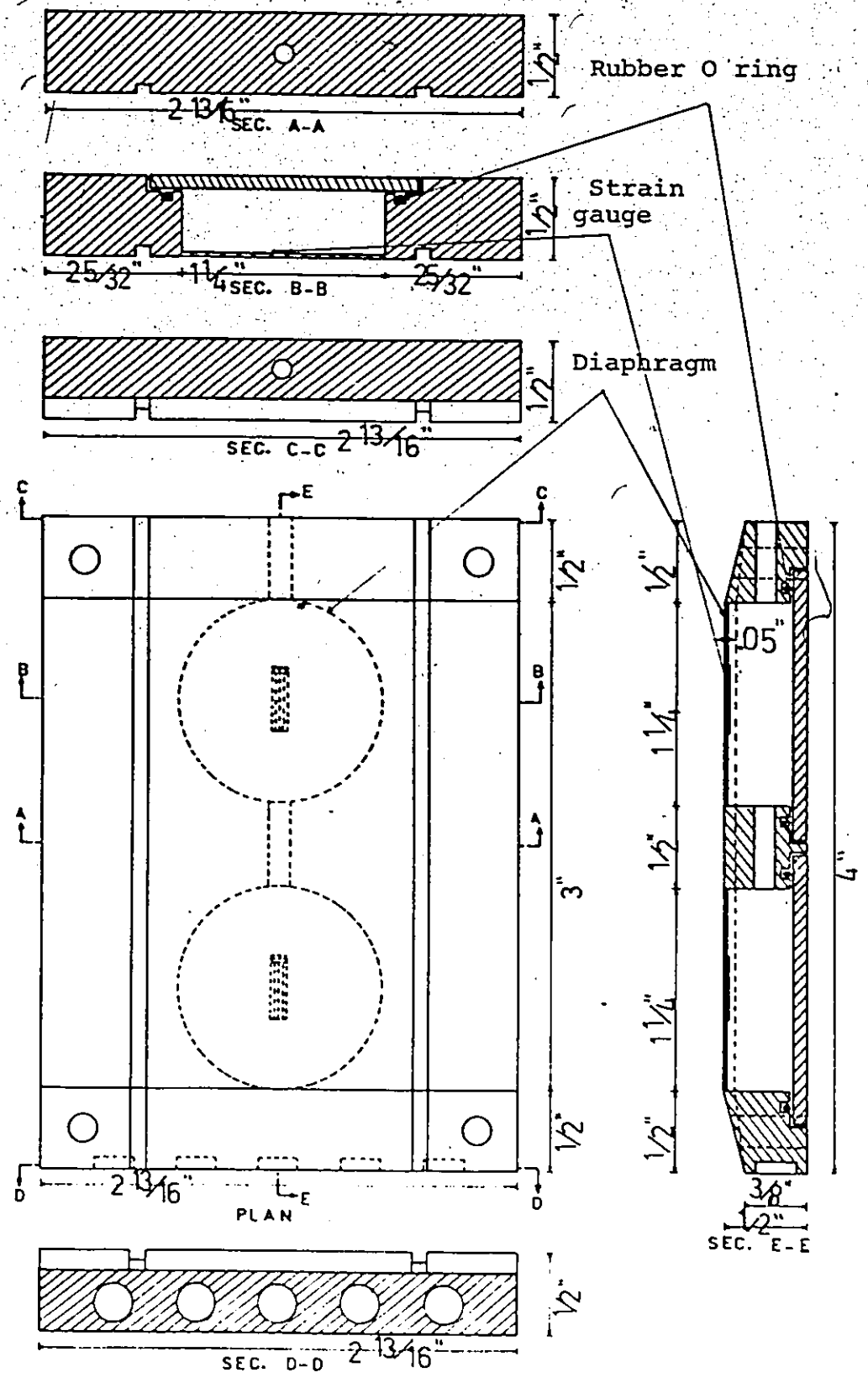


Figure (4.4) Instrumented Side Plate.

$$\sigma_{max} = \frac{3}{2}(1 + \mu)\frac{p}{\pi h^2}\left(\text{Log}_e \frac{a}{c} + \frac{c^2}{4a^2}\right) \qquad (4.1)$$

where $p = \pi a^2 q$, $c = a$ in this case as shown in Figure (4.5),

q is the assumed intensity of the uniform pressure,

a is the radius, a = .625 in.

$\sigma_{max}$ is the maximum allowable tensile stress for stainless steel where $\sigma_{max}$ = 50,000 psi,

$\mu$ is Poisson's ratio.

For stainless steel materials $\mu = 0.3$, and for the assumption of a maximum q = 100 psi, $p = 3.14 \times .625^2 \times 100 =$ 122.7 lbs. (maximum operating levels were about 0.5 p, i.e., safety factor = 2).

From Equation (4.1) $h^2$ is equal to

$$h^2 = \frac{3}{2}(1 + \mu)\frac{p}{\pi\sigma_{max}}\left(2.3\ \text{Log}_{10} \frac{a}{c} + \frac{c^2}{4a^2}\right.$$

$h^2 = .00038$ in.$^2$

$h = .0194$ in.

From these calculations we can conclude that the thickness of the stainless steel diaphragms should be .0194 in. and this thickness is within the elastic range.

4.3.2 Strain Gauge Calibrations

Strain gauges were installed on the internal surface of the circular diaphragms. Calibration curves were obtained by stressing the diaphragms in the triaxial cell without a soil sample in place. Voltage readings were recorded on a digital recorder as shown in Tables (4.1) and (4.2) in the

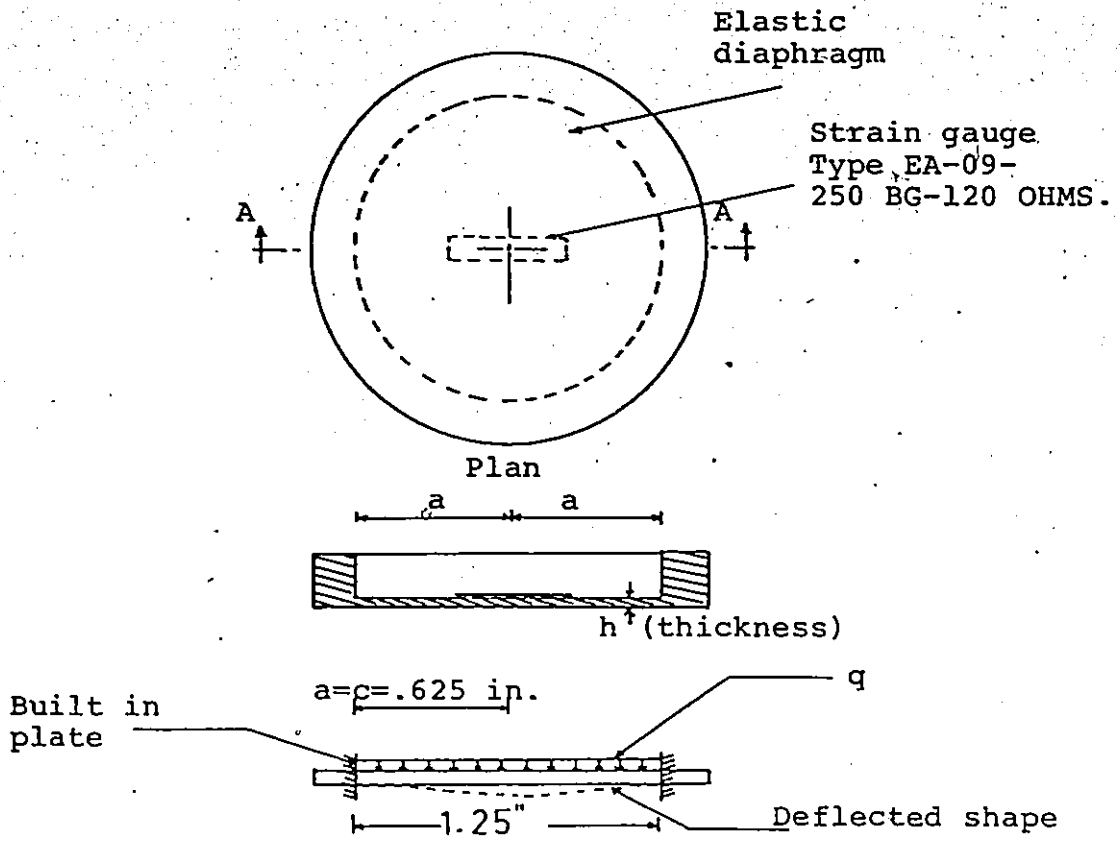


Figure (4:5) Elastic Diaphragm.

Appendix.

To reduce electrical difficulties, air pressure was used in the triaxial cell, instead of water, to provide the confining pressure ($\sigma_3$). Leakage to the diaphragms was prevented by using rubber O-rings, and heavy glue was applied externally to the clearance between the diaphragm's covers and the side plate to provide extra precautions against any possible leakage.

The results obtained using air pressure showed very stable scanning on the digital voltmeter. Figure (4.6) shows the calibration curves of four strain gauges for increasing and decreasing cell pressure. These curves were obtained after two cycles of preloading. A zero shift was noticed clearly on one of the strain gauges as shown in Figure (4.6). This zero shift was about -20% on the decreasing pressure curve. Readings from this gauge were not used in the calculations of the experimental results. In each calibration run the strain gauges were balanced and set at zero before testing commenced.

Also, it was noted that the decreasing pressure calibration curves differ from the increasing pressure calibration curves. This is believed to be due to the possible leakage and/or the hysteresis of the strain gauges. Figure (4.6) shows a difference in slope, which may mean that there are different sensitivies to the strain gauges, which may be due to the thickness of the diaphragms and the placement of the strain gauges.

Finally, these calibration curves permit the measurement

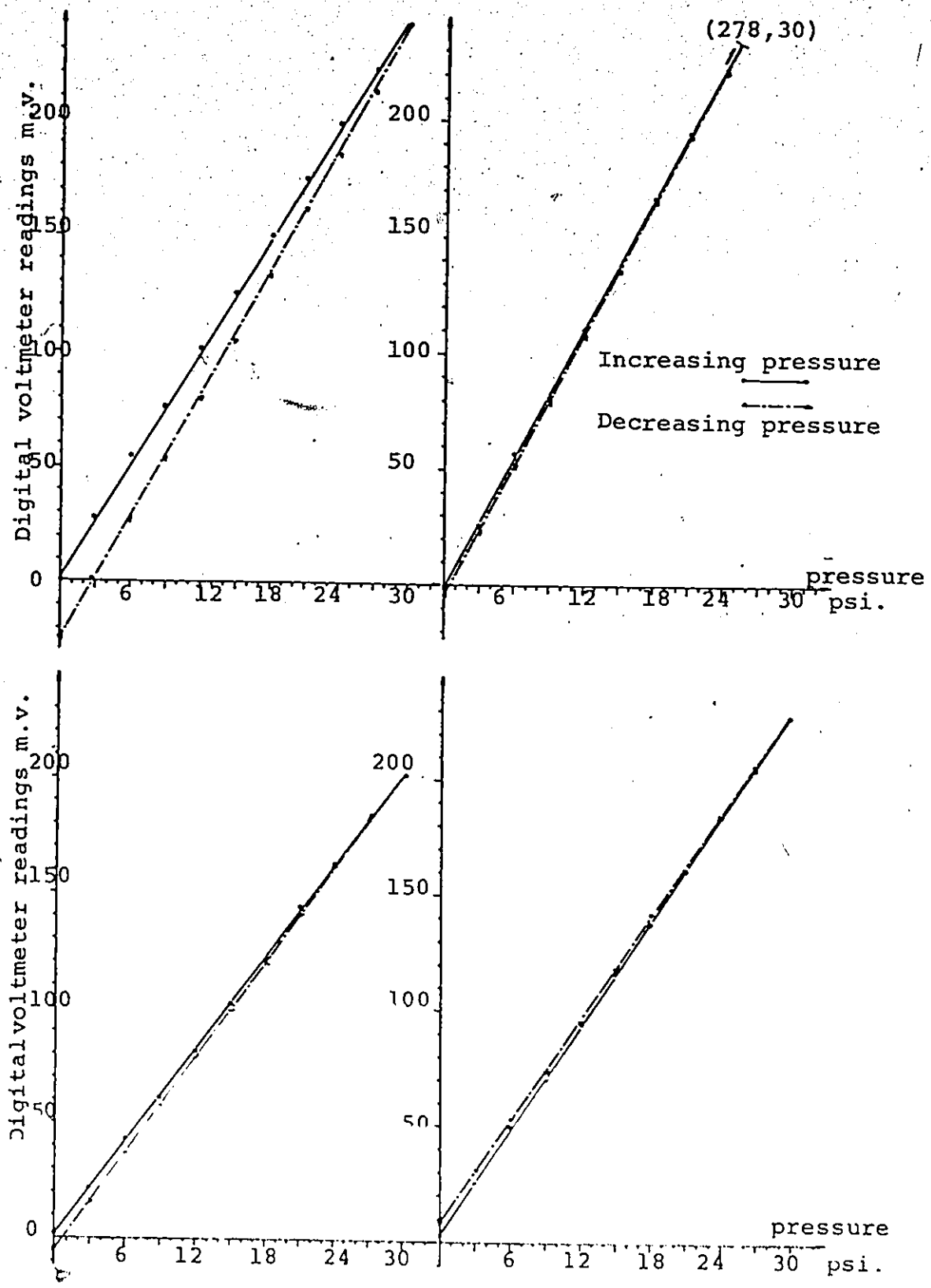


Figure (4.6) Strain Gauges Calibration Curves

of the intermediate principal stress ($\sigma_2$) during the shear test.

## 4.4 Plane Strain Base

The plane strain brass base was made in order to support the side plates through two sets of 1/4" dia. springs. These springs were located and directed vertically through circular slots on the top of the brass base. The use of the springs was to reduce the friction between the side plates and the sample during the shear test. The base was tightly mounted on the top of the triaxial base as shown in Figure (4.7). Also, Figure (4.7) shows the location of the rubber membrane which was sealed by a set of four screws to prevent leakage. The O-ring was located in a special slot. The cell pressure was applied through a longitudinal slot inside the base.

## 4.5 Bearing Plate and Top Platen

The bearing plate and the top platen were made from Lucite. Figure (4.8) shows the location of the rubber membrane which was sealed by a set of four screws to prevent leakage. The O-ring was located in a slot on the top of the top platen.

The bearing plate and the top platen were connected together by a set of screws as shown in Figure (4.8). The vertical load was transferred uniformly to the sample by a regular loading ram.

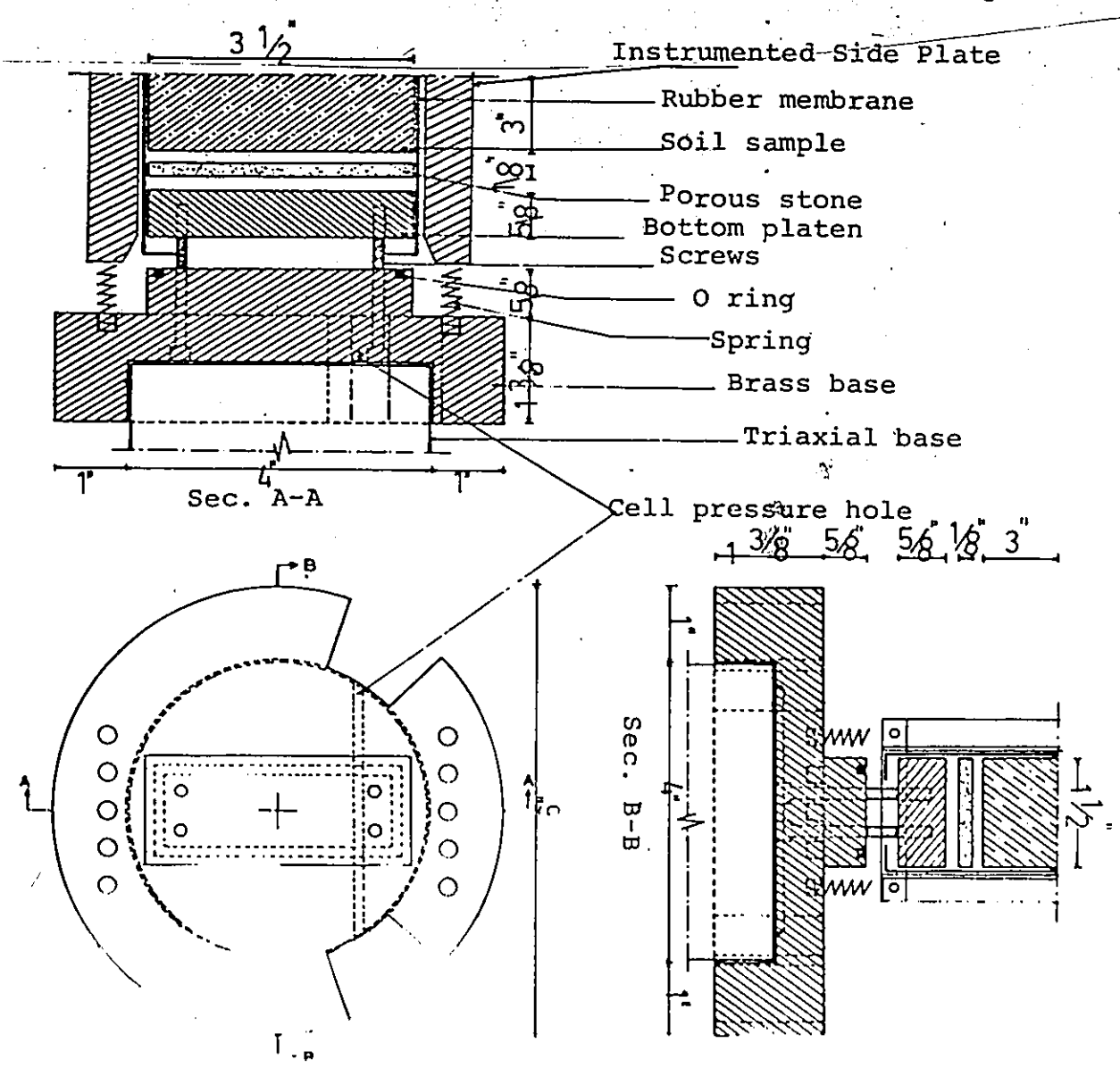


Figure (4.7) Plane Strain Base.

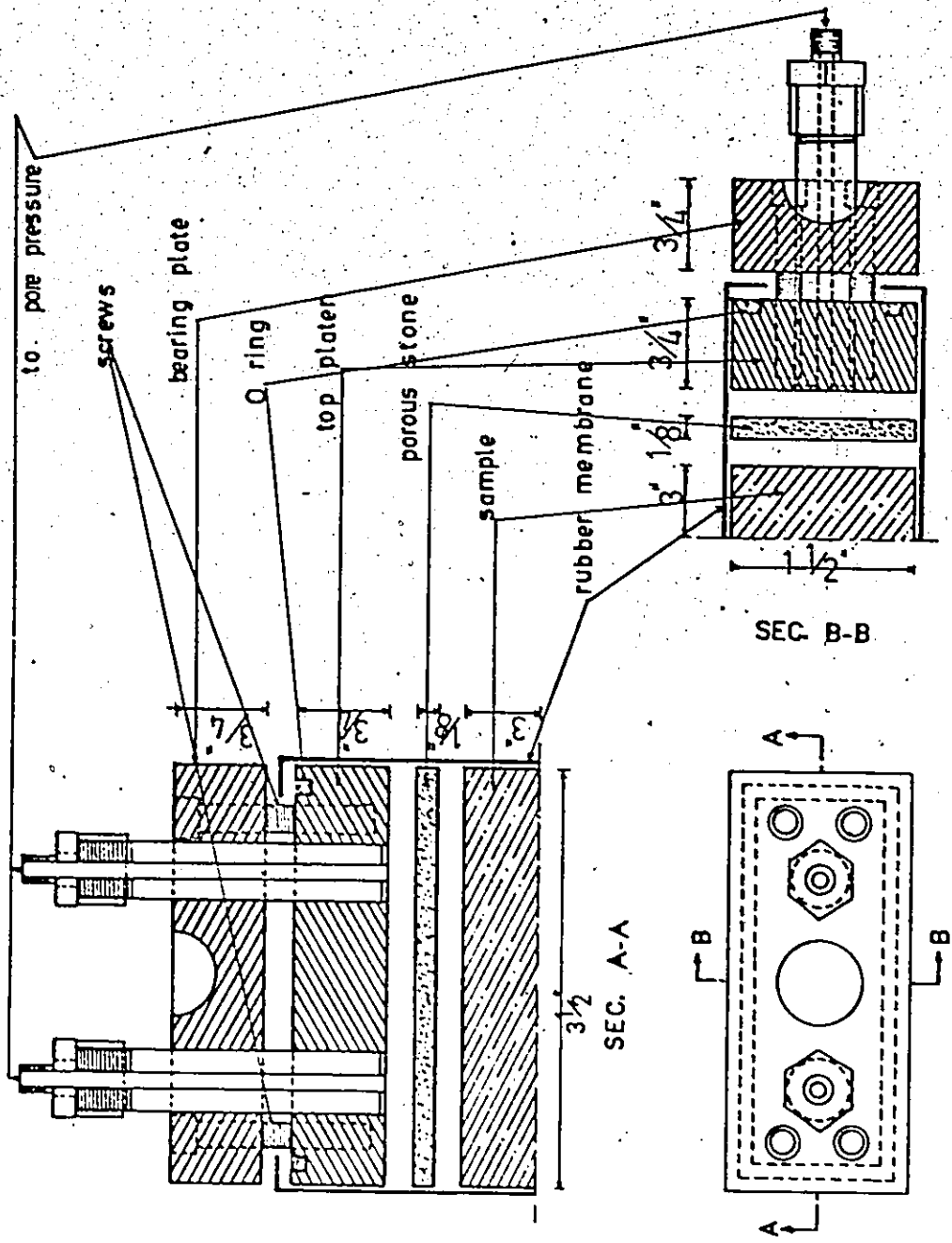


Figure (4.8) BEARING PLATE AND TOP PLATEN.

## 4.6 Rubber Membrane

Rectangular rubber membranes were made in the Geotechnical Laboratories in order to enclose the plane strain specimen during the shear test, the porous stones (1/8 in. thick), top perspex platen, and the bottom brass platen.

The procedure of making these rectangular rubber membranes was taken from Campanella and Vaid (1973).

The procedure was commenced as follows:

1. Cleaning the impervious aluminum mold. This mold was made 6 in. high, 1.5 in. wide and 3.5 in. long. The edges were rounded to small radii and a steel rod was threaded into the mold for suspension purposes.
2. The clean mold was dipped into a coagulant solution (calcium nitrate tetrahydrate and pure alcohol). This solution causes a film to build up through coagulation of the latex (National Rubber Latex) particles in the intermediate contact areas. The concentration of the coagulant was 20% by weight.
3. The mold with dried coagulant film was immersed very slowly with a steady motion into the rubber latex for a minimum period of one minute, then the mold was withdrawn with the same motion.
4. The latex film was allowed to dry in the air at room temperature for at least 12 hours, then followed by drying it in an oven at 60°C for 24 hours. The mold was allowed to cool before stripping and dusting with talc powder.

All rectangular rubber membranes were uniform and were

tested against water leakage before they were used in the shear tests. The measured average thickness was about .020 in.

# CHAPTER 5

# TESTING PROCEDURE AND RESULTS

Shear tests were carried out on dry sand under triaxial compression and plane strain conditions in order to compare the shear parameters in both methods and to study the effect of the intermediate principal stress on the shear strength. The state of density of the sand used in all tests was in the range of dense to very dense. The following sections are limited to the description of the materials used, testing procedure, and experimental results.

## 5.1 Material Description

Grain size distribution tests were carried out on the tested sand in order to classify the size of the particles. Figure (5.1) shows two grain size curves which were obtained by using the mechanical method. The tested sand can be classified as coarse to medium uniform sand with a very small portion of fine grains. Microscope observations showed that the particles possess fairly round shapes. Sieve analysis tests showed that sand particles have in the main two sizes: particles retained on #30 sieve, and particles retained on #50 sieve. The coefficient of uniformity ($C_u$) for both tests

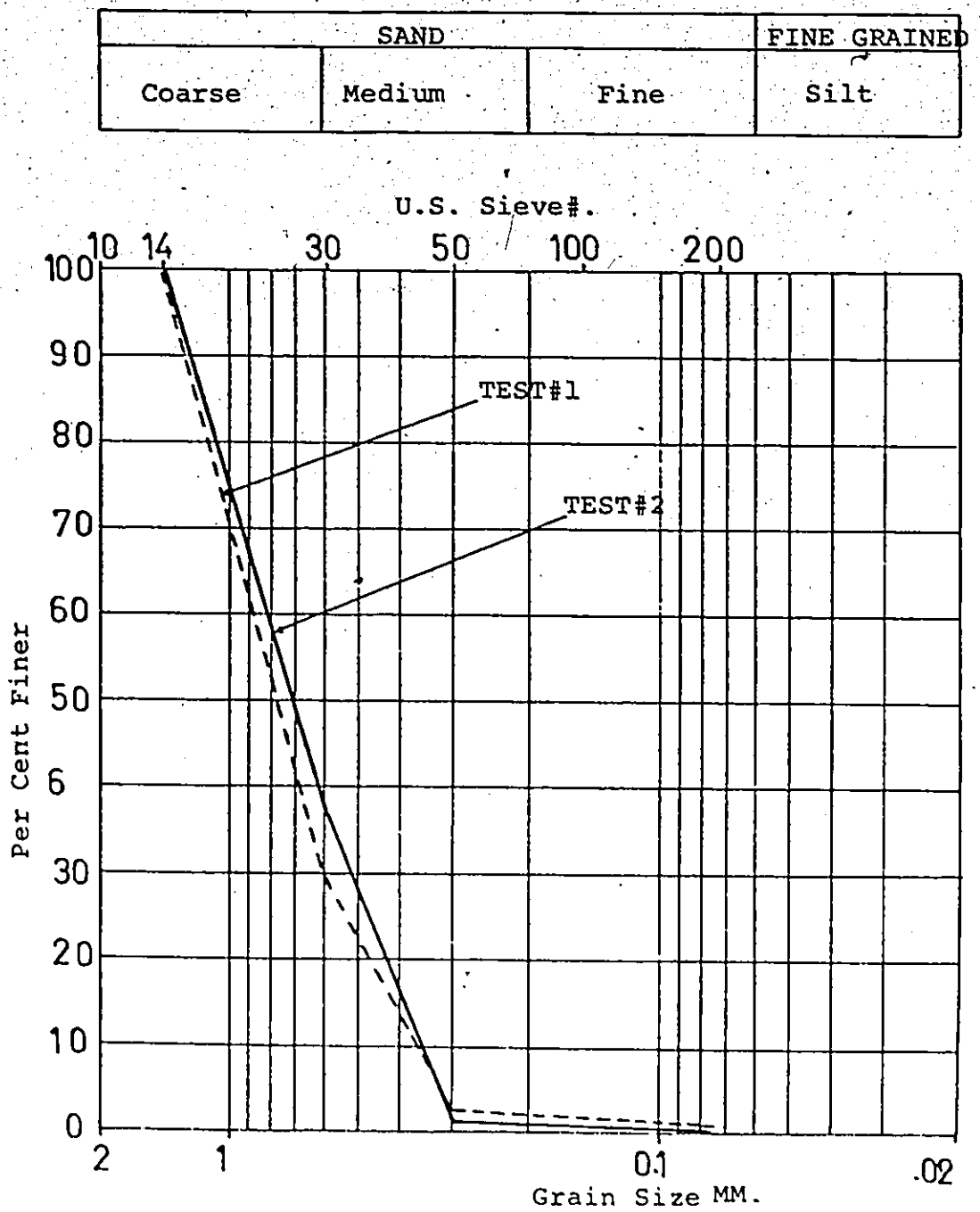


Figure (5.1) Grain Size Distribution Curves.

is equal to 2.3. This supports the fact that the tested sand is uniform. The dominant colour is white without any organic material.

## 5.2 Densities Determination

The densest and loosest values of the dry unit weight of the tested sand were determined by using the conventional standard compaction mold (Bowles, 1970).

### 5.2.1 Determination of $\gamma_{dmax}$ (Densest State)

Five trials were carried out to obtain the maximum dry unit weight by placing the dry sand in the 1/30 cu. ft. compaction mold in five layers, confining the layers and rapping the side of the mold 25 times with the rubber mallet. The soil used was mixed with the remaining soil before the next trial.

The largest weight of sand was equal to 3.672 lb.

$$\therefore \quad \gamma_{dmax} = \frac{3.672}{.0333} = 110.264 \text{ lb/ft}^3, \quad e_{min} = 0.50$$

### 5.2.2 Determination of $\gamma_{dmin}$ (Loosest State)

The sand was carefully poured through a large funnel into the mold, distributing the discharge in a circular motion over the mold. Extra care was taken not to vibrate the mold.

The smallest weight of sand in the five trials was equal to 3.229 lb.

$$\therefore \quad \gamma_{dmin} = \frac{3.229}{.0333} = 96.970 \text{ lb/ft}^3, \quad e_{max} = 0.71$$

## 5.3 Triaxial Compression Tests and Procedure

A series of three tests was carried out on dry sand with three different cell pressures: 5 psi, 10 psi and 15 psi. For each test the sample was subjected to a constant pressure $\sigma_3'$ during the application of the axial deviator stress ($\sigma_1' - \sigma_3'$); the deviator stress was gradually increased at an almost constant strain rate up to failure. The rate of strain for all triaxial tests was .0024 inches per minute. Air pressure was used to provide confining pressure. The average diameter of the samples was equal to 1.37 in. and the average height was equal to 2.85 in.

The testing procedure and the specimen preparation followed for the cohesionless material was similar to the conventional way which is described in many soil mechanic textbooks (Bishop and Henkel,1962).

Triaxial compression test measurements and results were recorded as shown in Tables (5.1), (5.2) and (5.3) of the Appendix.

## 5.4 Plane Strain Tests and Procedure

In conventional geotechnical triaxial tests the intermediate principal stress ($\sigma_2'$) is equal to the minor principal stress ($\sigma_3'$) and is considered to have no effect on the shear strength of the soils. This assumption is not applicable for many plane strain problems. In this case a testing program was carried out on dry sand with three different cell pressures: 5 psi, 10 psi and 15 psi under plane strain conditions where $\sigma_2' > \sigma_3'$.

The plane strain sample was subjected to three different principal stresses: $\sigma_1'$, $\sigma_2'$ and $\sigma_3'$ where $\sigma_1' > \sigma_2' > \sigma_3'$. In all tests the minor principal stress ($\sigma_3'$) was held constant and the axial stress $\sigma_1'$ increased to failure. The intermediate principal stress ($\sigma_2'$) started at a value equal to $\sigma_3'$ at the beginning of the test and increased to a failure value.

The testing procedure and assembly were carried out according to the following steps:

1. A plane strain soil specimen was enclosed by a rectangular rubber membrane. The membrane was attached to the plane strain base and the top platen as described in the previous chapter.
2. Side plates were assembled with two thin aluminum plates to establish a former around the membrane. This enables the formation of the granular sample in the desired rectangular cross section. The aluminum plates were located vertically through vertical slots on the side plates. All samples were vibrated by rapping the sides of the former in order to get a dense sample.
3. Dry sand was weighed and poured inside the membrane in a similar way as in the triaxial test.
4. A vacuum pressure was applied to the sample and then the aluminum plates (which act as a former) were removed.
5. The predetermined cell pressure was applied.
6. The vertical loads were applied as in the triaxial test.
7. Friction was reduced between the piston and cell top

plate between the sample and the side plates by adding silicon grease.

8. The intermediate principal stress ($\sigma_2$) was measured by the strain gauge technique as voltage units and was subsequently converted to pressure units by using the calibration curves of the strain gauges. The deviator stresses and the vertical displacements were measured in the usual way common in triaxial testing. The rate of strain for all plane strain tests was equal to 0.0024 inches per minute.

Plane strain test data were recorded in Tables (5.4), (5.5) and (5.6) of the Appendix.

# CHAPTER 6

# EXPERIMENTAL RESULTS AND DISCUSSION

## 6.1 Failure Criteria

In order to compare the experimental results in triaxial and plane strain conditions, a full understanding of various failure criteria is necessary. Failure criteria determine the physical constants or parameters of strength for a sample at the point of failure. This may mean the rupture of the material or the beginning of loss of shearing resistance (Newmark, 1960). Failure criteria describe the relationships between shear strength parameters and the results can be applied to engineering problems. Soil parameters are expressed in terms of effective stresses.

One of the principal types of failure criteria is the Mohr-Coulomb theory which, at the point of failure, describes the relationships between effective prinicpal stresses, effective shearing resistance angle, and effective cohesion. All these parameters are used for stress-strain analyses and for both axially symmetric and plane strain conditions. The Mohr-Coulomb failure criterion neglects the influence of the intermediate principal stress ($\sigma_2$). The mathematical formula for the Mohr-Coulomb failure criterion is given by,

$$(\hat{\sigma}_1 - \hat{\sigma}_3) = \sin \hat{\phi} \ (\hat{\sigma}_1 + \hat{\sigma}_3) + 2 \hat{C} \cos \hat{\phi} \qquad (6.1)a$$

The Mohr-Coulomb equation for cohesionless soils is given by:

$$(\hat{\sigma}_1 - \hat{\sigma}_3) = \sin \hat{\phi} \ (\hat{\sigma}_1 + \hat{\sigma}_3) \qquad (6.1)b$$

There are more elaborate failure criteria, such as the octahedral shear theory, based on the extended Tresca and the extended Von Mises theories. These theories imply that the intermediate principal stress, $\hat{\sigma}_2$, does affect the principal stresses at failure. The mathematical formulae for such criteria are given below in terms of the effective stresses $\hat{\sigma}_1$, $\hat{\sigma}_2$, $\hat{\sigma}_3$ which are the major, intermediate and minor effective principal stresses respectively (Bishop, 1666):

Extended Tresca

$$(\hat{\sigma}_1 - \hat{\sigma}_3) = \alpha\left(\frac{\hat{\sigma}_1 + \hat{\sigma}_2 + \hat{\sigma}_3}{3}\right) \qquad (6.2)$$

Extended Von Mises

$$(\hat{\sigma}_1-\hat{\sigma}_2)^2 + (\hat{\sigma}_2-\hat{\sigma}_3)^2 + (\hat{\sigma}_3-\hat{\sigma}_1)^2 = 2\alpha^2\left(\frac{\hat{\sigma}_1 \ \hat{\sigma}_2 \ \hat{\sigma}_3}{3}\right)^2 \qquad (6.3)$$

where $\alpha$ is a failure constant.

In triaxial compression tests, where $\hat{\sigma}_2 = \hat{\sigma}_3$, Equations (6.2) and (6.3) can be reduced to:

$$(\hat{\sigma}_1 - \hat{\sigma}_3) = \alpha\left(\frac{\hat{\sigma}_1 + 2\hat{\sigma}_3}{3}\right) \qquad (6.4)$$

The intermediate principal stress at failure is related to the major principal stress and the minor principal stress by the following parameter:

$$b = \frac{(\hat{\sigma}_2 - \hat{\sigma}_3)}{(\hat{\sigma}_1 - \hat{\sigma}_2)} \qquad (6.5)$$

For triaxial tests the value of b is equal to zero as $\hat{\sigma}_2 = \hat{\sigma}_3$, for plane strain tests where $\hat{\sigma}_3 < \hat{\sigma}_2 < \hat{\sigma}_1$, $0 < b < 1$. (Bishop, 1966 and Green, 1971)

The Mohr-Coulomb equation becomes:

$$\frac{(\hat{\sigma}_I - \hat{\sigma}_3)}{(\hat{\sigma}_1 + \hat{\sigma}_3)} = \sin \hat{\phi} \qquad (6.6)$$

The extended Tresca becomes:

$$\frac{(\hat{\sigma}_1 - \hat{\sigma}_3)}{(\hat{\sigma}_1 + \hat{\sigma}_3)} = \frac{1}{\frac{1}{3} + \frac{2}{\alpha} - \frac{2}{3}b} \qquad (6.7)$$

The extended Von Mises becomes:

$$\frac{(\hat{\sigma}_1 - \hat{\sigma}_3)}{(\hat{\sigma}_1 + \hat{\sigma}_3)} = \frac{1}{\frac{1}{3} + \frac{2}{\alpha}\sqrt{1 - b + b^2} - \frac{2}{3}b} \qquad (6.8)$$

## 6.2 Evaluation of Various Failure Criteria

The Mohr-Coulomb criterion states that (Harr, 1966):

$$\hat{\sigma}_{max} - \hat{\sigma}_{min} = f(\hat{\sigma}_{max} + \hat{\sigma}_{min}) \qquad (6.9)$$

The extended Tresca criterion states that failure occurs when the maximum shear stress ($\tau_{max}$) equals a critical constant value such as (Harr, 1966):

$$\tau_{max} = \frac{\hat{\sigma}_{max} - \hat{\sigma}_{min}}{2} = b = \text{const} \qquad (6.10)$$

The extended Von Mises criterion states that failure surface is given by (Harr, 1966):

$$(\hat{\sigma}_1 - \hat{\sigma}_2)^2 + (\hat{\sigma}_2 - \hat{\sigma}_3)^2 + (\hat{\sigma}_3 - \hat{\sigma}_1)^2 = 2k^2 = \text{const} \qquad (6.11)a$$

and by using the formula

$$\tau_{oct} = \frac{1}{3}\sqrt{(\hat{\sigma}_1 - \hat{\sigma}_2)^2 + (\hat{\sigma}_1 - \hat{\sigma}_2)^2 + (\hat{\sigma}_3 - \hat{\sigma}_1)^2}$$

Equation (6.11)a can be written as (Harr, 1966):

$$(\tau_{oct})_{max} = \frac{\sqrt{2}}{3}k = \text{const} \qquad (6.11)b$$

These criteria can be represented in $(\hat{\sigma}_1, \hat{\sigma}_2, \hat{\sigma}_3)$ a stress space (Roscoe, Schofield and Thurairajah, 1963), and

form pyramid-shaped surfaces which have apices at the origin and are symmetrical about the stress-space diagonal (hydrostatic axis) where, $\hat{\sigma}_1 = \hat{\sigma}_2 = \hat{\sigma}_3$. Right sections of these pyramids which are formed by planes perpendicular to the space diagonal are:

1) Irregular hexagons (equal sides but not parallel) for Mohr-Coulomb criterion.
2) Regular hexagons for extended Tresca criterion.
3) Circles for extended Von Mises criterion.

These sections are shown in Figure (6.1).

Of the three failure criteria Mohr-Coulomb neglects the influence of the intermediate principal stress on the strength. In the triaxial compression test where $\hat{\sigma}_2 = \hat{\sigma}_3$, failure occurs at point A as shown in Figure (6.1); in the case of triaxial extension tests where $\hat{\sigma}_2 = \hat{\sigma}_1$, Equations (6.2) and (6.3) can be reduced to $\hat{\sigma}_1 - \hat{\sigma}_3 = \alpha(\frac{2\hat{\sigma}_1 + \hat{\sigma}_3}{3})$, and failure occurs at point C for Mohr-Coulomb criterion and at point B for both extended Tresca and extended Von Mises criteria in Figure (6.1). Plane strain tests, where $\hat{\sigma}_2$ has an intermediate value, mean that the Mohr Coulomb criterion is not applicable. However, plane strain data is not sufficient to determine a definite conclusion as to the relevant criteria that can be applied for sands (Roscoe, Schofield, and Thurairjah, 1963).

Results obtained by Roscoe (1971) from triaxial compression and extension tests showed that the Mohr Coulomb criterion underestimates the strength at failure while the extended Von Mises overestimates it.

Equation (6.9) shows that the Mohr Coulomb criterion

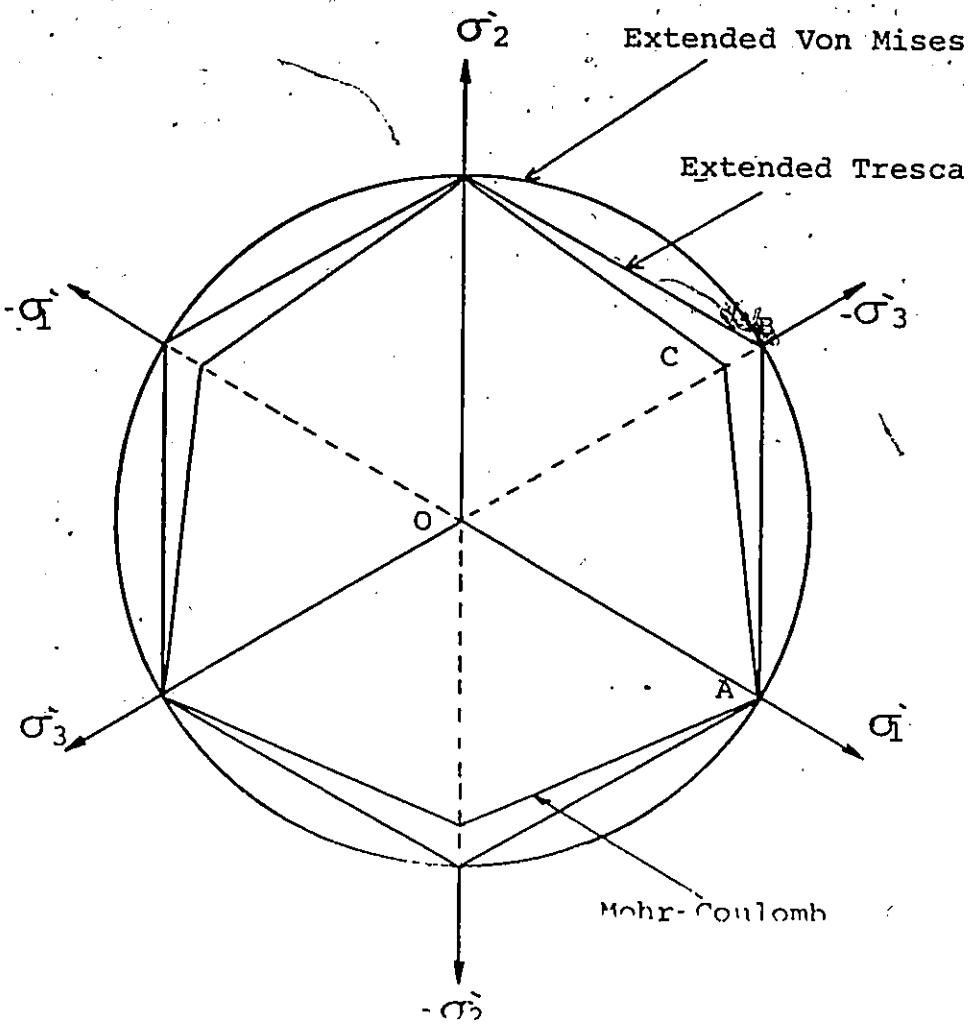


Figure (6.1) Representation of Failure Criteria Showing Right Sections of the Failure Surfaces.

neglects the influence of $\hat{\sigma}_2$ and generates a single failure surface (irregular hexagon); this failure locus is on the deviatoric plane where $\hat{\sigma}_1 + \hat{\sigma}_2 + \hat{\sigma}_3 = 0$ (Harr, 1966). Equation (6.10) shows that the extended Tresca failure criterion is independent of the intermediate principal stress and produces a regular hexagon as a failure surface. Equation (6.11) shows that the extended Von Mises failure criterion is dependent on the intermediate principal stress and generates a circle as a failure surface, as shown in Figure (6.1).

Bishop (1966) stated that the extended Tresca and the extended Von Mises criteria are unrealistic as generalizations; however, they give a better agreement than the Mohr-Coulomb criterion over a very limited range of b values ($b = (\hat{\sigma}_2 - \hat{\sigma}_3)/(\hat{\sigma}_1 - \hat{\sigma}_3)$). This statement was based on the measured value of $\hat{\phi}_f$ ($\hat{\phi}_f = 39°$) of dense Ham river sand in triaxial compression which was compared with predicted values by the three failure criteria. Furthermore, Bishop (1966) stated that with the knowledge of $\hat{\sigma}_2$, the values of $\hat{\phi}_f$ (defined by Equation (6.6)) can be compared with those predicted by various failure criteria (Equations (6.7) and (6.8)) as b varies between 0 and 1. A further comparison for loose Brasted sand (Cornforth, 1964) showed that results fit the Mohr-Coulomb failure criterion, whereas the extended Tresca and the extended Von Mises criteria predict values which differ completely from the observed values. For dense sand, Mohr-Coulomb gives again better agreement. In triaxial and plane strain compression tests, only the extended Tresca is in better agreement. Finally, all experimental evidences

strongly support the Mohr-Coulomb failure criterion (Bishop, 1966).

Plane strain compression results obtained by the author showed that the values of the angle of shearing resistance at failure which were determined by both the Mohr-Coulomb and the extended Tresca criteria are identical. This supports the argument that the extended Tresca criterion is independent of the value of the intermediate principal stress, that is, this conclusion is valid for values of b which vary between .080 and .241 (values of b obtained from our plane strain tests #I and #II). Values of $\phi_f$ which were determined by the extended Von Mises criterion (Equation (6.8)) are very high and unrealistic if compared with values obtained by the Mohr-Coulomb or extended Tresca criteria ($\phi_f = 63°$ for plane strain test #I, $\phi_f = 64°$ for plane strain test #II).

The previous evaluations of different failure criteria together with the experimental results suggest the use of the Mohr-Coulomb criterion as a yield condition for sand. The following paragraph gives details about the Mohr-Coulomb theory of failure and the use of this criterion in the determination of shear strength parameters at failure and the stress-strain analysis.

## 6.3 Mohr-Coulomb Theory

The Mohr-Coulomb theory has been widely used as a strength criterion. The failure state in this theory is denoted by sliding of grains which occurs as a result of shear stresses. The shear strength is the maximum value of shear

stress at the failure point (slip plane), where the failure point is the upper limit of the strain equilibrium.

The Mohr-Coulomb theory describes the relationship between the angle of shearing resistance at failure ($\phi'_f$) and the principal stresses ($\sigma'_1$ and $\sigma'_3$) at failure (Equation (6.1)b or (6.6)).

Figure (6.2) shows the Mohr-Coulomb theory which neglects the influence of the intermediate principal stress ($\sigma'_2$); that is, sin $\phi'_f$ is given in both triaxial and plane strain conditions by the ratio $(\sigma'_1 - \sigma'_3)/(\sigma'_1 + \sigma'_3)$ at the point of failure.

Equation (6.1)b describes the envelope of failure for circles with radii $1/2\ (\sigma'_1 - \sigma'_3)$ and centers at $1/2\ (\sigma'_1 + \sigma'_3)$. The shear strength ($\tau_f$) on the failure plane is given by:

$$\tau_f = \sigma'_f \tan \phi'_f \quad \text{Coulomb's equation} \qquad (6.12)$$

The relationship between the principal stresses at failure ($\sigma'_1$ and $\sigma'_3$) in terms of $\phi'_f$ is equal to:

$$\sigma'_1 = \sigma'_3 \tan^2(45 + \phi'_f/2) \qquad (6.13)$$

where $(45 + \phi'_f/2)$ is the angle of the slip plane at failure to the plane of the major principal stress ($\sigma'_1$) as shown in Figure (6.2).

The cohesionless materials slide at failure without volume change (Rowe, 1962), just as in the case of two blocks of material in a simple friction test. This is because at the point of failure, the interlocking between soil grains has decreased to the point where continuous shear deformation can proceed without further volume change (Lambe and Whitman, 1969). However, volume change does occur before the failure state is reached. Lambe and Whitman (1969) stated that dense

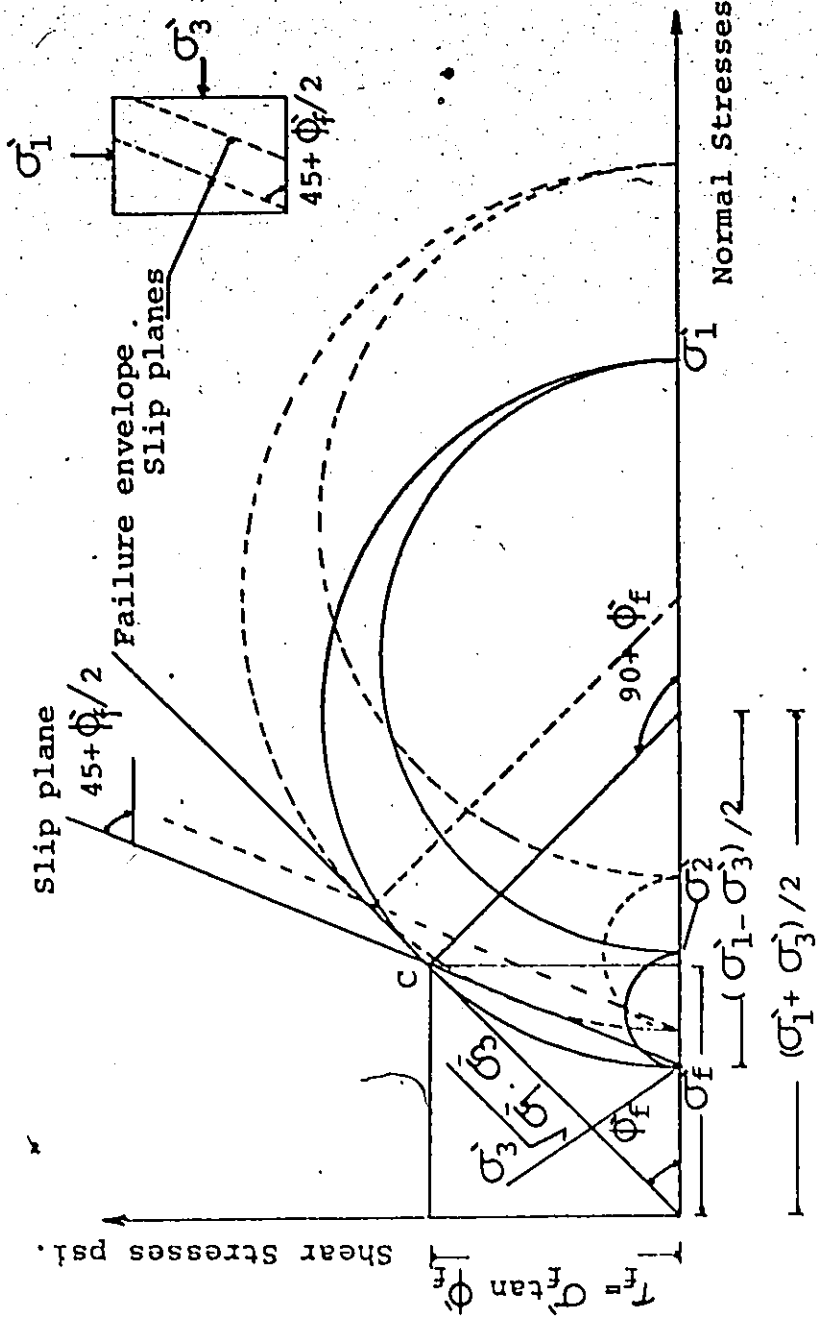


Figure (6.2) Mohr-Coulomb Failure Criterion for Cohesionless Materials.

sand tends to expand, while loose sand first tends to contract (decrease in volume), then expands again, and finally ends up at almost the initial volume. Slip planes (failure surfaces) are influenced by volumetric changes in the samples and the states of density; that is, at the point of failure dense samples tend to produce very limited failure zones and loose samples tend to produce fairly large failure zones. At these failure zones, the material becomes weaker and the applied stress ratio decreases (Rowe, 1962).

## 6.4 Experimental Values of $\phi_f$ in Both Triaxial and Plane Strain Conditions

The angle of shearing resistance at failure, $\phi_f$, for dry sand was determined according to the Mohr-Coulomb failure criterion in both triaxial and plane strain tests.

Figure (6.3) (triaxial sample #1) shows that $\phi_f = 47\frac{1}{2}°$, at call pressure $\sigma_3 = 5$ psi (.35 kg/cm$^2$). The density of the triaxial sample is 108.46 lb/ft$^3$ (1.74 g/cm$^3$), the void ratio (e) is .524 and the relative density of the sample $R_d = 87.9\%$ which is considered to be in a very dense state.

Figure (6.4) (triaxial sample #2) shows that $\phi_f = 47°$ at cell pressure $\sigma_3 = 10$ psi (.7 kg/cm$^2$). The density of the triaxial sample was 106.98 lb/ft$^3$(1.71 g/cm$^3$), the void ratio (e) is .538 and the relative density of the sample $R_d = 77.5\%$ which is also considered to be in a dense state.

Figure (6.5) (triaxial test #3) shows that $\phi_f = 47°$ at cell pressure $\sigma_3 = 15$ psi (1.05 kg/cm$^2$). The density of the triaxial sample is 106.69 lb/ft$^3$(1.71 g/cm$^3$), the void ratio (e) is .548 and the relative density of the sample $R_d = 75.5\%$

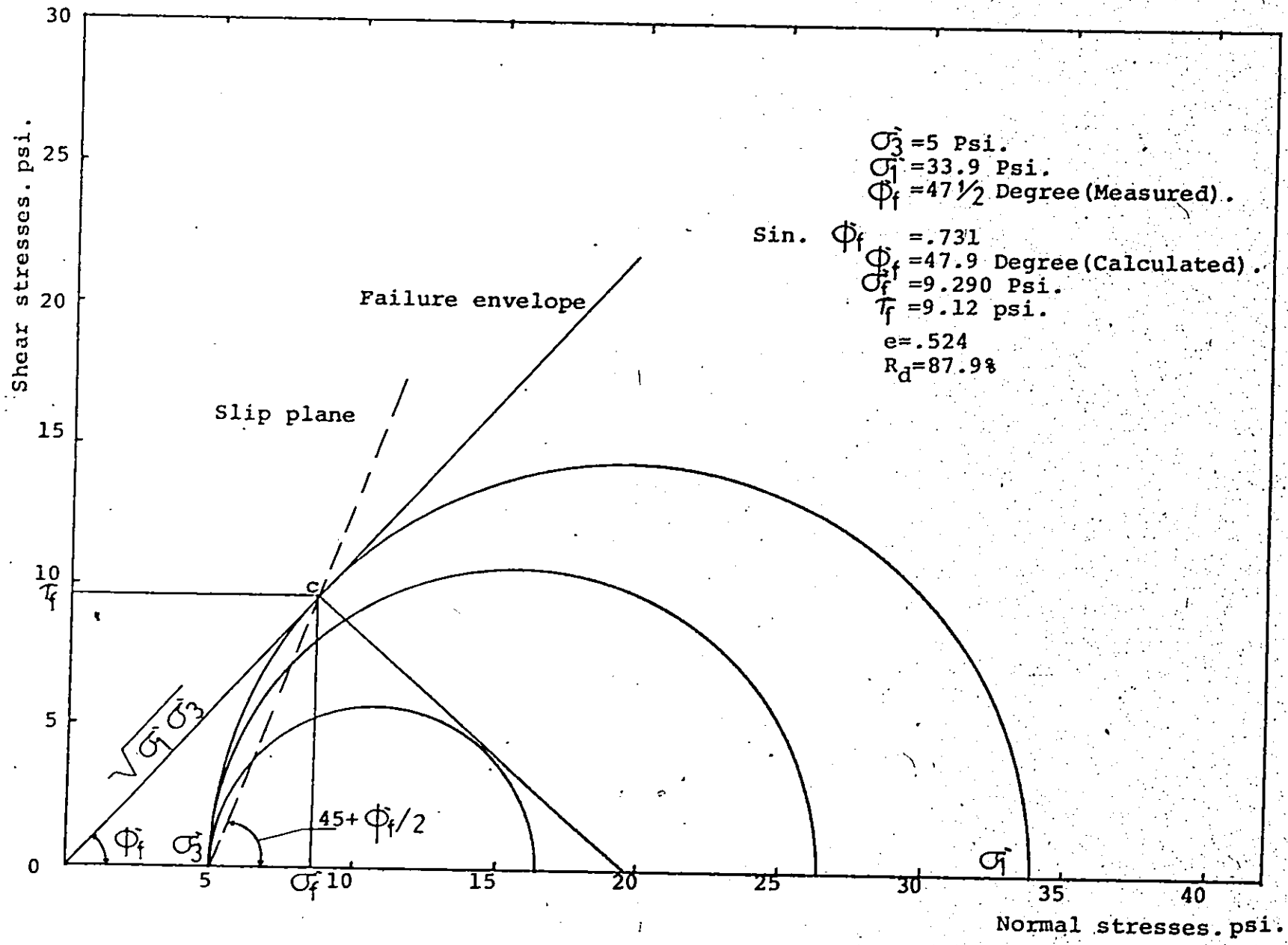


Figure (6.3) Mohr Circle representation, Triaxial Test #1.

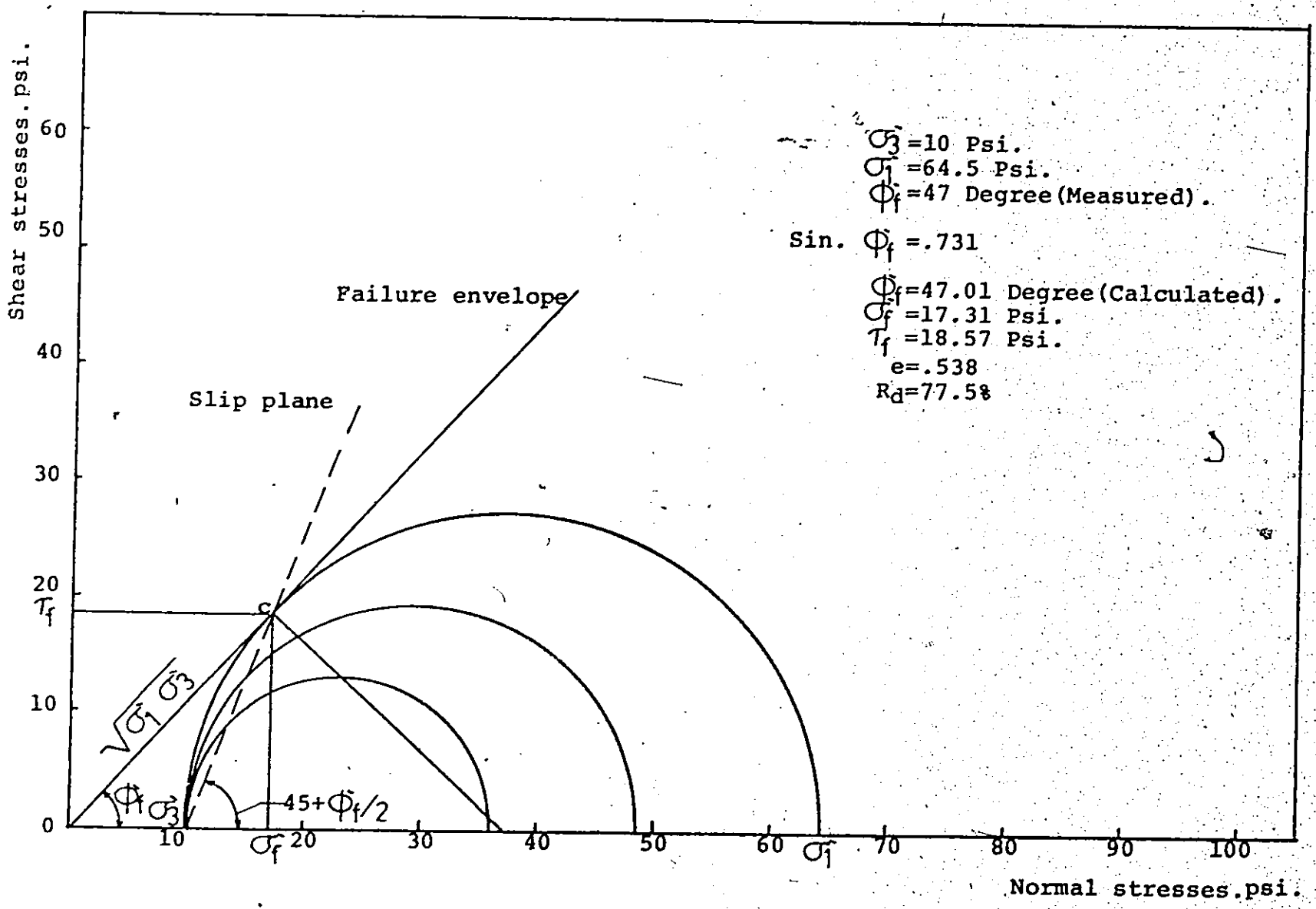


Figure (6.4) Mohr Circle Representation, Triaxial Test #2.

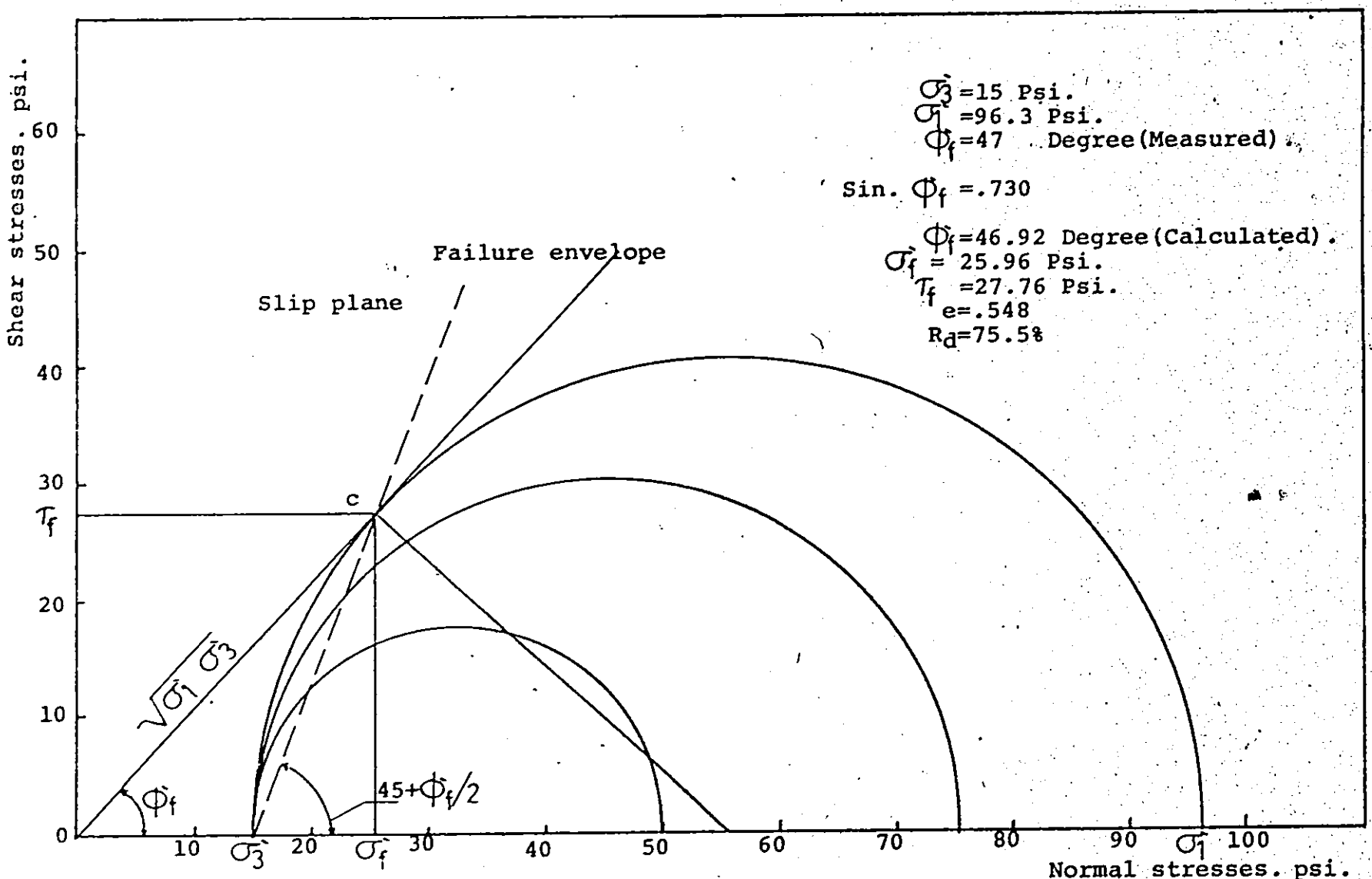


Figure (6.5) Mohr Circle Representation, Triaxial Test #3.

which is again considered to be in a dense state.

Figures (6.3), (6.4) and (6.5) show that the average value of the angle of shearing resistance $\phi_f$ is about 47° for triaxial tests #1, #2 and #3 at cell pressures: 5 psi, 10 psi and 15 psi, this value is fairly high for dense uniform sand. Comments and corrections will be presented later. Figures (6.3), (6.4) and (6.5) show the values of shear strengths and normal stresses at failure. These values will be compared with plane strain values.

The values of the angle of shearing resistance $\phi_f$, at failure in plane strain compression tests are being determined by using the limiting values of $\sigma_1$ and $\sigma_3$ in the Mohr-Coulomb theory, as shown in Figure (6.2).

Figure (6.6) (plane strain test #I) shows that $\phi_f = 55°$, at cell pressure $\sigma_3 = 5$ psi. The density of the plane strain sample is 108.36 lb/ft$^3$ (1.74 g/cm$^3$), the void ratio (e) is .530 and the relative density of the sample $R_d = 87.2\%$ which is considered to be in a very dense state.

Figure (6.7) (plane strain test #II) shows that $\phi_f = 56°$ at cell pressure $\sigma_3 = 10$ psi. The density of the plane strain sample is 109.65 lb/ft$^3$ (1.76 g/cm$^3$), the void ratio (e) is .523 and the relative density of the sample $R_d = 95.9\%$ which is considered to be in a very dense state.

Figure (6.8) (plane strain sample #III) shows that $\phi_f = 55°$ at cell pressure $\sigma_3 = 15$ psi. This value of $\phi_f$ is not the failure value and was measured by considering the highest value of $\sigma_1$; it could be assumed that $\phi_f$ at failure for this test is 57°. The density of the plane strain sample

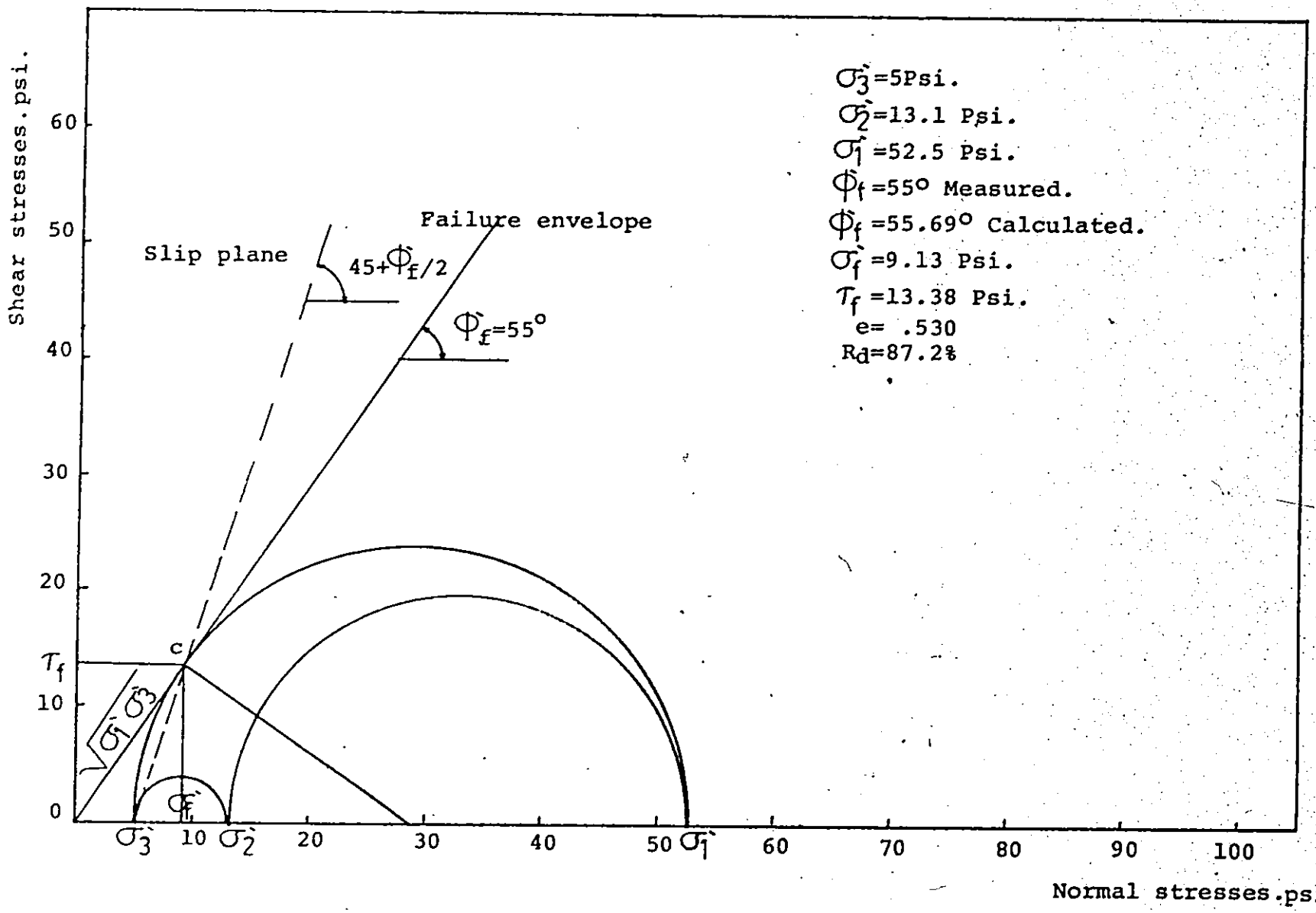


Figure (6.6)Mohr Circle Representation, Plane Strain Test #I.

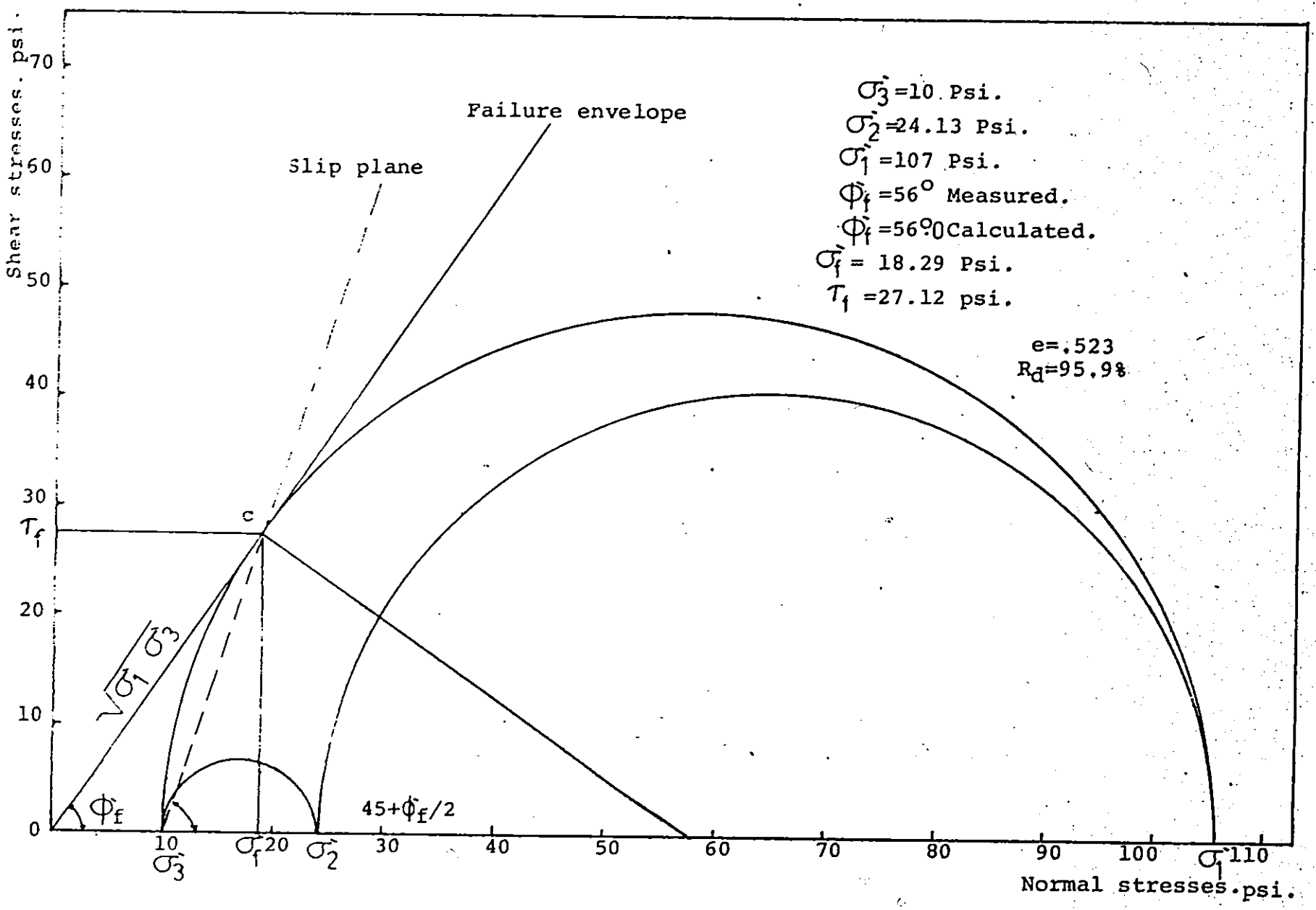


Figure (6.7) Mohr Circle Representation, Plane Strain Test #II.

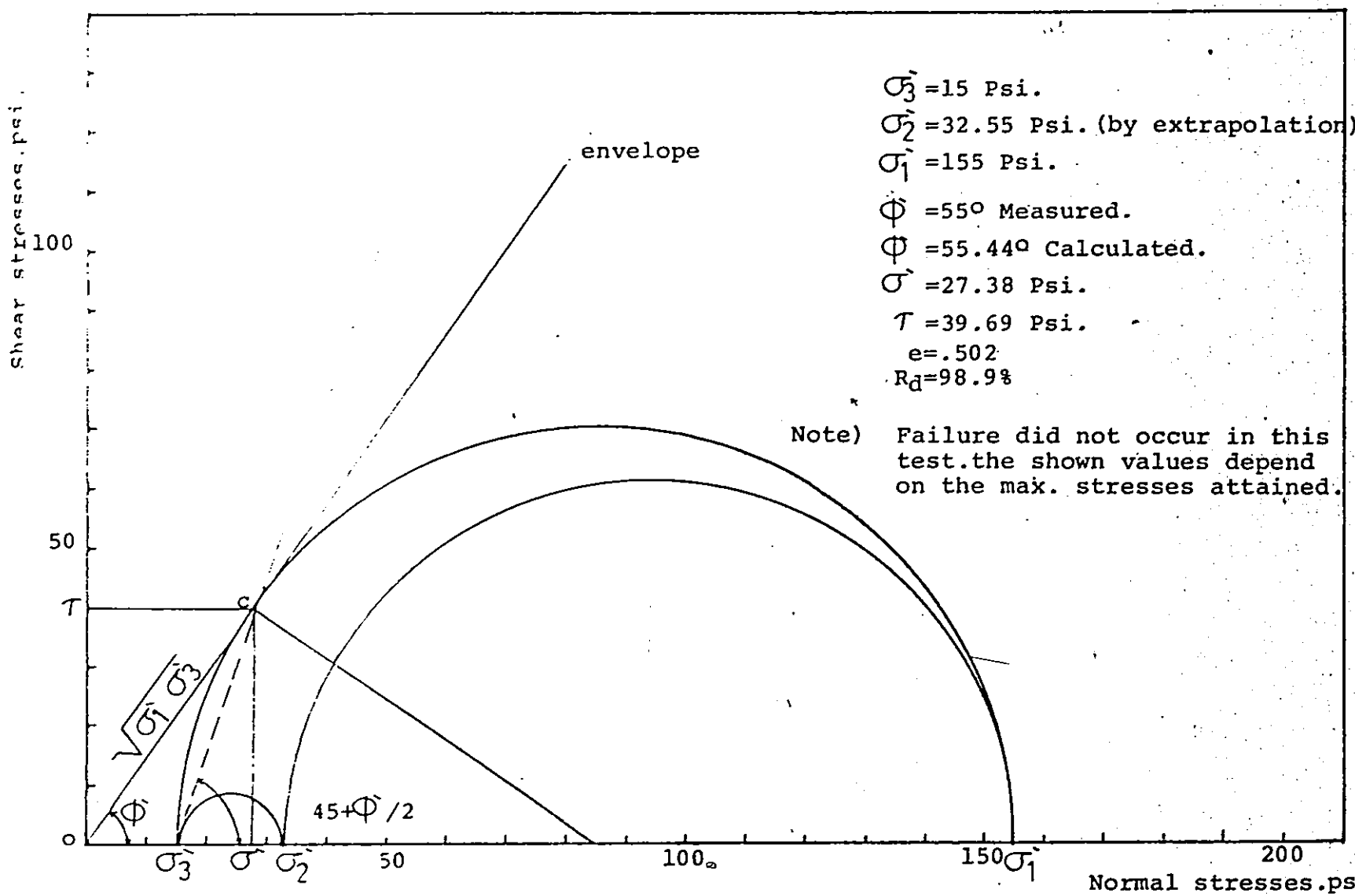


Figure (6.8)Mohr Circle Representation, Plane Strain Test #III.

is 110.10 lb/ft$^3$ (1.76 g/cm$^3$), the void ratio (e) is .502 and the relative density of the sample $R_d$ = 98.9% which is considered to be in a very dense state.

Figures (6.6), (6.7) and (6.8) show that the average value of the angle of shearing resistance $\phi_f$ is about 56° for plane strain tests #I, #II and #III at cell pressures: 5 psi, 10 psi and 15 psi. Comments and corrections will be presented regarding this high value of $\phi_f$. Figures (6.6), (6.7) and (6.8) give the values of shear strengths and normal stresses at failure for plane strain tests.

### 6.4.1 Sources of Error in Triaxial and Plane Strain Tests Which Affect the Values of $\phi_f$

A) Friction Forces: - There are two types of friction forces which can be developed: (1) friction forces developed in triaxial and plane strain tests when the loading ram passes through a bush in the top of the triaxial cell, and (2) friction forces developed in plane strain tests between plane strain samples and the rigid side plates. As friction forces have not been measured and in spite of the lubrication process, it was felt that a correction factor should be applied to all tests in order to obtain more accurate results. Bishop and Henkel (1962) stated that for most commercial and simple testing cells a correction to the axial load can be made. Studies concluded that friction forces would lie between 1% and 3% of the axial load for most of the loading range. For the particular case where a specimen failed on a single plane (in the case of dense samples) and where large lateral forces may be developed, tests indicate that the error increases with axial strain. For instance, at 5%

axial strain the error would be about 1% of the axial load. Thus, using the Bishop and Henkel (1962) a 5% correction factor should be applied to the axial load to reduce the magnitude of the axial load in both triaxial and plane strain tests.

Friction forces between the plane strain samples and the rigid plates were reduced by lubrication. No experimental evidence on the correction of such friction forces is available.

B) Rubber Membrane Correction: - A rubber membrane correction should be applied in both triaxial and plane strain tests. The computations of such a factor were obtained by Henkel and Gilbert (1952) as follows:

$$\sigma_t = \pi \frac{D \cdot M \cdot \varepsilon}{A_t} \qquad (6.14)$$

where $\sigma_t$ is the correction factor for triaxial tests,

$A_t$ is the initial cross section of the triaxial sample,

D = diameter of the triaxial sample,

M is the extension modulus of the membrane,

$\varepsilon$ is the axial strain.

The correction factor ($\sigma_p$) for plane strain tests was modified by Cornforth (1961) as follows:

$$\sigma_p = 2 \frac{(b+t) M \cdot \varepsilon}{A_p} \qquad (6.15)$$

where $A_p$ is the initial cross section of the plane strain sample and 2(b+t) is the initial perimeter of the plane strain sample.

Tests showed that the extension modulus of the membrane is M = 175.T and where T is the thickness of the membrane in

inches, M is given in lb/in.

In triaxial tests, $A_t$ = 1.45 in$^2$, D = 1.36 in., T = .02 in. (two membranes were used for each test). By considering that failure occurred at 5% axial strain, a correction factor $\sigma_t$ = .52 psi should be applied to the values of $\sigma_1$.

In plane strain tests, $A_p$ = 4.89 in$^2$, 2(b+t) = 9.74 in., T = .03 in. (plane strain membranes are thick at the edges). By considering that failure occurred at 3% axial strain, a correction factor $\sigma_p$ = .31 psi should be applied to the values of $\sigma_1$.

The membrane corrections in both triaxial and plane strain tests are small and can be neglected.

C) Energy Corrections due to Confining Pressure and Void Ratio: - Many investigators suggested the use of energy corrections when analyzing the shear strength in cohesionless soils. The energy corrections should be applied when volume changes occur (Poorooshasb and Roscoe, 1961). As mentioned before, dense samples tend to expand during shear while loose samples tend to contract. Lambe and Whitman (1969) stated that the volume changes are a function of the confining pressure, that is, the volume change is greater in the case of the test with a small confining pressure than in the case of the test with large confining pressure. Volume increase is less in the case of the test with larger confining pressure.

In this research very small confining pressures were used (e.g., 5 psi, 10 psi and 15 psi). Those pressures produced an additional volume change (increase). In this case, the energy put into soil structure by external loads is ex-

pended (1) to expand the soil against the confining pressure, and (2) to overcome the frictional resistance between particles. Poorooshasb and Rosooe (1961) stated that the energy correction for cohesionless dense soils which must be applied to the observed deviator stress $(\sigma'_1 - \sigma'_3)$ in order to obtain the corrected deviator stress is given by:

$$-\sigma'_3 \, (\delta v/\delta \varepsilon_1) \qquad (6.16)$$

where $\delta v = \delta(\Delta V)/V_o$

$V_o$ is the original volume of the sample. When $V_o$ increases in volume to V due to $\sigma'_1$ and $\sigma'_3$, $\Delta V = V - V_o$

The energy considerations are very important and could significantly affect the value of $\phi'_f$ at failure. Unfortunately, volume changes were not measured during shear tests in both triaxial and plane strain conditions, so that the energy correction factor is an assumption and cannot be estimated accurately.

Consequently, corrections should be applied to the measured strengths in all triaxial and plane strain tests to account for the effect of friction forces, rubber membrane stiffness, energy considerations and other factors such as the non-uniformity of deformation at failure. These corrections could significantly reduce the values of $\phi'_f$ at failure. The reduction could be between 5° and 10°. Keeping in mind that these corrections are just estimates as experimental measurements were not available. Thus, all values of $\phi'_f$ are subjected to a correction factor in both triaxial and plane strain tests.

### 6.4.2 Comparison of the Experimental Values of $\phi_f$ for Both Methods

The shear strength characteristics of sand are a very sensitive function of the void ratio of the sand. That is, the angle of shearing resistance of sand varies largely with the void ratio (state of density). Lambe and Whitman (1969) stated that the denser the sand, the greater the interlocking, hence the greater the shear resistance and the higher the angle of shearing resistance. The effect of the void ratio on $\phi_f$ can be explained by the concept of interlocking, which states that the energy that is put into a soil by external loads is expended to overcome the frictional forces between particles. Thus, the denser the sand, the greater the energy which is needed to shear the soil (higher value of $\phi_f$).

In order to compare the values of $\phi_f$ at failure in both triaxial and plane strain tests, samples should possess the same initial void ratio. The concept of extrapolation could be used to compare the values of $\phi_f$, as the testing program did not cover a wide range of densities because all tests were performed on samples which had a dense to very dense state of density.

In Figure (6.9), the calculated values of $\phi_f$ at failure in both triaxial and plane strain tests were plotted against the initial porosities ($n = \frac{e}{1 + e}$) of the samples.

Figure (6.9) shows that $\phi_f$ is a function of the initial porosity in both triaxial and plane strain tests, that is, $\phi_f$ increases as the initial porosity decreases. The values of $\phi_f$ are higher in plane strain tests than in triaxial tests.

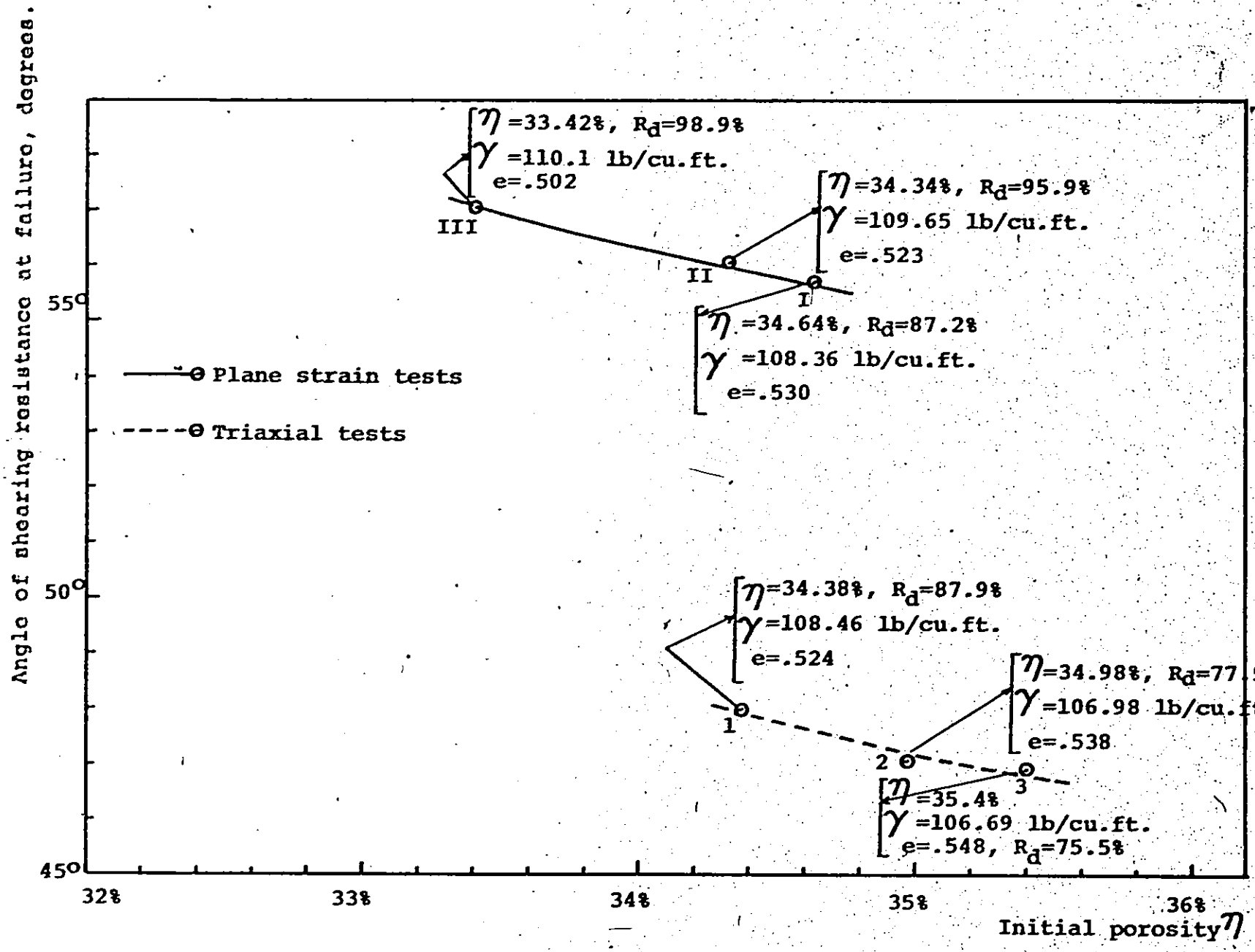


Figure (6.9) $\phi_f$ Values Versus Initial Porosity in Plane Strain and Triaxial Tests.

Figure (6.9) shows that plane strain test #II has almost the same density as triaxial test #1; the angle of shearing resistance in plane strain test #II is 56° while this angle in triaxial test #1 is ∿ 48°. The angle of shearing resistance $\phi_f$ in plane strain test #II is higher by 8° than triaxial test #1. The values of $\phi_f$ in both methods are rather high and are subjected to a correction factor as mentioned before.

The work done by Cornforth (1964) on Brasted sand in both plane strain and triaxial compression tests showed a tendency to higher values of the angle of shearing resistance ($\phi_f$) in dense samples than in loose samples. The angle of shearing resistance of sand varies largely with density, that is, the denser the sample the higher the value of $\phi_f$ and the looser the sample the lower the value of $\phi_f$. Cornforth's results indicated that the value of $\phi_f$ in plane strain tests was higher by 4° than triaxial tests at the densest state, and higher by 1/2° at the loosest state.

In Figure (6.10), the values of shear strength ($\tau_f$) at failure in both plane strain and triaxial tests were plotted versus cell pressures. Figure (6.10) shows that plane strain tests give higher values of $\tau_f$ than triaxial tests. This conclusion is valid if the compared samples possessed the same state of density.

## 6.5 Stress-Strain Analysis in Both Triaxial and Plane Strain Tests

In order to study the behaviour of the soil structure under applied stresses and to compare the failure character-

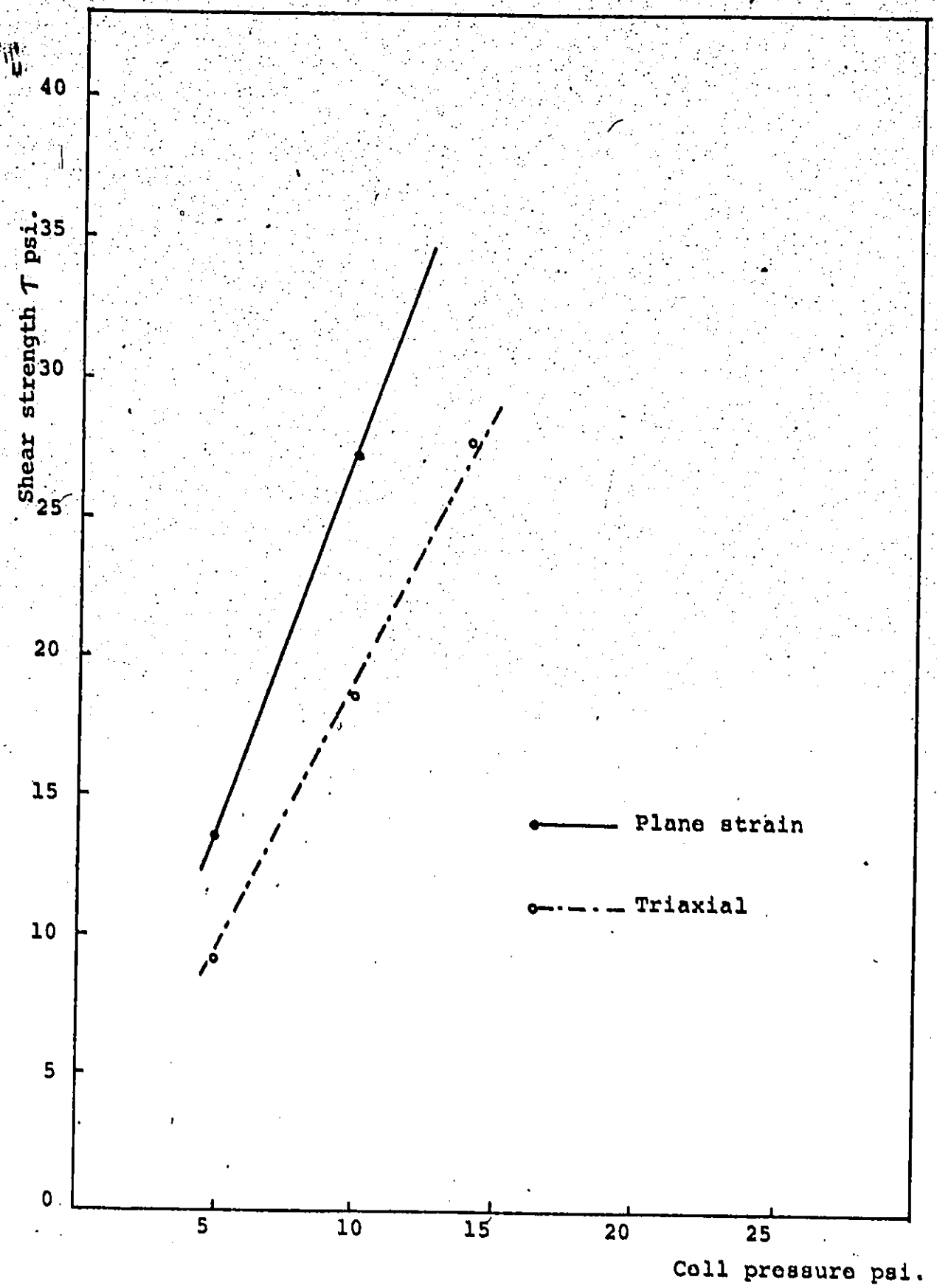


Figure (6.10) Shear Strength Values.

istics between triaxial and plane strain tests, a stress-strain analysis and a study of the effect of the intermediate principal stress ($\sigma_2$) on the stress-strain behaviour of cohesionless soils are essential.

Finn and Mittal (1963) indicated that if the soil is tested with the intermediate principal stress, $\sigma_2$, greater than the minor principal stress, $\sigma_3$:

A) The stress-strain curve in plane strain test will be similar in shape to the curve obtained by the conventional triaxial compression test.

B) The maximum stress ratio ($\sigma_1/\sigma_3$) is greater in a plane strain test than in a triaxial test.

C) The maximum stress ratio in a plane strain test will occur at a smaller axial strain than in a triaxial test as shown in the representative Figure (6.11).

In Figures (6.12), (6.13) and (6.14) stresses were plotted against axial strains which were based on Tables (5.1), (5.2) and (5.3) respectively in the Appendix. An area correction factor $(1 - \varepsilon)$ was applied to all triaxial tests data, the adjusted area ($A'$) is equal to: $A' = A_o/(1 - \varepsilon)$, where $A_o$ is the original area of the sample and $\varepsilon$ is the axial strain.

Figures (6.12), (6.13) and (6.14) show typical stress-strain curves for triaxial tests #1, #2 and #3, at cell pressures 5 psi, 10 psi and 15 psi, respectively. The maximum values of $\sigma_1$, for triaxial tests #1, #2 and #3 are 33.90 psi, 64.50 psi and 96.30 psi, respectively, at axial strains equal to 5.0%, 4.5% and 5.0%. The cell pressure was held constant

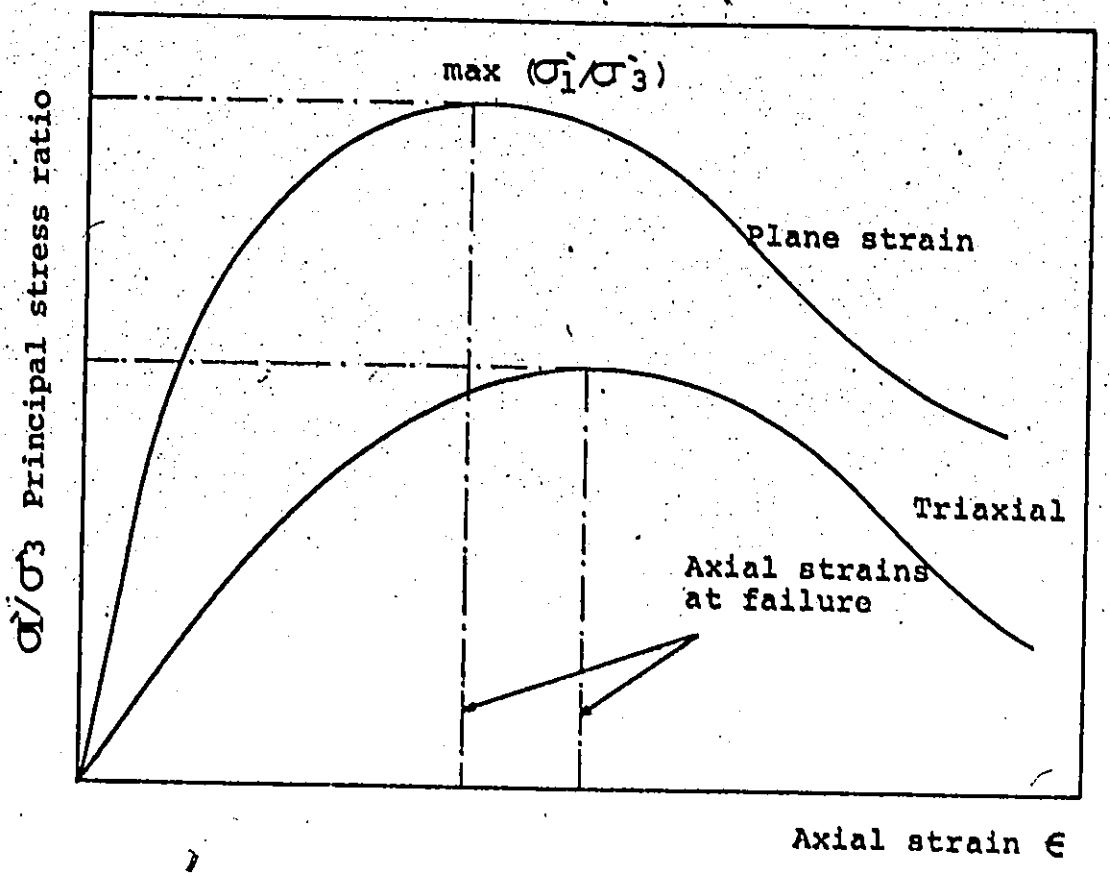


Figure (6.11) Representative Stress-Strain Curves for Plane Strain and Triaxial Tests.

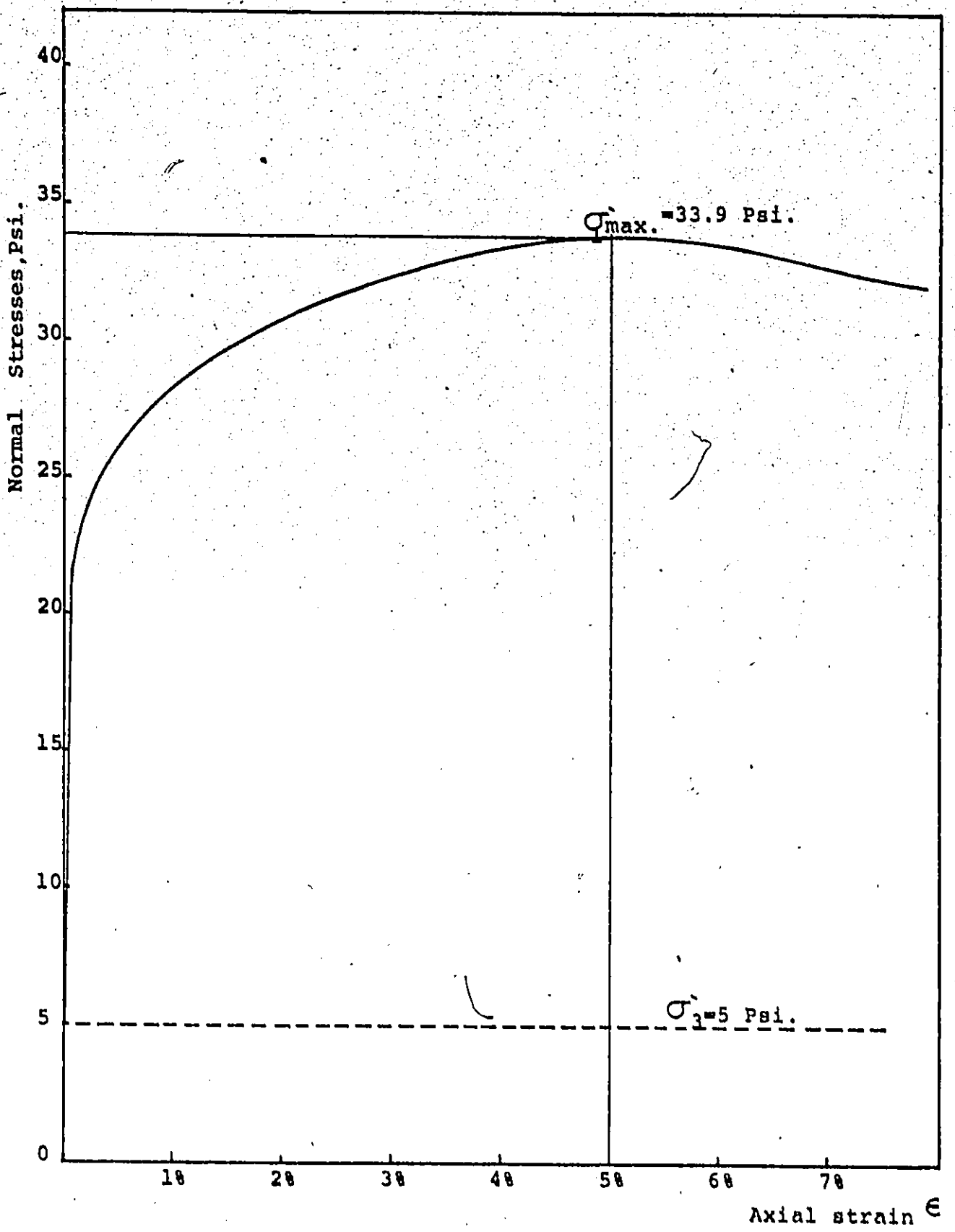


Figure (6.12) Stress-Strain Curves, Triaxial Test #1.

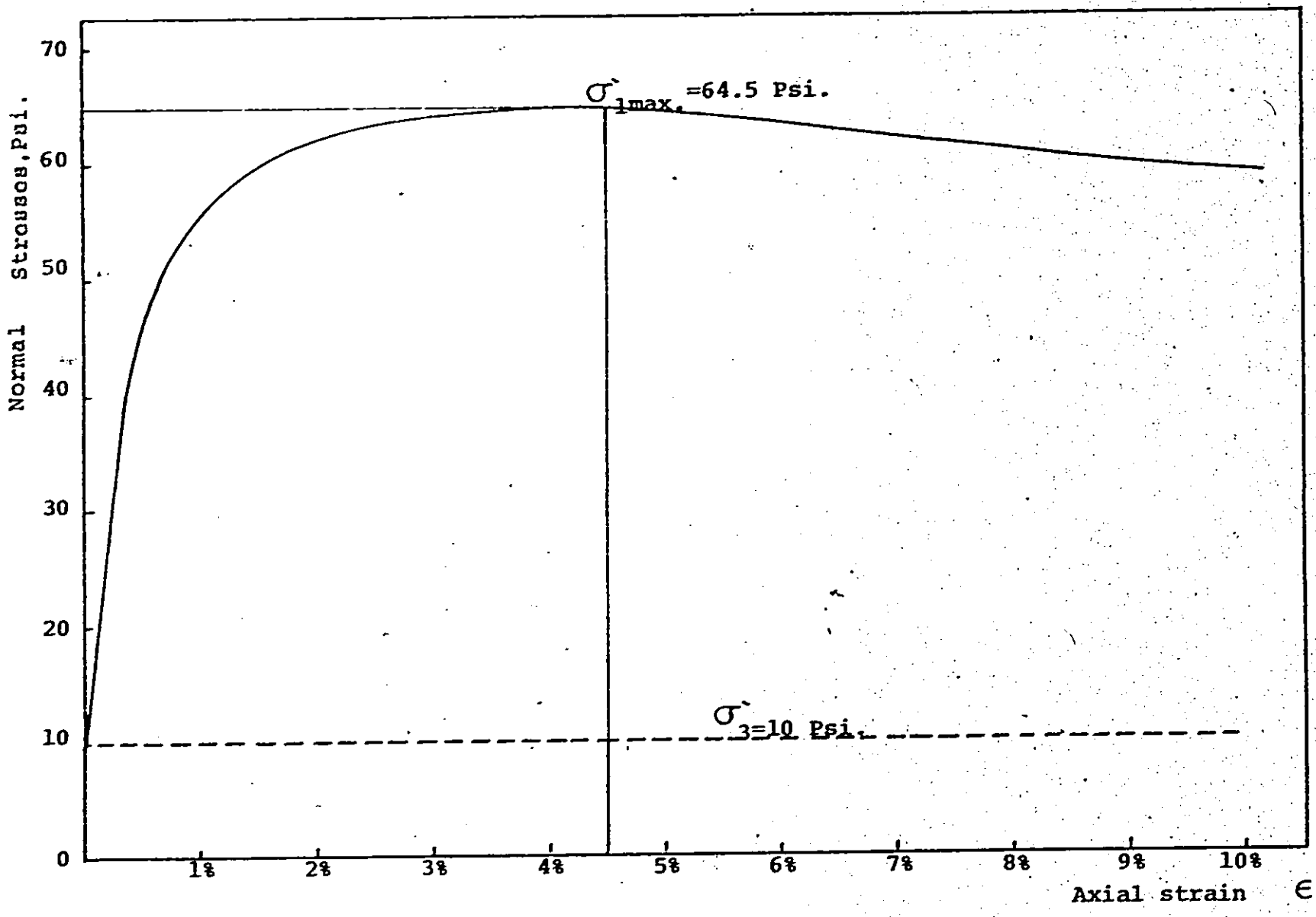


Figure (6.B ) Stress-Strain Curves, Triaxial Test #2.

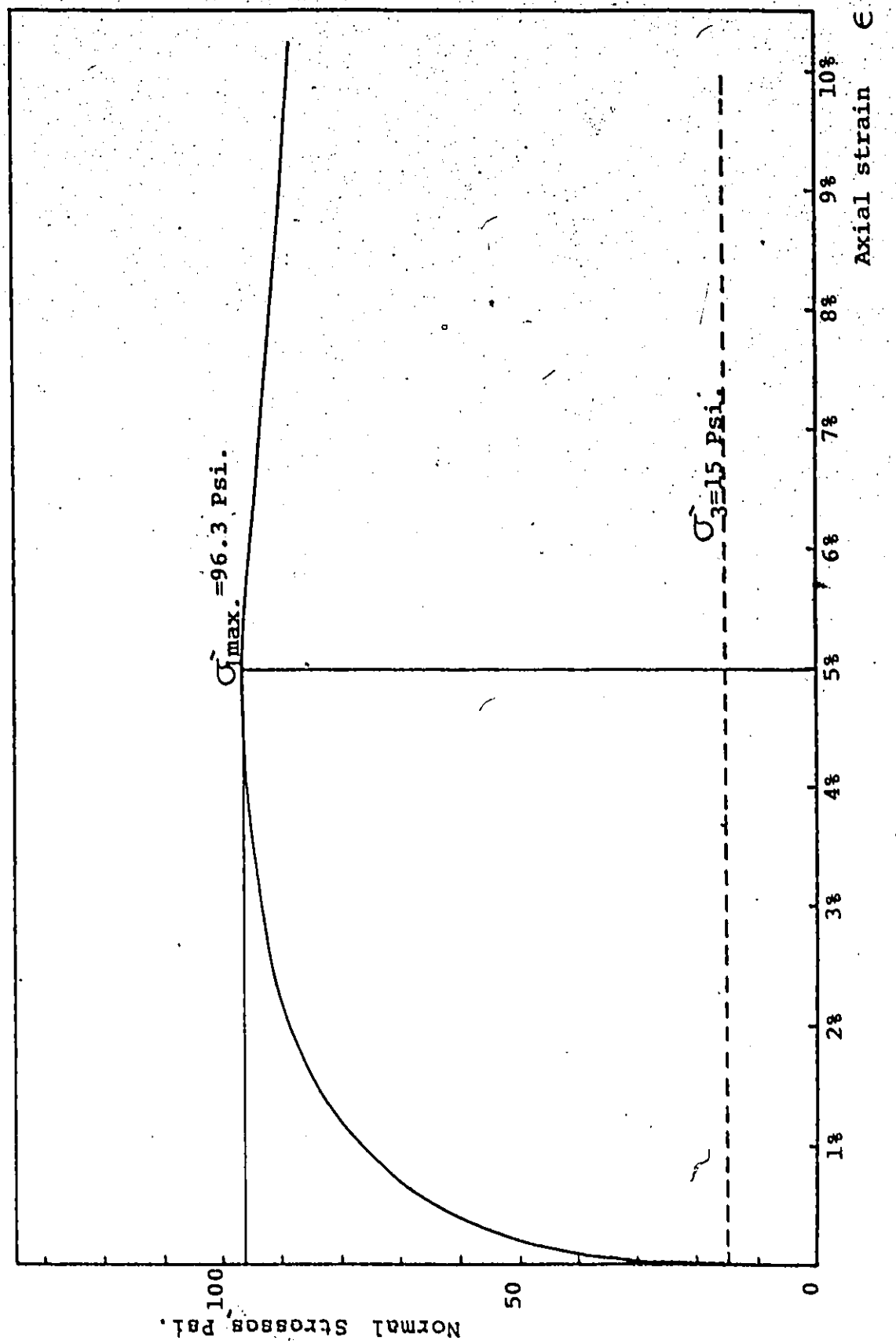


Figure (6.14) Stress-Strain Curves, Triaxial Test #3.

during shear while $\sigma_1$ increased to failure in all triaxial tests.

In Figures (6.15), (6.16) and (6.17) stresses were plotted against axial strains which were based on Tables (5.4), (5.5) and (5.6) respectively in the Appendix. An area correction factor was applied to all plane strain tests.

Figures (6.15) and (6.16) show typical stress-strain curves for plane strain tests #I and #II, at cell pressures 5 psi and 10 psi, respectively. The maximum values of $\sigma_1$ for plane strain tests #I and #II, are 52.5 psi and 107 psi, respectively, at axial strains equal to 2% and 3%. The values of the intermediate principal stress at failure for plane strain tests #I and #II are 13.10 psi and 24.13 psi respectively. The cell pressure was held constant during shear while $\sigma_1$ increased to failure.

Figure (6.17) shows that failure did not occur for plane strain test #III. The maximum value of $\sigma_1$ attained (not a failure value) was 155.00 psi and the value of $\sigma_2$ is 32.55 psi at an axial strain equal to 3.75%.

The maximum values of stresses are greater in plane strain tests than triaxial compression tests for the same cell pressure. In plane strain tests the peak values of $\sigma_1$ occurred at lower values of axial strains than in triaxial compression tests. The higher values of $\sigma_1$ in plane strain tests than triaxial tests can be explained by assuming that (Finn and Mittal, 1963), as the intermediate principal stress ($\sigma_2$) varies between $\sigma_3$ and $\sigma_1$, the soil structure exhibits increasing stiffness to the major principal stress, $\sigma_1$.

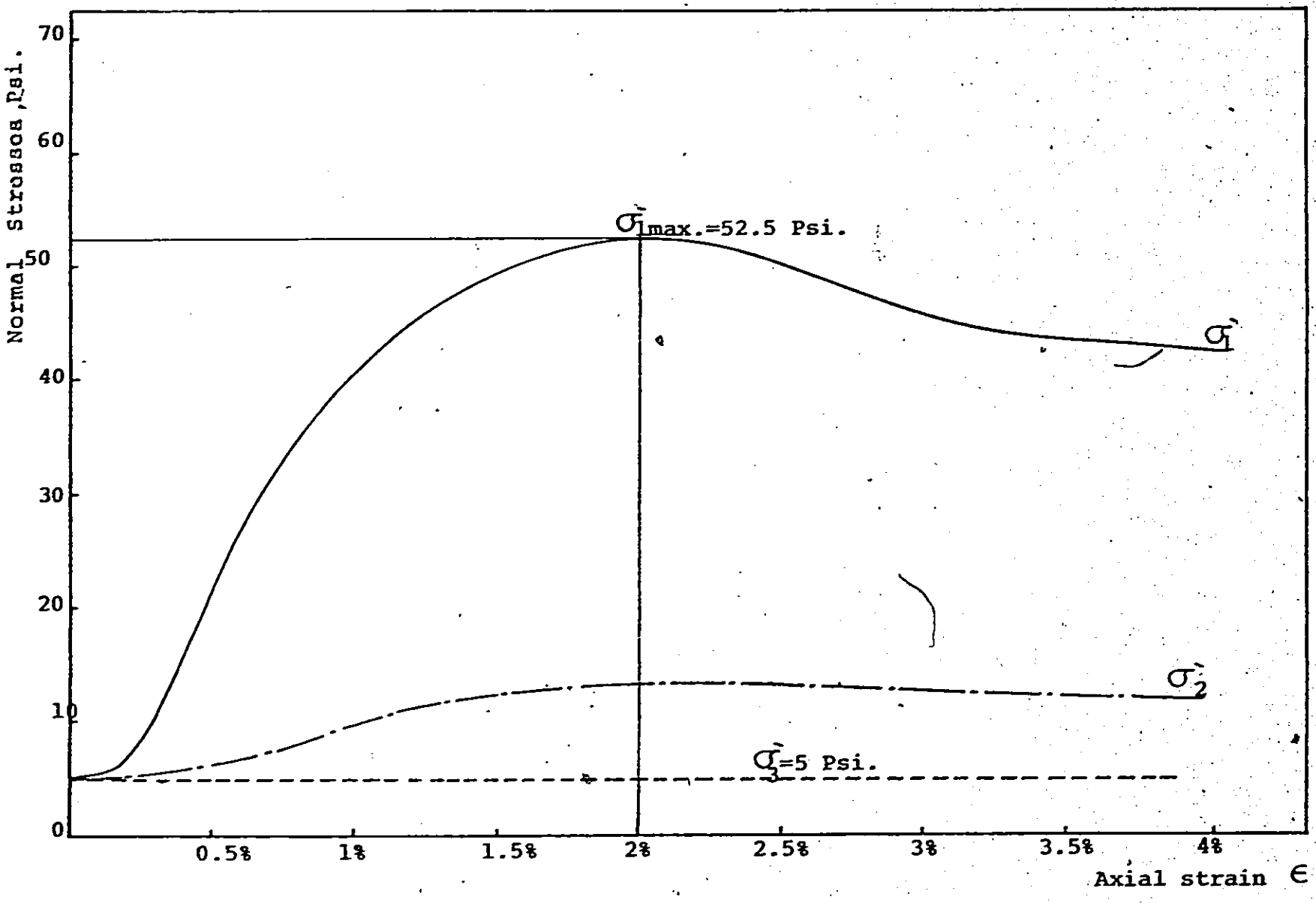


Figure (6.15) Stress-Strain Curves, Plane Strain Test #I.

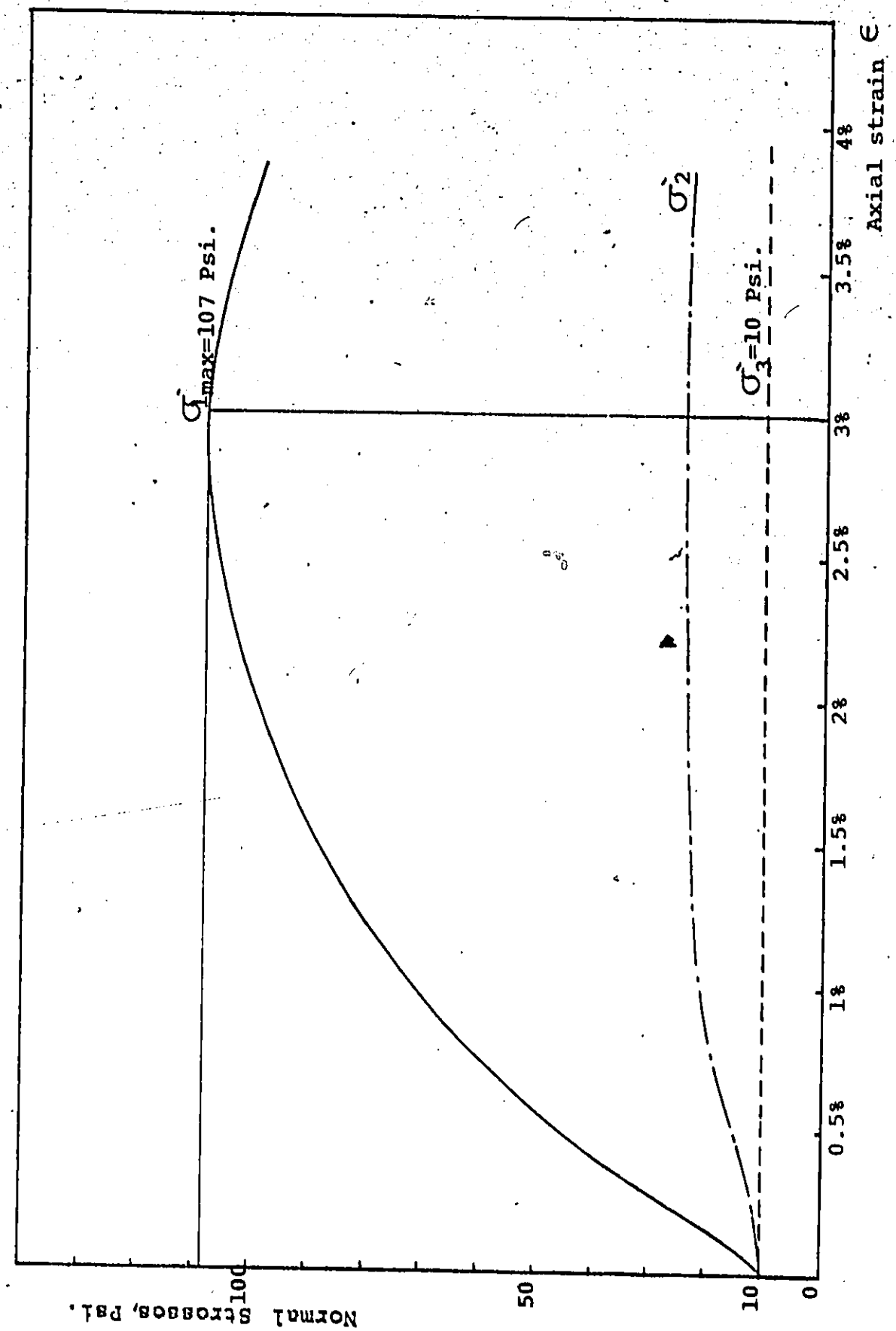


Figure (6.16) Stress- Strain Curves, Plane Strain Test #II.

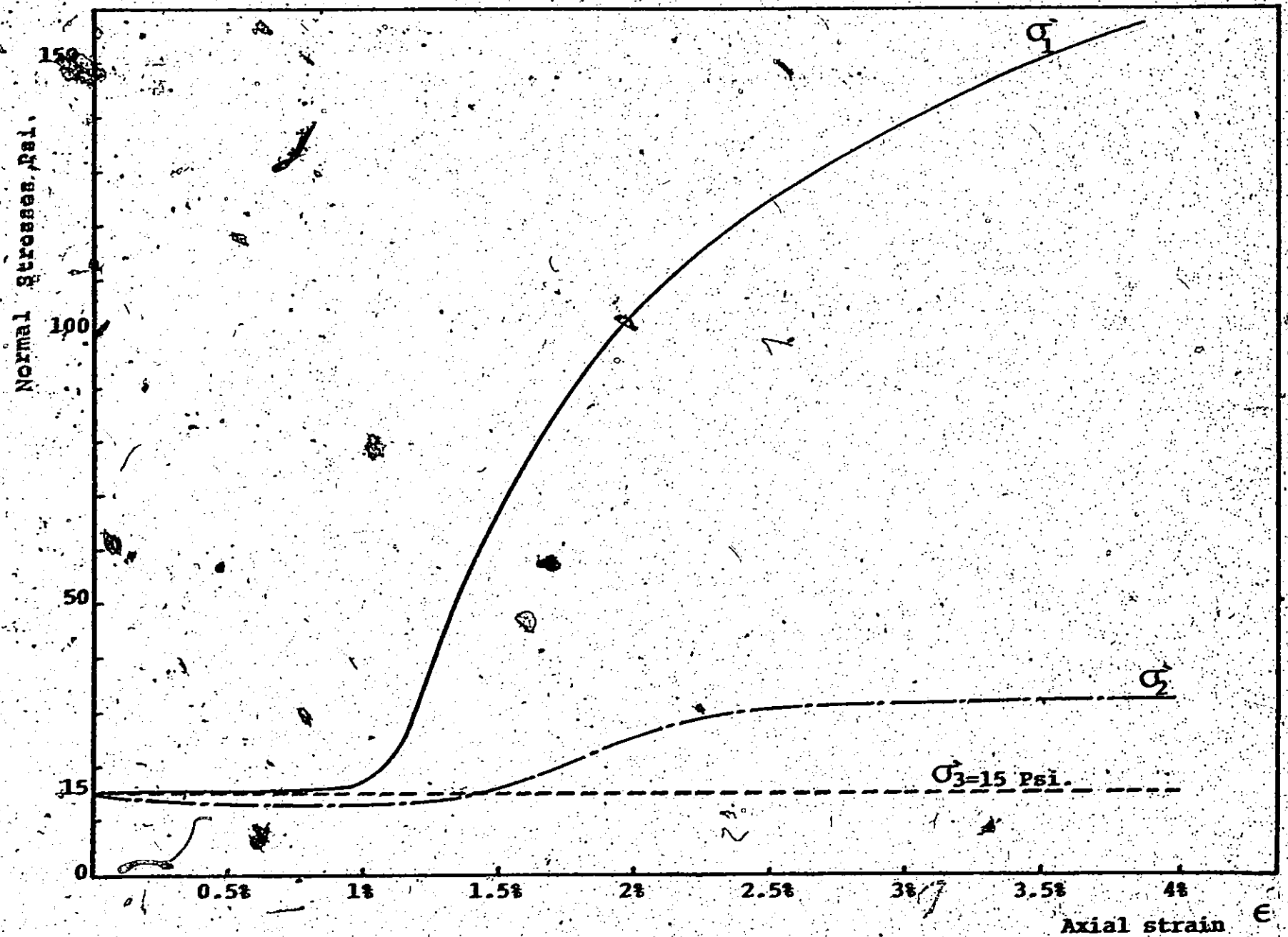


Figure (6.17) Stress-Strain Curves, Plane Strain Test #III.

Hence, more energy or more axial load is necessary.

Also, the values of $\sigma_1$ in plane strain tests occurred at smaller strains than in triaxial tests. This is because of the difference in stiffness in both tests.

## 6.6 Octahedral Stresses in Plane Strain and Triaxial Conditions

As mentioned before, octahedral stresses (normal and shear stresses) exist in a particular plane where the normal to this plane has direction cosines equal to $1/\sqrt{3}(\phi = 54.73°)$ with the x, y and z axes. The derivations of these stresses can be found in any textbook dealing with the theory of elasticity (Scott, 1963). Our concern is to use the octahedral stress equations in the analysis of the experimental data.

The octahedral normal stress ($\sigma_{oct}$) is given by:

$$\sigma_{oct} = \frac{(\sigma_1 + \sigma_2 + \sigma_3)}{3} \qquad (6.17)$$

in which $\sigma_1$, $\sigma_2$, $\sigma_3$ are major, intermediate and minor effective principal compressive stresses, respectively.

In the case of triaxial compression tests, the octahedral normal stress ($\sigma_{oct}$) can be derived by substituting $\sigma_2 = \sigma_3$, that is:

$$\sigma_{oct} = \frac{(\sigma_1 + 2\sigma_3)}{3} \qquad (6.18)$$

Also, the octahedral shear stress can be expressed by the following equation:

$$\tau_{oct} = 1/3\ \sqrt{(\sigma_1 - \sigma_2)^2 + (\sigma_2 - \sigma_3)^2 + (\sigma_3 - \sigma_1)^2} \qquad (6.19)$$

The octahedral shear stress can be derived to satisfy the triaxial compression tests by substituting $\sigma_2 = \sigma_3$.

$$\tau_{oct} = 1/3\ \sqrt{2\sigma_1^2 + 2\sigma_3^2 - 4\sigma_1\sigma_3} \qquad (6.20)$$

$$\tau_{oct} = \frac{\sqrt{2}}{3}(\sigma_1 - \sigma_3)$$

Figures (6.18), (6.19) and (6.20) show plots of the octahedral normal stresses and the octahedral shear stresses, for both triaxial compressions and plane strain tests, against the axial strains. Octahedral shear stresses and normal stresses should be drawn against the octahedral shear strains ($\gamma_{oct}$) and against the octahedral normal strains ($\epsilon_{oct}$), respectively in order to obtain more meaningful comparisons. Further experimental data is required to compute $\epsilon_{oct}$ and $\gamma_{oct}$. $\epsilon_{oct}$ can be computed if the measurement of the volume change is available, because $\Delta V/V = \epsilon_1 + \epsilon_2 + \epsilon_3$ and $\epsilon_{oct} = 1/3(\epsilon_1 + \epsilon_2 + \epsilon_3)$, (Newmark, 1960), also $\gamma_{oct}$ can be obtained if the values of the linear strains $\epsilon_1$, $\epsilon_2$ and $\epsilon_3$ are available. Since the computations of $\epsilon_{oct}$ and $\gamma_{oct}$ depend on further experimental work, the use of the axial strain was suggested.

The following points can be concluded from the curves:

A) The maximum octahedral normal stresses are higher in plane strain tests than in the triaxial compression tests and occurred at lower values of axial strains.

B) The maximum octahedral shear stresses are higher in plane strain tests than the triaxial compression tests and occurred at lower values of axial strains.

C) The octahedral normal and shear stresses in both triaxial and plane strain have a similar shape to the major principal stresses, where these stresses rose to a peak at failure and then decreased with increas-

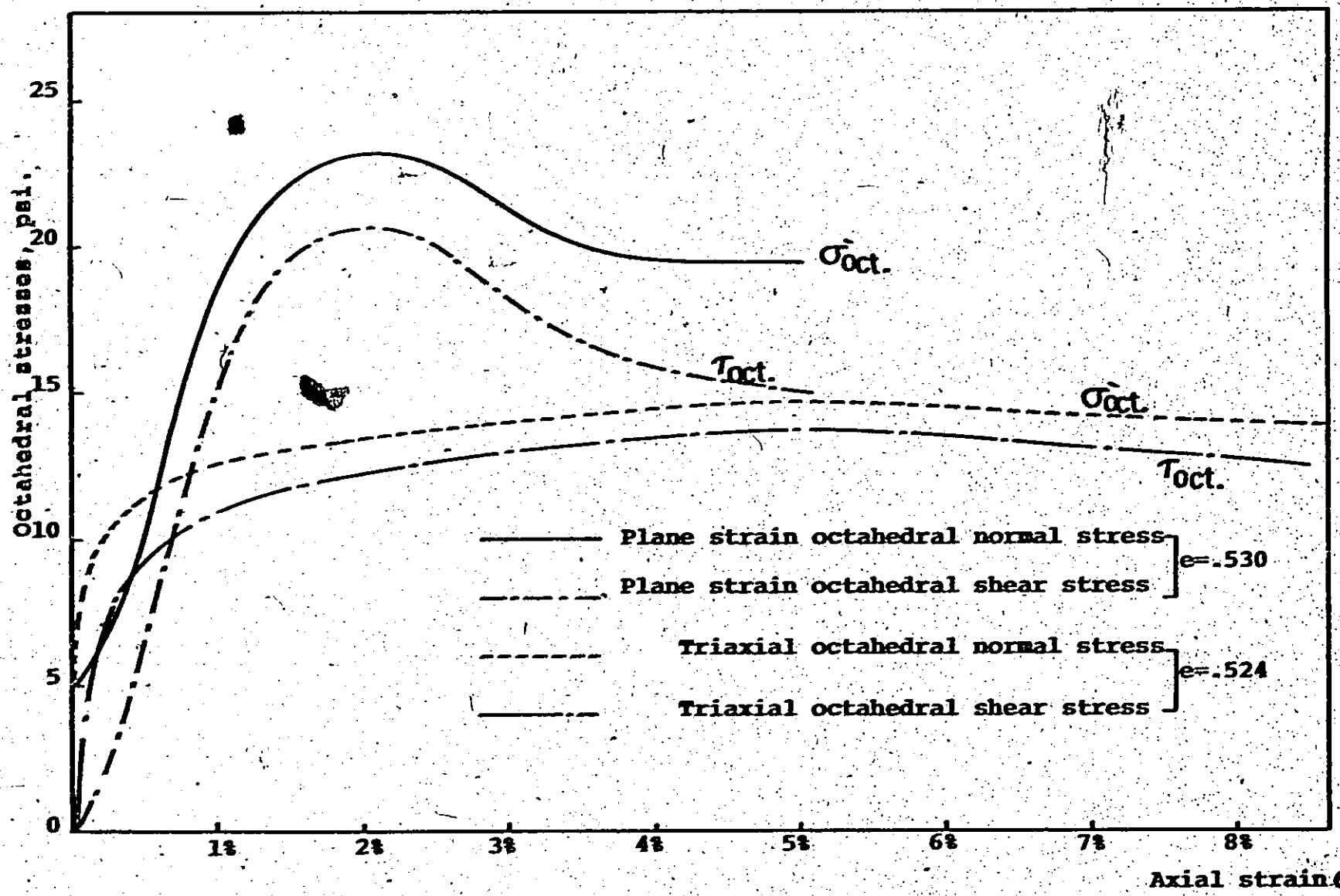


Figure (6.18) Octahedral Stresses, Triaxial Test #1 & Plane Strain Test #I.

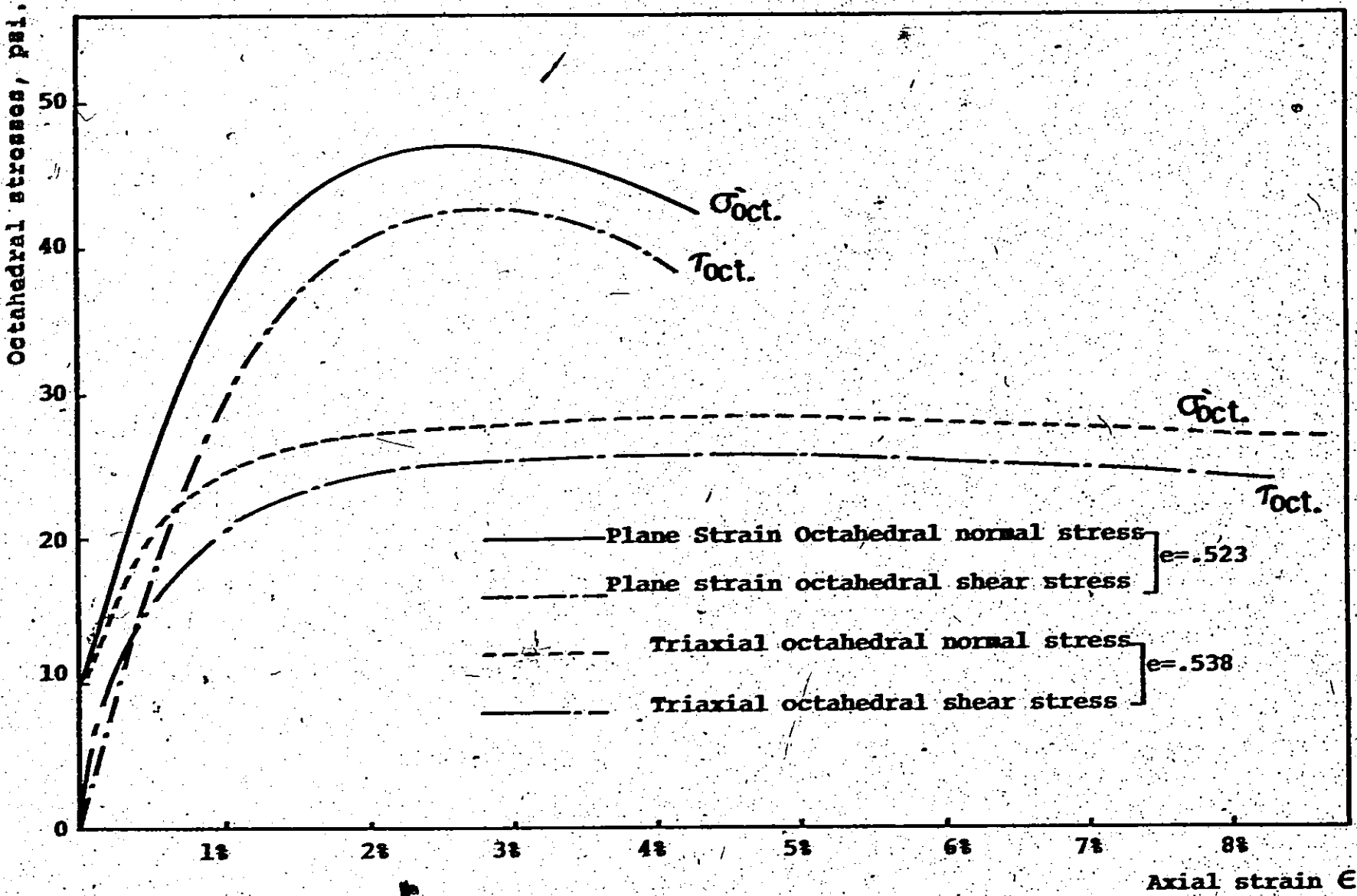


Figure (6.19) Octahedral Stresses, Triaxial Test #2 & Plane Strain Test #II.

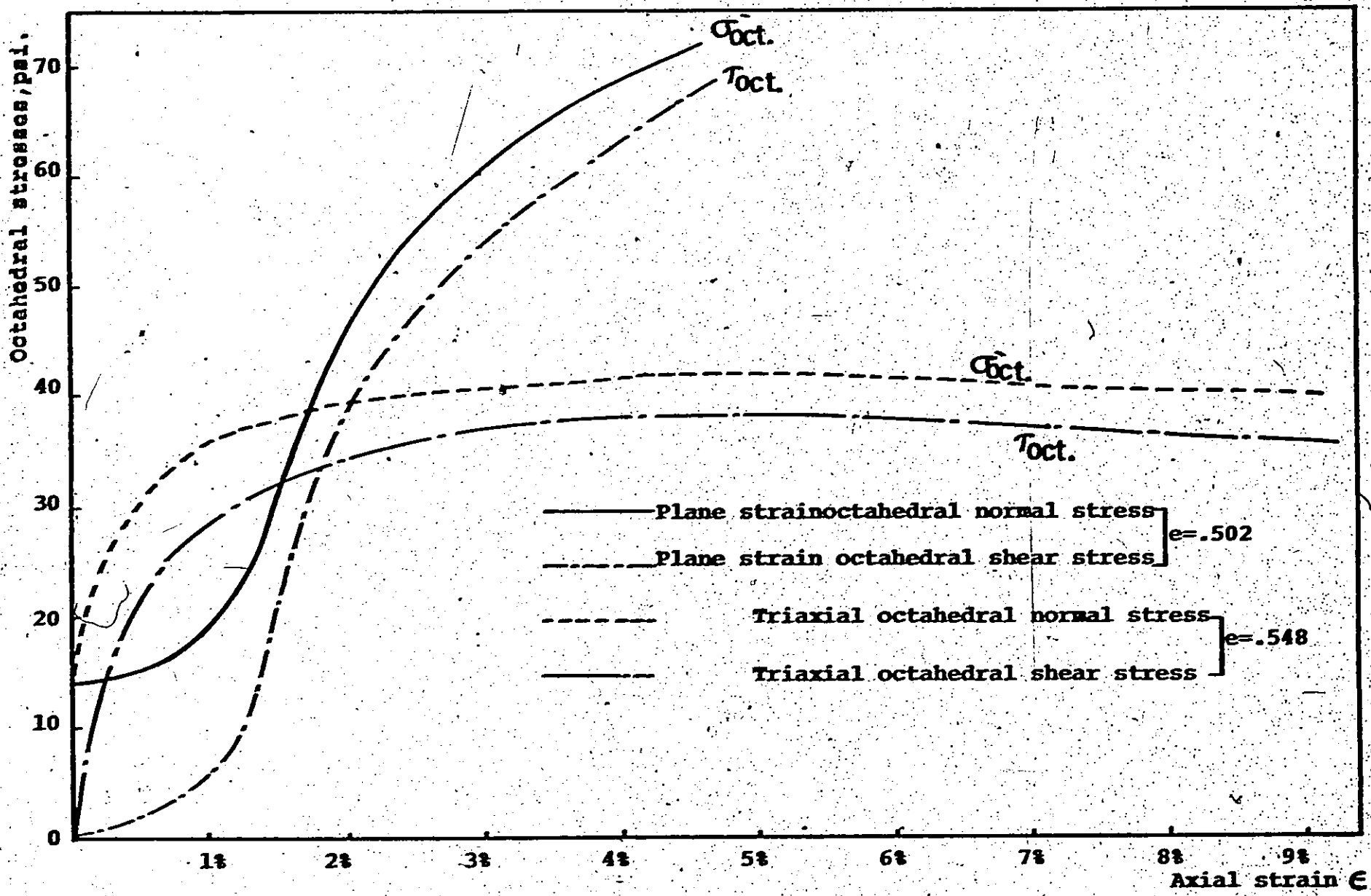


Figure (6.20) Octahedral Stresses, Triaxial Test #3 & Plane Strain Test #III.

ing axial strains.

## 6.7 Intermediate Principal Stress ($\sigma_2$) in Plane Strain Conditions

In plane strain conditions, the ratio between the intermediate principal stress and the other principal stresses ($\sigma_1$ and $\sigma_3$) at failure can be written, depending on the theory of elasticity, as

$$\sigma_2 = \nu(\sigma_1 + \sigma_3)$$

in which $\nu$ is the Possion's ratio. The lower portion of Figure (6.21) shows the experimental values of Possion's ratio ($\nu$) for dry sand in a very dense state which is plotted against the initial porosity. The ratio of the intermediate principal stress to the sum of the other two principal stresses (i.e., experimental values of $\nu$) varied from .19 to .23. The values of $\nu$ obtained by Cornforth (1964) varied from .25 to .27 for very dense samples.

Also, Figure (6.21) shows a graph of the intermediate principal stress ratios $\sigma_2/\sigma_1$, $\sigma_2/\sigma_3$ versus the initial porosity.

The ratio of $\sigma_2/\sigma_1$ varied from .21 to .25 and the ratio of $\sigma_2/\sigma_3$ varied from 2.2 to 2.6.

Figure (6.21) shows Cornforth's results for the ratio $\sigma_2/\sigma_1$ which varied from .32 to .35, and the values of $\sigma_2/\sigma_3$ which varied from 1.75 to 2.05.

Generally, experimental trends observed from Figure (6.21), where the initial porosities vary from 33% to 35%, do agree with the results obtained by Cornforth (1964).

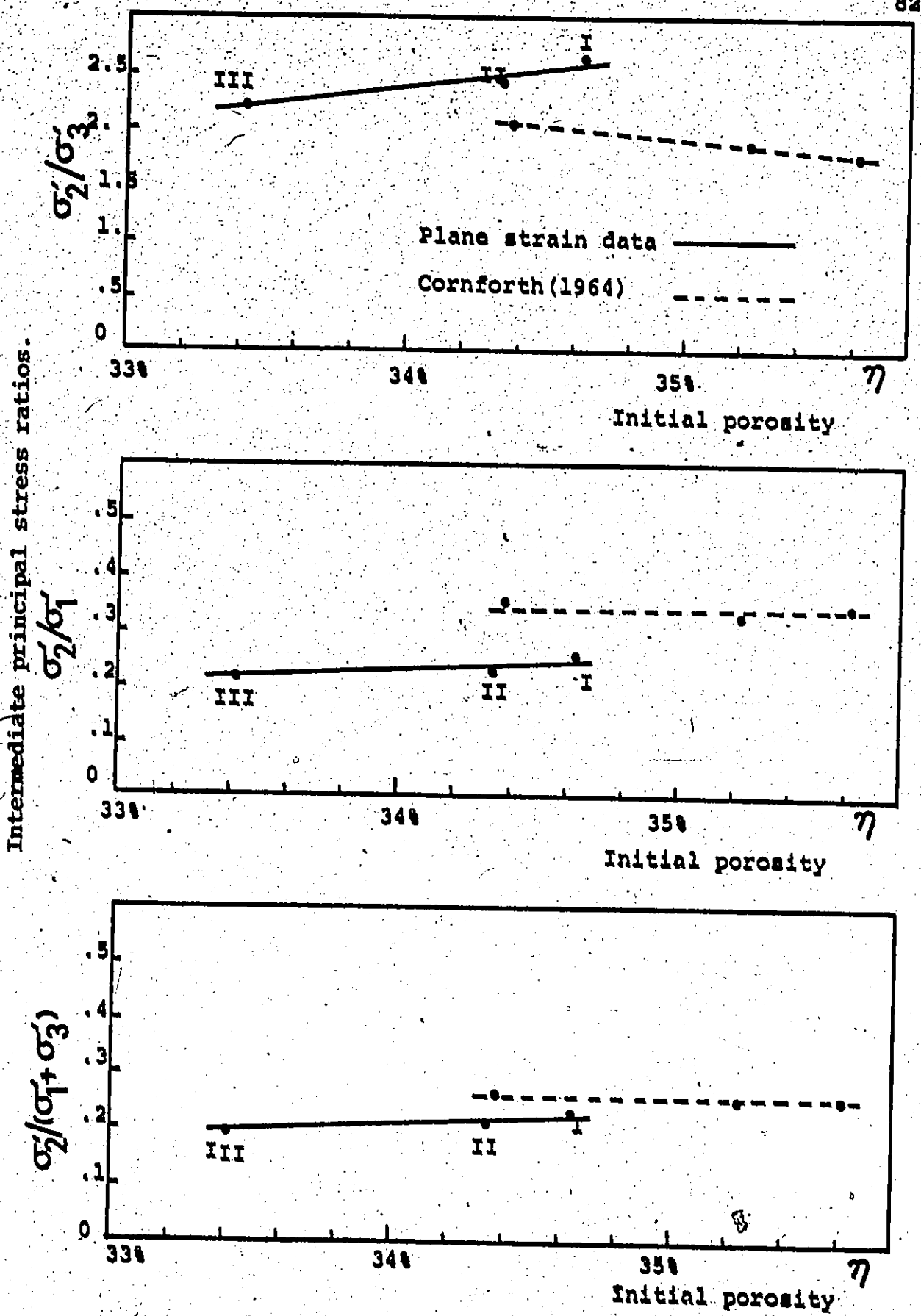


Figure (6.21) Intermediate Principal Stress Ratios Versus Initial Porosity.

# CHAPTER 7

# CONCLUSIONS AND RECOMMENDATIONS

## 7.1 Conclusions

Experimental results for plane strain compression tests and triaxial compression tests on dry uniform sand in the densest state have been obtained and considered for some typical failure relationships. The results indicated that:

A) The angle of shearing resistance at failure is considerably higher in plane strain tests than in triaxial compression tests. This difference was about 7 to 8 degrees in the densest state. In addition, the values of $\phi_f$ in triaxial tests and plane strain tests were higher than expected. The values of $\phi_f$ in both methods must be subjected to correction factors (reduction in the value of $\phi_f$). The correction factors which significantly affect the values of $\phi_f$ include the following:

   i) A correction factor due to friction forces developed when the loading ram passes through a bush in the top of the triaxial cell in both plane strain and triaxial tests.

   ii) A correction factor due to friction between the

plane strain samples and the instrumented side plates. These friction forces could be very high in spite of the lubrication process.

iii) A correction factor due to the thickness of the rubber membrane. This factor is negligible in triaxial tests, and could be important in plane strain tests because of the thick edges of the rectangular rubber membrane.

iv) An energy correction factor due to low confining pressures and initial void ratios must be applied to the observed deviator stress in order to obtain the corrected deviator stress. In this case the energy corrections could significantly reduce the value of $\phi'_f$. This is because when samples are sheared under low confining pressures, extra energy is needed to expand the sample against the confining pressure (Lambe and Whitman, 1969).

B) The angle of shearing resistance is a function of the initial porosity of the samples, that is, the angle increases with decreasing porosities.

C) All curves of principal stress ratios versus axial strains show similar trends in both plane strain and triaxial tests. Also, the peak values of such ratios are higher in plane strain tests and occurred at smaller strains. This is because the soil structure exhibits increasing stiffness to the major principal stress as the intermediate principal stress varies between the values of $\sigma'_3$ and $\sigma'_1$, or $\sigma'_3 < \sigma'_2 < \sigma'_1$.

(Finn and Mittal, 1963).

D) Graphs of the octahedral normal and shear stresses versus axial strains have similar shapes in both plane strain and triaxial tests. Octahedral normal and shear stresses at failure are higher in plane strain tests than triaxial tests and occur at lower values of axial strains.

E) Intermediate principal stress ratios $\sigma_2/\sigma_1$, $\sigma_2/\sigma_3$ and $\sigma_2/(\sigma_1 + \sigma_3)$ give similar values to those obtained by other soil investigators. Also, the experimental value of the ratio $\sigma_2/(\sigma_1 + \sigma_3)$ falls in the range of 0.19 to 0.23.

F) Finally, by considering the plane strain conditions, the intermediate principal stress $\sigma_2$ has an effect on the shear strength parameters, characteristics and failure criteria of cohesionless materials.

## 7.2 Recommendations

In order to obtain more representative results for plane strain tests on cohesionless soils, the testing program should include a series of tests with a wide range of densities, especially tests on loose sand as it is harder to perform these tests with loose samples. This will give the opportunity to study the effect of $\sigma_2$ on shear strengths of loose samples. Samples should be tested under a wide range of confining pressures together with the measurements of the volume change in order to compute the energy correction factor which could significantly affect the values of $\phi_f$ at failure. With minor

modifications (thin membranes, thinner diaphragms, accurate installment of strain gauges and their electrical connections) of the present equipment, reasonable results can be produced which would improve our knowledge of the behaviour of cohesionless soils during plane strain testing. Also, additional installations are needed for the present equipment (pore pressure connections and tranducers) in order to measure pore water pressure and to determine the effective shear parameters of cohesive and cohesionless soils.

These changes and modifications would lead to more accurate and useful results.

## REFERENCES


(1) Bardon, L., Ismail, H. and Tong, P., 1969. "Plane Strain Deformation of Granular Material at Low and High Pressures", Geotechnique 19, No. 4, p.441.

(2) Bares, R., 1969. "Tables for the Analysis of Plates, Slabs and Diaphragms", Baverlog, Germany.

(3) Bishop, A.W., 1966. "The Strength of Soils as Engineering Materials", 6th Rankine Lecture, Geotechnique, Vol. 16, No. 2, pp.91-130.

(4) Bishop, A.W., and D.J. Henkel, 1962. "The Measurements of Soil Properties in the Triaxial Test", Edward Arnold, London, 2nd Ed.

(5) Bowles, J.E., 1970. "Engineering Properties of Soils and Their Measurements", McGraw Hill, New York.

(6) Campanella, R.G., and Y.P. Vaid, 1973. "Influence of Stress Path on the Plane Strain Behaviour of Sensitive Clay", Proc. 8th Int. Conf. on Soil Mechanics and Foundation Engineering, Moscow, U.S.S.R.

(7) Cornforth, D.H., 1964. "Some Experiments on the Influence of Strain Conditions on the Strength of Sand", Geotechnique, Vol. 16, p.143.

(8) Cornforth, D.H., 1961. "Plane Strain Characteristics of Saturated Sand", Ph.D. Thesis, University of London.

(9) Finn, W.D.L., and Mittal, H.K., 1963. "Shear Strength of Soil in a General Stress Field", Proc. Symposium on Laboratory Shear Testing of Soils, ASTM Special Technical Publication No. 361, p.42.

(10) Frydman, S., 1974. "Yielding of Sand in Plane Strain", Journal of the Geotechnical Eng. Division, Proc. of the A.S.C.E., Vol. 100, GT5, p.491.

(11) Green, G.E., 1971. "Strength and Deformation of Sand Measured in an Independent Stress Control Cell", Proceedings of the Roscoe Memorial Symposium, Cambridge University.

(12) Harr, M.E., 1966. "Foundations of Theoretical Soil Mechanics", McGraw Hill, New York.

(13) Henkel, D.J., and Gilbert, G.D., 1952. "The Effect of the Rubber Membrane on the Measured Triaxial Compression Strength of Clay Samples", Geotechnique, Vol. 3, pp.20-29.

(14) Kjellman, W., 1936. "Reports on an Apparatus for Consummate Investigation of the Mechanical Properties of Soils", Proc. 1st Int. Conf. Soil Mech., 2, pp.16-20.

(15) Lambe, T.W., and Whitman, R.V., 1969. "Soil Mechanics", John Wiley, New York.

(16) Mitchell, R.J., 1973. "An Apparatus for Plane Strain and True Triaxial Testing of Undisturbed Soil Samples", Can. Geotch. J., 10, p.520.

(17) Newmark, N.M., 1960. "Failure Hypotheses for Soils", Proc. of the A.S.C.E., Res. Conference Shear Strength of Cohesive Soils, June 1960.

(18) Poorooshasb, H.B., and Roscoe, K.H., 1961. "The Correlation of the Results of Shear Tests With Varying Degrees of Dilatation", Proc. 5th Int. Conf. Soil Mech., Vol. 1, p.287.

(19) Roscoe, K.H., 1971. "Stress-Strain Behaviour of Soil", Proceedings of the Roscoe Memorial Symposium, Cambridge University.

(20) Roscoe, K.H., Schofield, A.N., and Thurairajah, A, 1963. "An Evaluation of Test Data for Selecting a Yield Criterion for Soils", Proc. Symposium on Laboratory Shear Testing of Soils, ASTM Special Technical Publication No. 261, pp.111-133.

(21) Rowe, P.W., 1962. "The Stress-Dilatancy Relation for Static Equilibrium of an Assembly of Particles in Contact", Proc. R. Soc. A269, pp.500-527.

(22) Scott, R.F., 1963. "Principles of Soil Mechanics", Addison-Wesly, London.

(23) Vaid, Y.P., and R.G. Campanella, 1973. "Making Rubber Membranes", Can. Geotch. J., Vol. 10, No. 4, p.643.

(24) Wood, C.C., 1958. "Shear Strength and Volume Change Characteristics of Compacted Soil Under Conditions of Plane Strain". Ph.D. Thesis, University of London.

# APPENDIX

## Strain Gauge Calibrations -

TABLE (4.1) Increasing Pressure

| Pressure psi | VOLTMETER READINGS M.V. | | | |
|---|---|---|---|---|
| | Gauge No. 1 | Gauge No. 2 | Gauge No 3 | Gauge No. 4 |
| 0 | +4 | +2.5 | +1.5 | -1 |
| 3 | +25 | +22 | +27.5 | +26.5 |
| 6 | +50 | +43 | +55 | +57 |
| 9 | +70 | +61.5 | +76 | +81 |
| 12 | +94.5 | +81.5 | +101.5 | +111 |
| 15 | +116.5 | +102.5 | +125.5 | +139 |
| 18 | +138 | +121.5 | +150.5 | +167.5 |
| 21 | +161.5 | +144.5 | +175.5 | +196 |
| 24 | +184 | +164 | +199.5 | +223.5 |
| 27 | +205 | +184.5 | +223 | +252 |
| 30 | +227.5 | +202.5 | +243 | +278 |

## Strain Gauge Calibrations

TABLE (4.2) Decreasing Pressure

| Pressure psi | VOLTMETER READINGS M.V. | | | |
|---|---|---|---|---|
| | Gauge No. 1 | Gauge No. 2 | Gauge No. 3 | Gauge No. 4 |
| 30 | +227.5 | 202.5 | +243 | +278 |
| 27 | +206.5 | 183 | +213 | +250.5 |
| 24 | +183.5 | 162 | +185.5 | +222 |
| 21 | +160.5 | 141.5 | +162 | +194 |
| 18 | +142.5 | 120.5 | 133 | +166 |
| 15 | +119 | 99 | +104.5 | +136.5 |
| 12 | +95.5 | 78 | +80 | +108.5 |
| 9 | +74 | 57.5 | +53.5 | +80 |
| 6 | +53.5 | 36.5 | +27.5 | +52.5 |
| 3 | +31 | 16 | +1 | +23.5 |
| 0 | +8.5 | -5 | -23.5 | -4 |

TABLE (5-1) Triaxial Test # 1, $\sigma_3$ = 5 psi.

| Load Dial Reading .0001 | Deformation .0001" | Loads lbs. | Deformation ΔH Inches | ε=ΔH/HO Strain | 1-ε | A/1-ε in.2 | Deviator Stress psi. $\sigma_1-\sigma_3$ | $\sigma_1$ psi. |
|---|---|---|---|---|---|---|---|---|
| 0.0 | 0.0 | 0.0 | .0 | .00 | 0 | 0 | 0 | 5 |
| 65 | 10 | 16.2 | .0010 | .000361 | .99964 | 1.47 | 11 | 16 |
| 100 | 22 | 25 | .0022 | .000791 | .99921 | 1.47 | 17 | 22 |
| 122 | 90 | 30.2 | .0090 | .0032 | .9968 | 1.47 | 20.45 | 25.45 |
| 125 | 110 | 31.2 | .0110 | .0039 | .9961 | 1.47 | 21.20 | 26.20 |
| 128 | 155 | 32 | .0155 | .0055 | .9945 | 1.47 | 21.8 | 26.80 |
| 132 | 210 | 32.5 | .210 | .0075 | .9925 | 1.47 | 22.1 | 27.1 |
| 135 | 265 | 33.6 | .0265 | .0094 | .9906 | 1.47 | 22.8 | 27.8 |
| 138 | 300 | 34.4 | .0300 | .0107 | .0983 | 1.485 | 23.2 | 28.2 |
| 145 | 430 | 36.0 | .0430 | .0154 | .0846 | 1.49 | 24.2 | 29.2 |
| 150 | 500 | 37.1 | .0500 | .0178 | .9822 | 1.495 | 24.8 | 29.8 |
| 156 | 620 | 38.5 | .0620 | .0220 | .9780 | 1.50 | 25.7 | 30.7 |
| 160 | 700 | 39.7 | .0700 | .0250 | .9750 | 1.51 | 26.3 | 31.3 |
| 165 | 810 | 40.8 | .0810 | .0290 | .9710 | 1.515 | 26.9 | 31.9 |
| 168 | 915 | 41.6 | .0915 | .0327 | .9673 | 1.52 | 27.4 | 32.4 |
| 171 | 1015 | 42.2 | .1015 | .0362 | .9638 | 1.525 | 27.6 | 32.6 |
| 174 | 1100 | 43.0 | .1100 | .0393 | .9607 | 1.53 | 28.1 | 33.1 |
| 176 | 1200 | 43.4 | .1200 | .0428 | .9572 | 1.535 | 28.2 | 33.2 |
| 179 | 1300 | 44.2 | .1300 | .0464 | .9536 | 1.54 | 28.7 | 33.7 |
| 179.5 | 1410 | 44.6 | .1410 | .0500 | .9500 | 1.545 | 28.9 | 33.9 |
| 180.5 | 1470 | 44.7 | .1470 | .0525 | .9475 | 1.55 | 28.8 | 33.8 |
| 181.5 | 1560 | 45 | .1560 | .0557 | .9443 | 1.56 | 28.85 | 33.85 |
| 181 | 1870 | 44.8 | .1870 | .0667 | .9333 | 1.57 | 28.6 | 33.6 |
| 180.5 | 1960 | 44.7 | .1960 | .0700 | .9300 | 1.58 | 28.3 | 33.3 |
| 179 | 2010 | 44.2 | .2010 | .0715 | .9285 | 1.585 | 27.9 | 32.9 |
| 178 | 2060 | 44.1 | .2060 | .0735 | .9265 | 1.59 | 27.7 | 32.7 |
| 176.5 | 2100 | 43.5 | .2100 | .0750 | .9250 | 1.595 | 27.3 | 32.3 |
| 174 | 2200 | 43 | .2200 | .0785 | .9215 | 1.595 | 27 | 32 |

TABLE (5-2) Triaxial Test # 2, $\sigma_3$ = 10 psi.

| Load Dial Reading .0001" | Deformation .0001" | Loads lbs. | Deformation ΔH Inches | ε=ΔH/Ho Strain | 1-ε | A/1-ε in.$^2$ | Deviator Stress $\sigma_1-\sigma_3$ psi | $\sigma_1$ psi. |
|---|---|---|---|---|---|---|---|---|
| 0.0 | 0.0 | 0.0 | 0.0 | .000 | 1 | 1.47 | 0 | |
| 20 | 16 | 5 | .0016 | .00056 | .99944 | 1.47 | 3.4 | 13.4 |
| 50 | 35 | 12.4 | .0035 | .0012 | .9988 | 1.47 | 8.43 | 18.43 |
| 110 | 49 | 27.4 | .0049 | .0017 | .9983 | 1.475 | 18.60 | 28.60 |
| 200 | 127 | 49.5 | .127 | .0045 | .9955 | 1.475 | 33.6 | 43.60 |
| 233 | 180 | 57.8 | .0180 | .0063 | .9937 | 1.48 | 39 | 49 |
| 265 | 255 | 65 | .0255 | .0089 | .9911 | 1.48 | 43.8 | 53.80 |
| 280 | 300 | 69 | .0300 | .0105 | .9895 | 1.485 | 46.5 | 56.50 |
| 304 | 410 | 75 | .0410 | .0145 | .9855 | 1.49 | 50.4 | 60.40 |
| 317 | 510 | 78 | .0510 | .0180 | .982 | 1.49 | 52.5 | 62.5 |
| 321 | 570 | 79 | .0570 | .02 | .98 | 1.49 | 53 | 63 |
| 327 | 670 | 81 | .0670 | .024 | .976 | 1.505 | 53.5 | 63.5 |
| 330 | 785 | 81 | .0785 | .028 | .972 | 1.51 | 53.6 | 63.6 |
| 331 | 830 | 81 | .0830 | .029 | .971 | 1.51 | 53.6 | 63.6 |
| 332.5 | 905 | 82 | .0905 | .032 | .968 | 1.515 | 54 | 64 |
| 333 | 965 | 82 | .0965 | .034 | .966 | 1.515 | 54 | 64 |
| 333.5 | 1020 | 82.5 | .1020 | .036 | .964 | 1.525 | 54.1 | 64.1 |
| 335 | 1100 | 83 | .1100 | .039 | .961 | 1.53 | 54.4 | 64.4 |
| 335 | 1170 | 83 | .1170 | .041 | .959 | 1.535 | 54.2 | 64.2 |
| 335 | 1200 | 83 | .1200 | .042 | .958 | 1.535 | 54.2 | 64.2 |
| 335.5 | 1270 | 83.5 | .1270 | .045 | .955 | 1.535 | 54.5 | 64.5 |
| 335.5 | 1300 | 83.5 | .1300 | .046 | .954 | 1.54 | 54 | 64 |
| 336.5 | 1530 | 83.5 | .1530 | .054 | .946 | 1.55 | 53.5 | 63.5 |
| 342 | 1570 | 84 | .1570 | .055 | .945 | 1.55 | 54.2 | 64.2 |
| 341 | 1600 | 84 | .1600 | .056 | .944 | 1.55 | 53.8 | 63.8 |
| 340 | 1700 | 84 | .1700 | .060 | .940 | 1.55 | 53.8 | 63.8 |

TABLE (5-2) Continued

| Load Dial Reading .0001" | Deformation .0001" | Loads lbs. | Deformation ΔH Inches | ε=H/HO Strain | 1-ε | A/1-ε psi. | psi. Deviator Stress $\sigma'_1-\sigma'_3$ | psi. $\sigma'_1$ |
|---|---|---|---|---|---|---|---|---|
| 339 | .1890 | 83.5 | .1890 | .067 | .933 | 1.57 | 53.2 | 63.2 |
| 339 | 2000 | 83.5 | .2000 | .070 | .93 | 1.575 | 53 | 63 |
| 334.5 | 2500 | 82.5 | .2500 | .088 | .912 | 1.60 | 51.6 | 61.6 |
| 333 | 2710 | 82 | .2710 | .095 | .905 | 1.625 | 50.5 | 60.5 |
| 328 | 2880 | 81 | .2880 | .102 | .898 | 1.685 | 49.6 | 59.6 |

TABLE (5-3) Triaxial Test #3, $\sigma_3$ = 15 psi

| Load Dial Reading .0001" | Deformation .0001" | Loads lbs. | Deformation ΔH Inches | ε= H/HO | 1-ε | A/1-ε in.$^2$ | Deviator Stress $\sigma_1-\sigma_3$ psi | $\sigma_1$ psi. |
|---|---|---|---|---|---|---|---|---|
| 0 | 0 | 0 | 0 | 0.00 | 1.0000 | 1.415 | | |
| 15 | 11 | 3.7 | .0011 | .00039 | .99961 | 1.415 | 2.61 | 17.61 |
| 50 | 18 | 12.4 | .0018 | .00063 | .99937 | 1.415 | 8.76 | 23.76 |
| 100 | 30 | 24.8 | .0030 | .00106 | .99894 | 1.415 | 17.5 | 32.5 |
| 200 | 61 | 49.5 | .0061 | .0022 | .9978 | 1.42 | 35 | 50 |
| 300 | 141 | 74 | .0141 | .0050 | .9950 | 1.425 | 52 | 67 |
| 350 | 220 | 86 | .022 | .0078 | .9922 | 1.44 | 60.4 | 75.4 |
| 410 | 460 | 101 | .046 | .016 | .984 | 1.45 | 70.2 | 85.2 |
| 425 | 560 | 104 | .056 | .020 | .98 | 1.45 | 71.6 | 86.6 |
| 440 | 660 | 108 | .066 | 0.023 | .977 | 1.46 | 74.5 | 89.5 |
| 447 | 780 | 115 | .078 | 0.028 | .972 | 1.46 | 78.6 | 93.6 |
| 455 | 880 | 116 | .088 | .031 | .969 | 1.47 | 79.6 | 94.6 |
| 460 | 1010 | 118 | .101 | .036 | .964 | 1.47 | 79.2 | 94.2 |
| 464 | 1110 | 119 | .111 | .039 | .961 | 1.48 | 81 | 96 |
| 467 | 1220 | 119 | .122 | .043 | .957 | 1.48 | 80.5 | 95.5 |
| 468.5 | 1310 | 120 | .131 | .046 | .954 | 1.49 | 81.2 | 96.2 |
| 470.5 | 1410 | 121 | .141 | .050 | .95 | 1.495 | 81.3 | 96.3 |
| 471 | 1510 | 121 | .151 | .053 | .947 | 1.51 | 80.8 | 95.8 |
| 471 | 1750 | 121 | .175 | .062 | .938 | 1.51 | 79.2 | 94.2 |
| 471 | 1810 | 121 | .181 | .064 | .936 | 1.53 | 79.2 | 94.2 |
| 470 | 2130 | 120.5 | .075 | .075 | .925 | 1.545 | 78.8 | 93.8 |
| 468 | 2350 | 119.5 | .235 | .083 | .917 | 1.545 | 77.3 | 92.8 |
| 465 | 2435 | 119 | .2435 | .086 | .914 | 1.555 | 77.1 | 92.1 |
| 464 | 2500 | 119 | .25 | .088 | .912 | 1.555 | 76.5 | 91.5 |
| 460 | 2590 | 118 | .259 | .091 | .909 | 1.56 | 75.8 | 90.8 |
| 457 | 2650 | 117 | .265 | .093 | .907 | 1.56 | 75.2 | 90.2 |
| 449 | 2800 | 116 | .28 | .099 | .901 | 1.57 | 74.5 | 89.5 |

TABLE (5-4) Plane Strain Test #1 $\sigma_3$ = 5 psi.

| Time Sec. | Load Dial Reading .0001" | Displacement .0001" | VOLTMETER READINGS - DIGITAL RECORDER | | | |
|---|---|---|---|---|---|---|
| | | | Gauge #1 M.V. | Gauge #2 M.V. | Gauge #3 M.V. | Gauge #4 M.V. |
| | | | -8 | +7 | +8.5 | +2 |
| | 0.0 | 0.0 | +23 | +43.5 | +50 | +48 |
| | 3 | 40 | 27.5 | 41.5 | 52 | 48.5 |
| | 30 | 50 | 36.5 | 42.5 | 53 | 48.5 |
| | 100 | 73 | 36 | 40.5 | 51 | 51.5 |
| | 185 | 90 | 28.5 | 41.0 | 53.5 | 50.0 |
| | 260 | 105 | 29 | 44.5 | 57.5 | 53.5 |
| | 330 | 122 | 32 | 51 | 59.5 | 55.5 |
| | 400 | 141 | 38.5 | 54.5 | 66.5 | 59.5 |
| | 510 | 175 | 42.5 | 60.0 | 76 | 66.5 |
| | 615 | 210 | 51.5 | 69.5 | 85 | 73 |
| | 700 | 243 | 56.5 | 74 | 91 | 80 |
| | 810 | 302 | 65 | 80 | 106.5 | 86 |
| | 865 | 347 | 75 | 83 | 112.5 | 91 |
| | 935 | 450 | 77 | 85 | 123 | 96 |
| | 955 | 522 | 82.5 | 84 | 126 | 96.5 |
| | 942 | 610 | 85 | 80 | 127 | 94 |
| | 936 | 660 | 90.5 | 75.5 | 126 | 95.5 |
| | 915 | 690 | 94 | 79.5 | 125 | 95.5 |
| | 890 | 735 | 82.5 | 73 | 122.5 | 94.5 |
| | 850 | 800 | 80 | 72.5 | 120.5 | 95 |
| | 800 | 900 | 92 | 63 | 114 | 95 |
| | 780 | 960 | 84 | 60 | 113 | 94.5 |
| | 765 | 1010 | 82.5 | 58.5 | 111 | 95.5 |

TABLE (5.4) Continued, Plane Strain Test # I, $\sigma_3$ = 5 psi.

| Load lbs. | Displacement ΔH Inches | Intermediate Principal Stress Readings, $\sigma_2$ = psi | | | | $\epsilon = \frac{\Delta H}{H_o}$ | 1-ε |
|---|---|---|---|---|---|---|---|
| | | Gauge #1 | Gauge #2 | Gauge #3 | Gauge #4 | | |
| | | | .8 | 1.0 | .4 | | |
| 0.0 | 0.0 | | 5.8 | 5.6 | 5.4 | 0 | 1 |
| 0.75 | 0.004 | | 6.1 | 5.8 | 5.4 | .0016 | .9984 |
| 7.5 | .005 | | 6.2 | 5.9 | 5.4 | .0020 | .9980 |
| 25.0 | .0073 | | 5.9 | 5.7 | 5.7 | .0029 | .9971 |
| 45.0 | .0090 | | 6.3 | 6.0 | 5.6 | .0035 | .9963 |
| 65.0 | .0105 | | 6.8 | 6.4 | 6.0 | .0041 | .9959 |
| 81.0 | .0122 | | 7.0 | 6.5 | 6.2 | .0048 | .9952 |
| 98.0 | .0141 | | 7.9 | 7.3 | 6.6 | .0055 | .9945 |
| 125.0 | .0175 | | 9.1 | 8.3 | 7.3 | .0068 | .9932 |
| 151.0 | .0210 | | 10.2 | 9.4 | 8.0 | .0082 | .9918 |
| 172.0 | .0243 | | 10.9 | 10.0 | 8.8 | .0095 | .9905 |
| 198.0 | .0302 | | 12.8 | 11.6 | 9.4 | .012 | .988 |
| 211.0 | .0347 | | 13.6 | 12.2 | 9.9 | .014 | .986 |
| 228.0 | .0450 | | 14.9 | 13.3 | 10.5 | .018 | .982 |
| 232.0 | .0522 | | 15.3 | 13.6 | 10.5 | .020 | .980 |
| 230.0 | .0610 | | 15.4 | 13.65 | 10.3 | .024 | .976 |
| 228.0 | .0660 | | 15.3 | 13.6 | 10.4 | .025 | .975 |
| 223.0 | .0690 | | 15.2 | 13.5 | 10.4 | .027 | .973 |
| 218.0 | .0735 | | 14.8 | 13.3 | 10.3 | .029 | .971 |
| 208.0 | .0800 | | 14.6 | 13.0 | 10.4 | .031 | .969 |
| 196.0 | .0900 | | 13.8 | 12.4 | 10.4 | .035 | .965 |
| 191.0 | .0960 | | 13.7 | 12.3 | 10.3 | .038 | .962 |
| 188.0 | .1010 | | 13.6 | 12.2 | 10.4 | .039 | .961 |

Results Unsatisfactory

TABLE (5.4) Continued, Plane Strain Test # I, $\sigma'_3$ = 5 psi.

| $A_o/1-\varepsilon$ in.$^2$ | $\sigma'_1-\sigma'_3$ psi. | $\sigma'_1$ psi. | $\sigma'_2$ Average psi. | $\frac{\sigma'_2}{\sigma'_1}$ | $\frac{\sigma'_1}{\sigma'_3}$ | $\frac{\sigma'_2}{\sigma'_1+\sigma'_3}$ | $\frac{\sigma'_1+\sigma'_2+\sigma'_3}{3}$ psi. |
|---|---|---|---|---|---|---|---|
| | | | .73 | | | | |
| 4.87 | 0 | 5.00 | 5.6 | 1.12 | 1 | .56 | 5.2 |
| 4.87 | 1.54 | 5.15 | 5.8 | 1.00 | 1.02 | .57 | 5.32 |
| 4.87 | 1.54 | 6.54 | 5.8 | .89 | 1.31 | .5 | 5.78 |
| 4.88 | 5.12 | 10.12 | 5.8 | .57 | 2.02 | .38 | 6.97 |
| 4.89 | 9.22 | 14.22 | 6.0 | .42 | 2.84 | .31 | 8.41 |
| 4.89 | 13.3 | 18.3 | 6.4 | .35 | 3.66 | .27 | 9.9 |
| 4.90 | 16.6 | 21.6 | 6.6 | .31 | 4.32 | .25 | 10.07 |
| 4.90 | 20 | 25 | 7.3 | .29 | 5 | .24 | 12.43 |
| 4.91 | 25.6 | 30.6 | 8.2 | .27 | 6.12 | .23 | 14.6 |
| 4.91 | 35.03 | 35.9 | 9.2 | .26 | 7.18 | .22 | 16.7 |
| 4.92 | 34 | 39 | 9.9 | .25 | 7.8 | .23 | 17.97 |
| 4.94 | 40.5 | 45.5 | 11.3 | .25 | 9.1 | .22 | 20.6 |
| 4.94 | 43.2 | 48.2 | 11.9 | .25 | 9.64 | .22 | 21.7 |
| 4.96 | 46.7 | 51.7 | 12.9 | .25 | 10.34 | .23 | 23.2 |
| 4.97 | 47.5 | 52.5 | 13.1 | .25 | 10.5 | .23 | 23.53 |
| 4.99 | 47.1 | 52.1 | 13.1 | .25 | 10.42 | .23 | 23.4 |
| 4.99 | 46.6 | 51.6 | 13.1 | .25 | 10.32 | .23 | 23.23 |
| 5.01 | 43.5 | 48.5 | 13.0 | .27 | 9.7 | .24 | 22.17 |
| 5.03 | 41.35 | 46.35 | 12.8 | .28 | 9.27 | .25 | 21.38 |
| 5.05 | 40 | 45.0 | 12.7 | .28 | 9 | .25 | 20.90 |
| 5.06 | 38.8 | 43.8 | 12.2 | .28 | 8.76 | .25 | 20.33 |
| 5.06 | 37.75 | 42.75 | 12.1 | .28 | 9.55 | .25 | 19.95 |
| 5.07 | 37.08 | 42.08 | 12.1 | .29 | 8.42 | .26 | 19.73 |

TABLE (5-5) Plane Strain Test # II, $\sigma'_3$ = 10 psi.

| Time Sec. | Load Dial Reading .0001" | Displacement .0001" | M.V. Voltmeter Reading, Digital Recorder | | | |
|---|---|---|---|---|---|---|
| | | | Gauge #1 | Gauge #2 | Gauge #3 | Gauge #4 |
| | .0001" | | +1 | +6.5 | +17.5 | -1 |
| | 0 | 0 | +74 | +73.0 | +93.0 | +80.5 |
| | 50 | 22 | 73.5 | 76.5 | 84.5 | 85.0 |
| | 120 | 34 | 73.5 | 75.0 | 81.5 | 88.5 |
| | 230 | 50 | 72.0 | 75.5 | 75.0 | 92.0 |
| | 340 | 64 | 73.5 | 77.5 | 70.0 | 96.5 |
| | 430 | 76 | 74.5 | 77.5 | 65.5 | 102.5 |
| | 515 | 90 | 76.5 | 77.5 | 61.0 | 108.0 |
| | 615 | 108 | 86.0 | 81.0 | 57.5 | 115.5 |
| | 710 | 128 | 95.0 | 84.0 | 53.0 | 113.0 |
| | 815 | 152 | 113.0 | 89.0 | 47.5 | 139.0 |
| | 900 | 173 | 129.0 | 96.0 | 45.0 | 145.0 |
| | 1010 | 204 | 150.5 | 104.0 | 41.0 | 157.0 |
| | 1115 | 234 | 166.5 | 109.0 | 38.0 | 166.5 |
| | 1300 | 290 | 191.5 | 119.0 | 34.0 | 184.0 |
| | 1420 | 338 | 194.5 | 121.5 | 29.0 | 198.5 |
| | 1655 | 395 | 205.0 | 116.5 | 25.5 | 213.5 |
| | 1700 | 460 | 206.5 | 113.5 | 22.0 | 232.5 |
| | 1800 | 515 | 203.5 | 108.0 | 19.0 | 247.0 |
| | 1900 | 593 | 206.0 | 106.0 | 19.0 | 263.5 |
| | 1960 | 660 | 203.0 | 106.0 | 22.0 | 264.5 |
| | 1990 | 730 | 202.0 | 104.5 | 31.0 | 284.5 |
| | 1993 | 800 | 198.5 | 101.5 | 36.0 | 291.0 |
| | 1990 | 830 | 189.0 | 103.0 | 37.0 | 293.0 |
| | 1980 | 860 | 186.0 | 102.5 | 41.0 | 296.5 |
| | 1970 | 900 | 192.0 | 97.0 | 49.5 | 301.5 |
| | 1920 | 960 | 189.5 | 94.5 | 56.0 | 309.0 |

TABLE (5.5) Continued, Plane Strain Test # II, $\sigma_3$ = 10 psi.

| Load lbs. | Displacement ΔH Inches | Intermediate Principal Stress Readings, $\sigma_2$=psi | | | | Strain $\epsilon=\frac{\Delta H}{H_o}$ | 1 - ε |
|---|---|---|---|---|---|---|---|
| | | Gauge #1 | Gauge #2 | Gauge #3 | Gauge #4 | | |
| 0 | 0.00 | 9.4 | 10.6 | | 8.8 | .00 | 1 |
| 12.4 | .0022 | 9.4 | 11.2 | | 9.4 | .00082 | .99918 |
| 29.9 | .0034 | 9.4 | 10.9 | | 9.7 | .00082 | .99918 |
| 57.0 | .005 | 9.2 | 11.0 | | 10.0 | .0013 | .9987 |
| 84.0 | .0064 | 9.4 | 11.3 | | 10.5 | .0019 | .9981 |
| 105.0 | .0076 | 9.5 | 11.3 | | 11.72 | .0024 | .9976 |
| 126.0 | .0090 | 9.8 | 11.3 | | 11.7 | .0028 | .9972 |
| 151.0 | .0108 | 11.0 | 11.8 | | 12.6 | .0034 | .9966 |
| 174.0 | .0128 | 12.2 | 12.3 | | 12.3 | .0040 | .9960 |
| 200.0 | .0152 | 14.6 | 13.0 | | 15.0 | .0048 | .9952 |
| 220.0 | .0173 | 16.8 | 14.0 | | 15.8 | .0057 | .9943 |
| 245.0 | .0204 | 19.7 | 15.3 | | 17.0 | .0065 | .9935 |
| 271.0 | .0234 | 21.8 | 16.0 | | 18.0 | .0076 | .9924 |
| 316.0 | .029 | 25.2 | 17.5 | | 20.0 | .0087 | .9913 |
| 341.0 | .0338 | 25.6 | 17.8 | | 21.6 | .0108 | .9892 |
| 395.0 | .0395 | 27.0 | 17.2 | | 23.1 | .013 | .987 |
| 407.0 | .046 | 27.2 | 16.7 | | 25.0 | .015 | .985 |
| 431.0 | .0515 | 26.8 | 15.9 | | 26.6 | .017 | .983 |
| 455.0 | .0593 | 27.2 | 15.5 | | 28.5 | .019 | .981 |
| 471.0 | .066 | 26.8 | 15.5 | | 28.6 | .022 | .978 |
| 477.0 | .073 | 26.5 | 15.3 | | 30.6 | .025 | .975 |
| 477.0 | .08 | 26.1 | 14.8 | | 31.5 | .027 | .973 |
| 477.0 | .083 | 24.8 | 15.2 | | 31.7 | .030 | .970 |
| 475.0 | .086 | 24.4 | 15.2 | | 32.0 | .032 | .968 |
| 473.0 | .09 | 25.2 | 14.1 | | 32.6 | .034 | .966 |
| 461.0 | .096 | 24.8 | 13.8 | | 33.4 | .036 | .964 |

Unsatisfactory Results

TABLE (5.5) Continued, Plane Strain Test # II, $\sigma'_3$ = 10 psi.

| $A_o/1-\epsilon$ in? | psi. $\sigma'_1-\sigma'_3$ | psi. $\sigma'_1$ | psi. $\sigma'_2$ Average | $\frac{\sigma'_2}{\sigma'_1}$ | $\frac{\sigma'_1}{\sigma'_3}$ | $\frac{\sigma'_2}{\sigma'_1+\sigma'_3}$ | $\sigma'_{oct} = \frac{\sigma'_1+\sigma'_2+\sigma'_3}{3}$ psi. |
|---|---|---|---|---|---|---|---|
| 4.92 | 0 | 10 | 9.6 | .96 | 0 | 0.48 | 9.87 |
| 4.92 | 2.52 | 12.52 | 10.0 | .79 | 1.25 | 0.44 | 10.84 |
| 4.92 | 6.07 | 16.07 | 10.0 | .62 | 1.61 | 0.38 | 12.02 |
| 4.92 | 11.60 | 21.60 | 10.07 | .47 | 2.16 | 0.32 | 13.89 |
| 4.93 | 17.10 | 27.10 | 10.4 | .38 | 2.71 | 0.28 | 15.83 |
| 4.93 | 21.30 | 31.30 | 10.84 | .35 | 3.13 | .26 | 17.38 |
| 4.94 | 25.60 | 35.60 | 10.93 | .31 | 3.56 | .24 | 18.84 |
| 4.94 | 30.70 | 40.70 | 11.80 | .29 | 4.07 | .23 | 20.83 |
| 4.94 | 35.40 | 45.40 | 12.27 | .27 | 4.54 | .22 | 22.56 |
| 4.95 | 40.6 | 50.6 | 14.20 | .28 | 5.06 | .23 | 24.93 |
| 4.95 | 44.6 | 54.6 | 15.53 | .28 | 5.46 | .24 | 26.71 |
| 4.96 | 49.8 | 59.8 | 17.33 | .29 | 5.98 | .25 | 29.04 |
| 4.96 | 55.0 | 65.0 | 18.6 | .29 | 6.50 | .25 | 31.20 |
| 4.96 | 64.2 | 74.2 | 20.9 | .28 | 7.42 | .25 | 35.03 |
| 4.97 | 69.5 | 79.5 | 21.67 | .27 | 7.95 | .24 | 37.06 |
| 4.98 | 80.2 | 90.2 | 22.43 | .25 | 9.02 | .22 | 40.88 |
| 4.98 | 82.6 | 92.6 | 22.96 | .25 | 9.26 | .22 | 41.85 |
| 5.00 | 87.5 | 97.5 | 23.1 | .24 | 9.75 | .21 | 43.53 |
| 5.01 | 92.5 | 102.5 | 23.73 | .23 | 10.25 | .21 | 45.41 |
| 5.03 | 95.5 | 105.5 | 23.63 | .22 | 10.55 | .20 | 46.38 |
| 5.05 | 97.0 | 107.0 | 24.13 | .23 | 10.70 | .21 | 47.03 |
| 5.06 | 97.0 | 107.0 | 24.13 | .23 | 10.70 | .21 | 47.03 |
| 5.07 | 97.0 | 107.0 | 23.9 | .22 | 10.70 | .20 | 46.97 |
| 5.08 | 96.5 | 106.5 | 23.87 | .22 | 10.65 | .22 | 46.79 |
| 5.09 | 96.1 | 106.1 | 23.97 | .23 | 10.61 | .23 | 46.69 |
| 5.10 | 93.6 | 103.6 | 24.00 | .23 | 10.36 | .23 | 45.87 |

TABLE (5-6) Plane Strain Test #III, $\sigma_3$ = 15 psi.

| Time Sec. | Load Dial Reading .0001" | Displacement 0.0001" | VOLTMETER READINGS - DIGITAL RECORDER | | | |
|---|---|---|---|---|---|---|
| | | | Gauge #1 M.V. | Gauge #2 M.V. | Gauge #3 M.V. | Gauge #4 M.V. |
| | | | +2 | +10 | +9.5 | +2 |
| | 0 | 0 | +95.5 | +113 | +115.5 | +123 |
| | 10 | 60 | 103 | 112.5 | 97 | 125 |
| | 14 | 100 | 93 | 108 | 91.5 | 126.5 |
| | 20 | 140 | 97 | 108.5 | 90 | 124 |
| | 31 | 210 | 100 | 112.5 | 86.5 | 125 |
| | 60 | 265 | 96.5 | 111.5 | 81.5 | 125.5 |
| | 120 | 278 | 96.5 | 110 | 79.5 | 125.5 |
| | 225 | 287 | 94 | 113 | 76.5 | 126 |
| | 330 | 297 | 98.5 | 109 | 73 | 128.5 |
| | 420 | 307 | 96 | 104.5 | 60.5 | 118 |
| | 525 | 317 | 98.5 | 108 | 70 | 134.5 |
| | 725 | 339 | 103 | 106.5 | 63.5 | 149.5 |
| | 910 | 362 | 104.5 | 103 | 61 | 169.5 |
| | 1100 | 390 | 110.5 | 101 | 56.5 | 190.5 |
| | 1300 | 419 | 111 | 98.5 | 57.5 | 219.5 |
| | 1510 | 450 | 128 | 93 | 49 | 249 |
| | 1765 | 494 | 144.5 | 93.5 | 46 | 279 |
| | 1935 | 557 | 161 | 103 | 40.5 | 314.5 |
| | 2110 | 606 | 176.5 | 116.5 | 36 | 332 |
| | 2345 | 700 | 193 | 136.5 | 32.5 | 342 |
| | 2510 | 794 | 213.5 | 169.5 | 45 | 329.5 |
| | 2610 | 810 | 216.5 | 170.5 | 45 | 331.5 |
| | 2865 | 927 | 221.5 | 173.5 | 44.5 | 332 |

TABLE (5.6) Continued, Plane Strain Test #III, $\sigma_3$ = 15 psi.

| Load lbs. | Displacement ΔH Inches | Intermediate Principal Stress Readings, $\sigma_2$ = PSI | | | | Strain $\epsilon=\frac{\Delta H}{Ho}$ | 1 - ε |
|---|---|---|---|---|---|---|---|
| | | Gauge #1 | Gauge #2 | Gauge #3 | Gauge #4 | | |
| 0 | 0.0 | 12.3 | | | 13.4 | | 1 |
| 2.4 | .006 | 13.4 | | | 13.6 | .0024 | .9976 |
| 3.4 | .0100 | 12.0 | | | 13.8 | .0040 | .9960 |
| 5.0 | .014 | 12.5 | | | 13.5 | .0057 | .9943 |
| 7.6 | .021 | 12.9 | | | 13.6 | .0084 | .9916 |
| 14.9 | .0265 | 12.5 | | | 13.7 | .0107 | .9893 |
| 30.0 | .0278 | 12.5 | | | 13.7 | .0112 | .9888 |
| 55.8 | .0287 | 12.2 | | | 13.8 | .0115 | .9885 |
| 81.0 | .0297 | 12.7 | | | 14.0 | .012 | .9880 |
| 103.0 | .0307 | 12.5 | | | 12.8 | .0124 | .9876 |
| 129.0 | .0317 | 12.7 | | | 14.6 | .0128 | .9872 |
| 178.0 | .0339 | 13.4 | | | 16.2 | .0137 | .9863 |
| 222.0 | .0362 | 13.6 | | | 18.2 | .0146 | .9854 |
| 267.0 | .0390 | 14.3 | | | 20.6 | .0158 | .9842 |
| 316.0 | .0419 | 14.3 | | | 23.7 | .0169 | .9831 |
| 362.0 | .0450 | 16.7 | | | 27.0 | .0183 | .9817 |
| 423.0 | .0494 | 18.9 | | | 30.2 | .02 | .9800 |
| 464.0 | .0557 | 21.2 | | | 34.0 | .0225 | .9775 |
| 506.0 | .0606 | 23.2 | | | 35.8 | .0245 | .9755 |
| 563.0 | .0700 | 25.3 | | | 34.0 | .0282 | .9718 |
| 603.0 | .0794 | 28.1 | | | 35.6 | .032 | .9680 |
| 627.0 | .0810 | 28.5 | | | 35.7 | .0327 | .9673 |
| 688.0 | .0927 | 29.2 | | | 35.9 | .0375 | .9625 |

Unsatisfactory Results

Unsatisfactory Results

TABLE (5-6) Continued, Plane Strain Test # III , $\sigma'_3$ = 15 psi.

| $A_o/1-\varepsilon$ $in^2$ | psi. $\sigma'_1-\sigma'_3$ | psi. $\sigma'_1$ | psi $\sigma'_2$ Average | $\frac{\sigma'_2}{\sigma'_1}$ | $\frac{\sigma'_1}{\sigma'_3}$ | $\frac{\sigma'_2}{\sigma'_1+\sigma'_3}$ | $\sigma'_{oct} = \frac{\sigma'_1+\sigma'_2+\sigma'_3}{3}$ psi. |
|---|---|---|---|---|---|---|---|
| 4.88 | | 15 | 12.85 | .86 | $\phi$. | .86 | 14.28 |
| 4.89 | .49 | 15.49 | 13.50 | .87 | 1.03 | .44 | 14.66 |
| 4.90 | .69 | 15.69 | 12.90 | .83 | 1.05 | .42 | 14.53 |
| 4.91 | 1.03 | 16.03 | 13.00 | .81 | 1.07 | .42 | 14.68 |
| 4.92 | 1.56 | 16.56 | 13.25 | .80 | 1.10 | .42 | 14.94 |
| 4.93 | 3.07 | 18.07 | 13.10 | .72 | 1.20 | .40 | 15.39 |
| 4.94 | 6.15 | 21.15 | 13.1 | .62 | 1.41 | .36 | 16.42 |
| 4.94 | 11.40 | 26.40 | 13.0 | .49 | 1.76 | .31 | 18.13 |
| 4.94 | 16.60 | 31.60 | 13.35 | .42 | 2.11 | .29 | 19.98 |
| 4.94 | 21.10 | 36.10 | 12.65 | .35 | 2.41 | .25 | 21.25 |
| 4.94 | 26.4 | 41.40 | 13.65 | .33 | 2.76 | .24 | 23.35 |
| 4.95 | 36.5 | 51.5 | 14.8 | .29 | 3.43 | .22 | 27.10 |
| 4.95 | 45.5 | 60.5 | 15.9 | .26 | 4.03 | .21 | 30.47 |
| 4.96 | 54.6 | 69.6 | 17.45 | .25 | 4.64 | .21 | 34.02 |
| 4.96 | 64.7 | 79.7 | 19.0 | .24 | 5.31 | .20 | 37.90 |
| 4.97 | 74.0 | 89.0 | 21.85 | .24 | 5.93 | .21 | 41.96 |
| 4.98 | 86.6 | 101.6 | 24.55 | .24 | 6.77 | .21 | 47.05 |
| 4.99 | 94.5 | 109.5 | 27.6 | .25 | 7.3 | .22 | 50.70 |
| 5.00 | 103.5 | 118.5 | 29.5 | .25 | 7.9 | .22 | 54.33 |
| 5.02 | 115.0 | 130.0 | 29.65 | .23 | 8.67 | .20 | 58.22 |
| 5.04 | 123.5 | 138.5 | 31.85 | .23 | 9.23 | .21 | 61.78 |
| 5.04 | 128.5 | 143.5 | 32.1 | .22 | 9.57 | .20 | 63.53 |
| 5.07 | 140.0 | 155.0 | 32.55 | .21 | 10.33 | .19 | 67.52 |